Interaction Notes

Note 411

December 1981

POLE EXTRACTION IN THE FREQUENCY DOMAIN

Thomas B.A. Senior and Jeffrey Pond
Radiation Laboratory
Department of Electrical and Computer Engineering
The University of Michigan
Ann Arbor, Michigan 48109

Abstract

An investigation has been carried out to examine the practicality of extracting the SEM poles for scatterers from measured frequency domain data. The ultimate objective was to determine the poles, coupling coefficients and modes for a B-52G aircraft using data for the surface currents and charges measured using a small scale model, but this was not achieved. Three curve fitting and pole extraction algorithms were examined, and one of these was quite successful in fitting data. This particular program was applied to artificially generated data and to the measured longitudinal currents on a cylinder. Unfortunately, only the lowest order pole (at most) showed the positional invariance in the complex s plane required to separate the true (but unknown) poles from those generated by the curve fitting process. A detailed study using exact, artificially degraded and measured data for the surface fields on a sphere confirmed that accuracy of curve fit is not itself a guarantee of accuracy of (true) pole extraction, and showed that a relatively small amount of noise or other data degradation greatly affects the accuracy with which the poles can be located. When the same algorithm was applied to measured data for the B-52G for a

variety of incidence angles, not even the lowest order pole could be found with sufficient accuracy to justify acceptance of the residue.

Acknowledgements

We are grateful to Professor E. L. McMahon and Mr. C. J. Roussi for their assistance with the pole extraction algorithms, Ms. F. Movahhed for her help with the data manipulation, and Dr. V. V. Liepa who provided all of the experimental data used in this study.

CHAPTER 1: INTRODUCTION

The singularity expansion method (SEM) is based on the analytic properties of the electromagnetic response of a body as a function of the complex frequency s. For a passive body the singularities are confined to the left half of the complex s plane, and a knowledge of these singularities can serve to characterize the response to any excitation. If the body is finite and perfectly conducting, the only singularities in the finite part of the plane are poles, which are simple and occur in complex conjugate pairs (Baum, 1976: Sancer and Varvatsis, 1980), i.e., are symmetrically placed with respect to the negative real s axis.

It is fundamental to SEM that the poles are independent of the mathematical representation of the response and are a property of the body alone. In particular, their locations (but not the residues) are unaffected by a change in the illumination, and if a collection of poles is extracted from computed or measured data for the response, the SEM poles can be distinguished from numerical artifacts by their positional invariance. Cataloging the true poles is therefore a simple method of summarizing information about a body, and their extraction from measured data could serve as a means of target identification.

Theoretically any target response to a time harmonic field such as the surface current density is expressible as a residue series

$$\bar{J}(s) = \sum_{\alpha} \frac{\bar{A}(s_\alpha)}{s - s_\alpha}$$

in the complex frequency s $(= \sigma + i\omega)$ plane, where ω is the circular frequency and the s_α are the SEM poles representing the complex natural frequencies. Each residue can also be written as the product of a natural mode factor which is a function of position on the target and a coupling coefficient which depends on the incident field. When the target is illuminated by an electromagnetic pulse (EMP) which has a broad frequency spectrum, the degree to which the natural frequencies are excited depends on the coupling coefficients which are themselves functions of the angle of incidence and the polarization of the incident illumination. To determine the 'optimum' EMP simulation for the target, it is therefore important to understand this dependence. Moreover, if the natural frequencies and their coupling coefficients could be found, it might then be possible to develop an equivalent circuit which, when driven with the appropriate input waveform, could produce the same transient field as an EMP excitation.

Given data of sufficient accuracy for the frequency response, it is feasible that the SEM poles could be extracted and the residues decomposed in the manner indicated above. For most targets of practical interest, however, the only data available are experimental in origin, and it is by no means evident that all (or, indeed, any) of the analysis is still feasible. The objective of the present project was to attempt the analysis using data for the surface fields on a B-52G aircraft obtained from scale model measurements made in the Radiation Laboratory's surface field facility. Some data were available from a prior study (Liepa, 1980), but to the extent necessary it was required that additional data be gathered.

The initial and vital step on which all others in the sequence depend is the extraction of the SEM poles. The mathematical procedure is to fit the frequency response data using a rational function or its partial fraction expansion and to distinguish the true (SEM) poles from those generated by the curve fitting process by their positional invariance to a change in the excitation conditions. Several numerical algorithms exist for fitting the data. One of these is an iterative method developed by Sharpe and Roussi (1979) and based on a technique of Levy (1959). It is essentially a least squares method that fits the data with a rational function from which the poles and residues are then computed. The iteration linearizes the calculation and also reduces the excessive weighting of the higher frequencies that a straight least squares computation normally produces. Although the program is relatively inefficient, it had been our intent to rely exclusively on this; but at the beginning of the project difficulties were experienced in implementing the necessary extensions to the basic program described by Sharpe and Roussi. In the meantime we had been provided with an alternative program written by Dr. H. J. Price of the Mission Research Corporation which was considerably more efficient. The decision was made to use this instead.

The initial version of the program was dubbed MRC1 and used only the real part of the frequency response, but it was felt that useful experience could be gained by applying this to existing measured data for the B-52G aircraft. The program duly provided a fit to the data and yielded poles and their residues, but as we explored the effect of such parameters as the increment in frequency, the number of data points used, and the value of ω_{max}, certain peculiarities revealed themselves. In particular, the results obtained were extremely sensitive to the magnitude of ω_{max}, and differed substantially according to the manner in which the frequency was normalized.

So began an exercise in frustration, part of which is documented in Chapter 2. In an effort to resolve the problems, we now resorted to numerically generated data for specific rational functions whose poles and residues were known precisely. Sometimes the program accurately determined these and others not, and there seemed no logic to the successes and failures. Since we could discern no fault in the program itself, we had to believe that numerical round-off errors were responsible; and when we received the improved version (MRC2) of the program which accepted data for the real and imaginary parts of the frequency response, we turned to a CDC computer for which the program had been written rather than an Amdahl 470/V8 on which the MRC1 had been run. Unfortunately, neither the new program nor the new computer helped. A variety of techniques were tried some of which are described in Chapter 2. All were unsuccessful and when the extended version of the less efficient but more direct Sharpe-Roussi program became available we transferred our attention to it.

The program had no difficulty fitting the computer-generated data with which the MRC2 program had struggled, and the poles and residues were accurately recovered. To test its performance in a more realistic situation, the program was then applied to measured data for the surface fields on a metal cylinder for a variety of excitations. In each case a reasonable fit to the measured data was achieved, but there was no consistency in the pole locations. Indeed, the poles wandered to such an extent that it was impossible to distinguish the true poles from those generated by the curve fitting process; and though there were certain groupings that were believed to be associated with SEM poles, the spread was too large to justify an analysis of the residues.

It was once again time to retreat and consolidate. To better understand the capability of the program and, in particular, to appreciate the manner in which the orders of the rational function polynomials and the frequency span of the data affect the accuracy of the extracted poles, it seemed appropriate to examine the frequency response for a body whose poles and residues are known precisely. One of the few bodies for which this is true is a sphere. The results of applying the program to computed data for the surface fields on a perfectly conducting sphere are presented in Chapter 3. For 'exact' data accurate to six decimals, the program successfully extracted a handful of the dominant poles and determined their residues; but as the accuracy of the data was reduced, the accuracy of the results progressively decreased. Indeed, for data accurate to two decimals, only the dominant pole was located with sufficient precision for its residue to be accepted. The results obtained by adding noise to the computed data or using measured data were similar: only for the dominant (lowest order) pole was the information meaningful, and filtering the data produced no improvement.

The investigation described in Chapter 3 represents one of the major accomplishments of the project. It showed that the accuracy of curve fitting per se is not a measure of the accuracy with which the true SEM poles can be located, and a relatively small amount of noise or other degradation of the data has a major effect on the determination of the pole locations and their residues. In fact, with less noise than is typical of the best experimental data, only the dominant pole would be located with sufficient accuracy to justify a consideration of its residue. This finding agrees with the conclusion of our earlier study of the cylinder and was expected to hold in general; but since the sphere is a very special shape (and a less resonant one than, say, a thin cylinder), it was felt prudent to re-examine the cylinder data using those program parameters which had been found most effective in analyzing the sphere. The results are summarized in Appendix A and are virtually identical to those obtained earlier. Although it is possible to associate a particular grouping of extracted poles with a true SEM pole, the spread in pole locations is too great to ascribe any meaning to the residues computed. A brief and semi-quantitative discussion of the manner in which an error in pole location affects the residue is given in Appendix B.

While the sphere study was being completed, the surface fields on a scale model of the B-52G were measured at several locations on the aircraft, each for a variety of illumination and/or polarization conditions. With a heavy heart we now turned to the analysis of the data. There were no surprises, and only the dominant pole could be located. A selection of the data and a discussion of the analyses performed are given in Chapter 4.

CHAPTER 2: APPLICATION OF THE MRC PROGRAMS

Our original effort toward curve-fitting and the location of poles and residues was through the use of a program known as the Sharpe-Roussi program, written at the Radiation Laboratory. The Sharpe-Roussi program, however, was still in the process of being debugged when a complete program was supplied by Mission Research Corporation; it was therefore decided to use the latter program.

This first MRC program used only the real part of the data, which made it somewhat suspect; there was also some difficulty with ensuring that the poles and residues were generated in conjugate pairs. Before the program could be thoroughly evaluated, a second program was received from MRC and became the principal subject of investigation; it is referred to hereafter as MRC2.

The MRC2 program calculates a least-squares fit of a rational function to complex data in an indirect manner. After multiplying through by the unknown denominator to linearize the problem, the objective is to minimize separately the real and imaginary parts of

$$F(j\omega_i)D(j\omega_i) - N(j\omega_i) \quad , \qquad i = 1,2,\ldots,M$$

where $F(j\omega_i)$ is the given data, $D(j\omega_i)$ is the denominator, of order N, and $N(j\omega_i)$ the numerator, of order N + 1. Separating real and imaginary parts yields an overdetermined system of 2M equations in 2N + 3 unknowns, which can be written in the form

$$Aa = \delta$$

where A is generated from $F(j\omega)$, a is a vector of the unknown rational function coefficients, and δ is a vector of residuals which is to be minimized. Taking the inner product gives

$$\delta^t\delta = a^tA^tAa = a^tDa \quad .$$

To add the constraint

$$a^ta = 1 \quad ,$$

a Lagrangian multiplier is used and derivatives with respect to the coefficients are taken of

$$a^tDa - \lambda(a^ta - 1) \quad .$$

After some manipulation this yields

$$Da - \lambda a = 0 \quad .$$

Thus the λ's and a's are, respectively, eigenvalues and eigenvectors of D. Further manipulation gives

$$a^tDa - \lambda = 0 \quad .$$

Since it is desired to minimize a^tDa, the smallest eigenvalue is chosen; the corresponding eigenvector gives the coefficients of the desired rational-function approximation.

After the necessary editing and debugging to adapt the program to our system, it was checked using a test function of the form

$$\frac{A}{s - s_o} + \frac{A^*}{s - s_o^*} + 2s + 3$$

Runs were made with $\Delta\omega$ constant at 1.0 and the number N of data points (and thus ω_{max}) varying over 5,10,20,50,100. The best match was obtained for N = 5.

The test function was modified to the form

$$\frac{1 + j1}{s + 0.5 - j2} + \frac{0.5}{s + 1 - j4} + \text{conjugates} + 1.0 \quad .$$

The various parameter combinations tested and the results obtained are summarized in Table 2.1.

Table 2.1

$\Delta\omega$ \ N	5	10	20	40
1.0	$\omega_{max} = 5$ Adequate	$\omega_{max} = 10$ Excellent	$\omega_{max} = 20$ Excellent	$\omega_{max} = 40$ Very good
0.5	---	$\omega_{max} = 5$ Excellent	$\omega_{max} = 10$ Excellent	$\omega_{max} = 20$ Excellent
0.25	---	---	$\omega_{max} = 5$ Excellent	$\omega_{max} = 10$ Excellent

From these results it was concluded that $\Delta\omega$ was not critical so long as the function was adequately sampled. The case of N = 40 and $\Delta\omega$ = 1.0 was not as good as most of the others; it was felt that this was probably due to the large value of ω_{max}.

Taking the case N = 20, $\Delta\omega = 0.5$ as a reference and keeping N constant at 20, the pole locations, residues, and $\Delta\omega$ were scaled, first by a factor of 5 and then by a factor of 100. With the scale factor of 5, poles and residues were calculated with an accuracy of 3 significant figures; with the scale factor of 100, to within 10 to 15 percent. It was thus concluded that a reasonable amount of scaling was permissible but that a definite upper limit existed.

A more realistic test function, with five conjugate pole pairs, was then constructed and the program modified to accommodate it. The poles and residues of the new function were:

Pole	Residue	
$-0.5 \pm j2.0$	$2.0 \mp j0.1$	
$-0.15 \pm j6.0$	$2.5 \pm j0.8$	
$-1.6 \pm j12.0$	$.05 \pm j2.5$	Constant = 2.0
$-2.0 \pm j16.0$	$1.6 \mp j1.8$	
$-10.0 \pm j20.0$	$-0.2 \pm j0.4$	

This function was used for three different test runs, all with 800 data points and 11 poles, with $\Delta\omega$ (and thus ω_{max}) and the pole position scale factor ranging over two orders of magnitude. The results were extremely poor; none of the poles were located.

The test function was run again, with 80 data points. One pole was located with reasonable accuracy, although the residue was about 20 percent in error. A similar run with 15 poles was expected to give similar results with additional poles having small residues, but did not correlate with the previous run at all.

As it was felt that either N or ω_{max} was the limiting factor, the program was run again with N = 20 and $\Delta\omega$ = 1.0 (ω_{max} = 20) and N = 20, $\Delta\omega$ = 0.5 (ω_{max} = 10). For the first case, the lowest pole was located within about 2 percent and the residue within 10 percent. Although no other poles were located, the constructed function agreed quite well with the test data. For the second case, the first pole and its residue were found exactly, no other poles were found, and the constructed function agreed with the test data to five significant figures.

It was apparent that more insight was needed into the effects and interactions of the various paramters. These parameters were N, the number of data points; $\Delta\omega$, the frequency increment; ω_{max}, the maximum frequency; NP, the number of poles in the approximating function and the scale factor. Accordingly, a series of tests was devised to vary each of the parameters independently, to the extent possible. The earlier, two pole-pair, test function was used, as good results had been obtained previously with this function.

The first test runs gave results which did not agree with those previously obtained. It was at this point that an error was discovered in the program. The error was corrected, but all the results from the five pole-pair test function were invalidated.

Using the two pole-pair test function, the following tests were made:

1. To check ω_{max}, keep N constant and scale $\Delta\omega$, the pole positions, and the residues. Scaling by a factor of 10 caused no change; scaling by 100 caused only 1 to 2 percent change. It was concluded that ω_{max} was not a critical parameter.

2. To check N, multiply N and divide $\Delta\omega$ by the same factor. This was tried with a factor of four, producing no change and leading to the conclusion that N was not critical.

3. Since the test function was fairly constant over much of its range, the poles and residues were scaled by a factor of ten to concentrate the program on the "interesting" part of the function. This produced no change, indicating that the "constant" section of the function was not causing difficulty.

4. When NP was set equal to 11, the "real" poles and residues were calculated accurately. "False" poles were generated but their residues were at least four orders of magnitude smaller. It was concluded that NP, as long as it was made sufficiently large, should not cause problems.

5. To test the program capability at locating "weak" poles, the residues were scaled by a factor 0.01. The poles and residues were calculated to within 2 percent of the correct values.

The test procedure was quite inconclusive, in that none of the parameters had any appreciable effect on the performance of the program.

The five pole-pair test function was again tried, with N = 800 and $\Delta\omega$ = 0.1, 0.01, and 0.001, with the poles and residues correspondingly scaled. None of the poles were located in any of the three runs.

The two pole-pair function was tried again. With N = 800, $\Delta\omega = 0.025$, $\omega_{max} = 20$, the poles and residues were calculated correctly. With N = 20, $\Delta\omega = 1.0$, $\omega_{max} = 20$, and the poles and residues scaled down by a factor of 0.1, none of the poles were found. In this latter case, because of the scaling, a substantial part of the data record was almost constant; it was believed that this was the cause of the difficulty.

The constant was removed from the test function and the program run with N = 20, $\Delta\omega$ = 0.1, which gave results accurate to 3 percent, and with N = 20, $\Delta\omega$ = 1.0, and the poles and residues scaled by 0.1 which gave totally inaccurate results. It was felt that $\Delta\omega$ was too large for the rate of change of the function.

Using the same parameters of the first run above, but with the constant term set to 1.0, the poles were not located, indicating that the constant was indeed the source of difficulty.

The five, pole-pair test function was tried again, with the constant term set to zero. The results, although somewhat better than previous runs, were still insufficiently accurate to be of use. There was, however, some tendency toward accuracy as ω_{max} was decreased, leading to the conclusion that sampling a large part of the constant region was undesirable, even if the constant was zero.

A measure of success was attained using N = 50, $\Delta\omega$ = 0.1, ω_{max} = 5.0; the two lowest poles and their residues were calculated within 1 percent. With N = 800, $\Delta\omega$ = 0.025, ω_{max} = 20 four poles were located within 2 percent and their residues within 5 percent. In both cases, the program located poles with imaginary parts less than ω_{max} and tended not to locate poles with imaginary parts greater than ω_{max}.

Since the program did not appear capable of accurately calculating more than one or two pole-pairs per run, specifically those whose imaginary parts were in the frequency range scanned, it was decided to use a "windowing" technique, examining relatively small, overlapping frequency intervals.

After a number of false starts, the windowing technique was implemented and a number of runs made with test data. All the runs used $\Delta\omega = 0.1$ and a 50 percent overlap between successive windows; the number of points per window was varied from 20 to 50, with and without a constant term in the test function. With two exceptions, the poles were located within ten percent of the correct locations and the residues determined, although somewhat less accurately, particularly in regard to the angle. It did not appear, therefore, that window size was a critical parameter as long as it was kept reasonably small. In the two exceptions mentioned above, three pole-pairs were located and the fourth was not; in one case the test function contained a constant and in the other it did not, so the constant could not be considered the source of difficulty.

Since the windowing technique was producing generally satisfactory results it was decided to continue with it. A decision algorithm was formulated: if a pole appears in two (or more) successive windows within ± 10 percent of the same location it is a "real" pole, and its location and residue are taken as those generated in the window in which the pole is most nearly centered.

All of the testing of the window technique thus far having been done with smooth, highly accurate test data, the data was perturbed to simulate noise in experimental data. This perturbation consisted of the addition of a small, cosinusoidally varying term to the real part and a corresponding sinusoidally varying term to the imaginary part.

For this data the smaller window (20 points, $\Delta\omega = 0.1$) was definitely superior; two poles and their residues were located accurately and the imaginary part of the third was also found, although the real part and the residue were grossly inaccurate.

The test function was modified slightly to make the dominant pole less dominant and run with "noise" amplitudes of 0.07, 0.02, and 0.00. In the noisy cases only one pole was located, although it was located quite accurately, as was its residue.

Since the program obviously could not handle noisy data, it became necessary to filter. (It should be noted that while true least-squares fitting is itself a smoothing process, rational function fitting invariably involves a modified least-squares procedure and tends to be somewhat ill-conditioned.) An eighth-order filter with a cutoff of 110 cycles/plot was tried. There was considerable ringing in the filtered data due to the discontinuities at the ends of the data record; this was smoothed by eye. The results from the filtered data showed only a slight improvement; two poles were located with good accuracy, although the residue of the second one was in error by about 50 percent.

Surprisingly, when the same data was run with a much larger window encompassing all the poles, the results were much better. All the poles were located within about 10 percent and residues within about 20 percent. The small-window approach, which worked well with smooth data, was less effective than the large-window method for noisy data. This was confirmed by another run with a noise amplitude of 0.07; although the accuracy of the pole locations was poor, they were at least identifiable . The noise thus remained a major problem.

Since experimental data could not be expected to be accurate to more than one or perhaps two decimal places,[1] test data files with data rounded to varying degrees of accuracy were generated and tested. With one decimal place accuracy and small (20 point) windows, only the first pole was located, although it was located quite accurately both as to location and residue. The run was repeated with two-place data with essentially the same results, although in this case the fourth pole was identifiable, with about 15 percent error.

The same two data sets were tried with large (200 point) windows. With two decimal-place data, all the poles and residues were found within 1 percent. With one-place data all the poles were found within 15 percent in the worst case and 7 percent in the best case; the residue accuracy was not quite that good and tended to correlate with the accuracy of the corresponding pole. This last result was to be expected; if the pole location is incorrect, the residue must change to fit the data. These test results are summarized in Tables 2.2 and 2.3.

These results clearly indicated that noisy data must be filtered. As the filtering procedure was being implemented, work was also progressing on another curve-fitting routine, the Sharpe-Roussi program. This is a more direct, though less efficient, least-squares procedure. Since the Sharpe-Roussi program subsequently proved more accurate than the MRC2, further work on the latter was abandoned.

---

[1]Typically the best experimentally obtained frequency domain data is limited to an accuracy of at most 5 percent which, for a response comparable to unity, translates into one or two decimal accuracy.

Table 2.2

Large Window Test Results

Actual	Pole	-0.4±j2.0	-1.5±j6.0	-1.6±j12.0	-2.0±j16.0
	Residue	2.0±j0.1	2.5±j0.8	0.05±j2.5	1.6±j1.8
Noise Amp. 0.0		-0.39±j2.0	-1.47±j6.0	-1.6±j12.0	-2.0±j16.0
		1.9±j0.12	2.4±j0.74	-1.5±j2.5	1.6±j1.9
Noise Amp. 0.02		-0.39 ±j2.2	-1.6±j6.2	-1.6±j12.2	-1.9 ±j16.0
		1.7±j0.56	2.8±j0.29	0.47±j2.6	1.5±j1.5
Noise Amp. 0.07		-0.2±j2.75	-1.7±j7.9	-1.7±j13.1	-1.2±j16.0
		0.42±j1.1	0.43±j2.4	2.4±j1.6	0.89±j0.59
1 Decimal Place		-0.36±j2.3	-1.7±j6.5	-1.6±j12.3	-1.9±j15.9
		1.4±j0.78	2.8±j0.25	0.7±j2.4	1.6±j1.4
2 Decimal Places		-0.4±j2.0	-1.5±j6.0	-1.6±j12.0	-2.0±j16.0
		2.0±j1.3	2.5±j0.79	-0.065±j2.5	-1.6±j1.8

Table 2.3

Small Window Test Results

Actual	Pole	$-0.4\pm j2.0$	$-1.5\pm j6.0$	$-1.6\pm j12.0$	$-2.0\pm j16.0$
	Residue	$2.0\pm j0.1$	$2.5\pm j0.8$	$0.05\pm j2.5$	$1.6\pm j1.8$
Noise Amp. 0.0		$-0.4\pm j2.0$	$-1.6\pm j6.0$	$-1.7\pm j12.0$	$-2.1\pm j15.8$
		$2.0\pm j0.11$	$3.0\pm j1.2$	$-0.32\pm j2.8$	$2.5\pm j1.4$
Noise Amp. 0.02		$-0.4\pm j2.0$	---	---	---
		$2.0\pm j0.097$			
Noise Amp. 0.07		$-0.4\pm j2.0$	---	---	---
		$2.0\pm j0.08$			
1 Decimal Place		$-0.4\pm j2.0$	---	---	---
		$2.0\pm j1.2$			
2 Decimal Places		$-0.405\pm j2.0$	---	---	---
		$2,04\pm j0.115$			

CHAPTER 3. APPLICATION OF THE SHARPE-ROUSSI PROGRAM TO SPHERE DATA

3.1 Introduction

The Sharpe-Roussi program for determining the SEM poles from frequency domain data was developed by the Radiation Laboratory and is an iterative technique based on that of Levy (1959). It is essentially a least squares method that fits the data with a rational function from which the poles and residues are then computed. The program was initially applied to measured data for the axial current on a thick cylinder over a frequency range spanning the first five longitudinal modes. In every instance the rational function gave an excellent fit to the measured data, but of the poles extracted, only the lowest order (dominant) one was positionally invariant.

The extent to which the lack of success was due to the program itself, the selection of such parameters as the sampling interval and the order of the rational function, or to the noise and other inaccuracies in the measured data, was not apparent. In the time domain it is found (Cho and Cordaro, 1980) that pole extraction is quite sensitive to noise. To see if this same sensitivity exists in the frequency domain and, at the same time, gain experience in the application of the program, it is helpful to consider data whose accuracy can be controlled. The only finite body whose frequency response is easily obtained to any accuracy desired is the sphere, and in the following sections we consider the determination of the poles and residues from frequency domain data for the surface fields on a perfectly conducting sphere. For this body the SEM poles and residues are known precisely. After a brief description of the numerical algorithm and the computation of the exact surface fields, poles and residues (Section 3.2), the extraction of the poles and residues from the frequency response data is discussed (Section 3.3), along with the influence of the various parameters in the algorithm. In Section 3.4 we then consider the effect of noise and other data inaccuracies on the pole extraction process.

3.2 Formulation

Over any finite frequency range the electromagnetic response of a body can be approximated by a rational function whose poles can be found. It is assumed that a subset of these approximate the SEM poles which are dominant in this frequency range and can be distinguished by their positional invariance to a change in excitation of the body. It follows that the most effective pole extraction procedure is one that accurately determines the SEM poles and maximizes the subset.

Given a (complex) frequency response $F(\omega_\ell)$ where ω_ℓ, $\ell = 1,2,\ldots,L$, are sampled (real) frequencies, the numerical algorithm employed fits this with a rational function

$$\frac{N(\omega)}{D(\omega)} = \frac{a_0 + a_1\omega + \ldots + a_m\omega^m}{b_0 + b_1\omega + \ldots + b_n\omega^n} \quad (m \leq n) \quad . \tag{1}$$

The initial curve fit is obtained when the error

$$E = \sum_{\ell=1}^{L} \left| D(\omega_\ell)F(\omega_\ell) - N(\omega_\ell) \right|^2$$

is minimized, subject to the constraint $b_0 = 1.0$ by solving the simultaneous set of equations

$$\frac{\partial E}{\partial a_j} = 0 \quad , \qquad j = 0,1,\ldots,m$$

$$\frac{\partial E}{\partial b_j} = 0 \quad , \qquad j = 1,2,\ldots,n$$

for the coefficients a_j and b_j. The square of the resulting denominator is then used as a weighting factor in a further application of least squares to improve the rational function fit, giving rise to an iterative procedure. At the kth stage of iteration, the coefficients are obtained by minimizing

$$E = \sum_{\ell=1}^{L} \left| \left\{ D_k(\omega_\ell)F(\omega_\ell) - N_k(\omega_\ell) \right\} \left\{ D_{k-1}(\omega_\ell) \right\}^{-1} \right|^2 , \qquad (2)$$

and so on until the error is less than a pre-specified value.

A program has been written to implement this curve fitting routine. Apart from the frequency range and the sampling interval which are in general determined by the data at hand, there are three parameters which must be chosen at the outset. They are the orders of the numerator and denominator polynomials, M and N respectively, and the maximum allowed error which terminates the iteration. At the conclusion of the program, the poles and residues of the rational function approximation are computed. The process is then repeated using other (distinct) data for the response of the same body, and those poles which are common to most of the results are identified as SEM poles of the body.

To better understand the limitations of the method and to gain experience in the selection of the parameters involved, it is helpful to consider data for a frequency response whose poles and residues are known precisely. This is true in particular for the surface field on a perfectly conducting sphere.

A sphere of radius a is illuminated by the plane wave

$$\bar{E}^i = \hat{x}\, e^{i\omega x/c} \quad , \quad \bar{H}^i = -\hat{y}Y\, e^{i\omega x/c}$$

propagating in the direction of the negative z axis of the Cartesian coordinate system (x,y,z). Y is the intrinsic admittance of the surrounding free space medium, c is the velocity of light in vacuo, and a time factor $e^{i\omega t}$ has been assumed and suppressed. If (r,θ,ϕ) are spherical polar coordinates, the tangential components of the total magnetic field at the surface r = a are

$$H_\theta = YT_1\left(\frac{\omega a}{c}, \theta\right)\sin\phi \quad , \quad H_\phi = YT_2\left(\frac{\omega a}{c}, \theta\right)\cos\phi$$

(Bowman et al., 1969; pp. 396 and 397) with

$$T_1\left(\frac{\omega a}{c}, \theta\right) = \frac{c}{\omega a}\sum_{n=1}^{\infty} i^{n+1}\,\frac{2n+1}{n(n+1)}\left\{\frac{1}{\xi_n^{(2)'}\left(\frac{\omega a}{c}\right)}\,\frac{P_n^{(1)}(\cos\theta)}{\sin\theta} + \frac{i}{\xi_n^{(2)}\left(\frac{\omega a}{c}\right)}\,\frac{\partial}{\partial\theta}P_n^{(1)}(\cos\theta)\right\} \tag{3a}$$

$$T_2\left(\frac{\omega a}{c},\theta\right) = \frac{c}{\omega a}\sum_{n=1}^{\infty} i^{n+1}\,\frac{2n+1}{n(n+1)}\left\{\frac{1}{\xi_n^{(2)'}\left(\frac{\omega a}{c}\right)}\,\frac{\partial}{\partial\theta}P_n^{(1)}(\cos\theta) + \frac{i}{\xi_n^{(2)}\left(\frac{\omega a}{c}\right)}\,\frac{P_n^{(1)}(\cos\theta)}{\sin\theta}\right\} \tag{3b}$$

where $P_n^{(1)}(\cos\theta)$ is the Legendre function of degree n and order unity as defined by Stratton (1941, p. 401) and

$$\xi_n^{(2)}(x) = xh_n^{(2)}(x) \quad , \quad \xi_n^{(2)'}(x) = \frac{d}{dx}\left\{xh_n^{(2)}(x)\right\}$$

where $h_n^{(2)}(x)$ is the spherical Hankel function of the second kind of order n.

By appropriate truncation of the infinite series representations, it is a simple matter to compute T_1 and T_2 to any desired accuracy. A program was available (Senior, 1975) for the far zone scattered fields of a sphere and this was modified to compute T_1 and T_2 for $\theta = 0(45)180°$ and $0.2 \leq \omega a/c \leq 7.0$ to six decimal accuracy. In the limit as $\omega \to 0$, $T_1(0,\theta) = -(3/2)\cos\theta$ and $T_2(0,\theta) = -3/2$.

The functions $\xi_n^{(2)}(x)$ and $\xi_n^{(2)'}(x)$ are proportional to polynomials in x of orders n and n+1 respectively whose zeros are the SEM poles. In terms of the complex frequency $s = i\omega a/c$, the polynomials have positive real coefficients which ensures that all zeros lie in the left half plane, and those which do not lie on the negative real s axis occur in complex conjugate pairs. As shown, for example, by Martinez et al. (1972), the zeros can be arranged in layers lying successively further from the imaginary s axis. When ordered from the right, the odd (even) numbered layers are the electric (magnetic) mode resonances produced by the zeros of $\xi_n^{(2)'}(-is)$ and $\xi_n^{(2)}(-is)$ respectively. In general the dominant SEM poles are those in the first ($\ell = 1$) layer, and the nth pole numbered up from the negative real s axis is a zero of $\xi_n^{(2)'}(-is)$.

T_1 and T_2 can be expressed as

$$T_1(-is,\theta) = \sum_{m=1}^{\infty} \frac{R_1^m(\theta)}{s - s_m} \quad , \quad T_2(-is,\theta) = \sum_{m=1}^{\infty} \frac{R_2^m(\theta)}{s - s_m} \tag{4}$$

where the s_m are zeros of either $\xi_n^{(2)'}(-is)$ or $\xi_n^{(2)}(-is)$, and $R_1^m(\theta)$ and $R_2^m(\theta)$ are the residues of T_1 and T_2 respectively at $s = s_m$. The residues can be found by computing

$$\frac{d}{ds}\left\{-is\ \xi_n^{(2)'}(-is)\right\}\Bigg|_{s=s_m} \quad , \quad \frac{d}{ds}\left\{-is\ \xi_n^{(2)}(-is)\right\}\Bigg|_{s=s_m}$$

and then dividing these into the quantities

$$i^{n+1}\,\frac{2n+1}{n(n+1)}\,F_n(\theta)$$

where $F_n(\theta)$ is either $(\partial/\partial\theta)P_n^{(1)}(\cos\theta)$ or $P_n^{(1)}(\cos\theta)/\sin\theta$. For $\theta = 0$ the poles and residues of the first six poles in the first layer are given in Table 3.1. For comparison we note that for the first pole (at $s = -1$) in the second layer, $R_1(0) = R_2(0) = -i0.551819$.

Table 3.1: Exact poles and residues for first layer poles

m	s_m	$R_2^m(0)$
1	-0.500000 + i0.866025	-0.0946447 - i0.516674
2	-0.701964 + i1.80740	0.633323 - i0.0853256
3	-0.842862 + i2.75786	0.0802221 + i0.733736
4	-0.954230 + i3.71478	-0.822075 + i0.0767481
5	-1.04764 + i4.67641	-0.0741270 - i0.901805
6	-1.12891 + i5.64163	-0.0664705 + i0.223154

3.3 Exact Data Analysis

The curve fitting algorithm was applied to the computed data for T_2 as a function of frequency in an attempt to extract a handful of the lowest order SEM poles. The objective was to locate 4 or 5 pole pairs with sufficient accuracy to leave no doubt as to their identification as SEM (rather than curve fitting) poles, and to allow us to determine the θ dependence of their residues. Data were available for $0.2 \leq \omega a/c \leq 7.0$ in increments of 0.1 and 0.02, and in the expectation that the poles which could be accurately located would be the dominant ones with Im s_m within the frequency range covered by the data, it was anticipated that most (if not all) poles would lie in the first layer.

To apply the algorithm there are a number of parameters which must be chosen, some of which relate to the data and others to the curve fitting process. Regarding the data, there are the minimum, maximum and increments of $\omega a/c$ and, in our case, the choice of phase reference for the frequency response. Since our concern was with the lower order poles, it was natural to choose min $\omega a/c$ to be the smallest value for which data was available, namely 0.2; and to avoid handling more data than was clearly necessary, we initially selected max $\omega a/c = 4.0$ with increments of 0.1. The computed data of Section 2 are phase-referenced to a plane perpendicular to the z axis through the center of the sphere. For all θ except $\pi/2$, arg T_2 varies almost linearly as a function of frequency, and this translates into a roughly sinusoidal variation of the real and imaginary parts which are the inputs to the curve fitting process. The variation is greatly reduced if the phase is referenced to the point on the surface of the sphere where the field is computed, and since it is natural to expect that a smooth curve can be fitted more accurately than a rapidly varying one, arg T_2 was increased by $\omega a/c \cos \theta$ prior to the application of the algorithm. Once the curve fitting was accomplished and the poles and residues determined, the phase reference was returned to the original location.

Three parameters involved in the program itself are the orders M and N of the numerator and denominator polynomials and the maximum allowed error E_{max}. Since the set of SEM poles is infinite in number and the response remains finite as $\omega a/c \to \infty$, it would seem that the accuracy of curve fit should increase with M and N, and that a logical choice would be M = N. Numerically, however, problems are experienced when M and/or N are large due to the finite range of numbers that any computer can handle, whereas if N is small there are too few poles available to simulate the data. It was therefore anticipated that there would be an optimum range of N and, perhaps, M depending on the frequency span of the data and the particular characteristics of the computer.

The error E_{max} relates to the convergence of the iterative process and is not directly a measure of the curve fit nor, of course, the accuracy of pole extraction. When running the program, E_{max} was set at 10^{-8} and the iteration was terminated when this value was achieved, or after 20 iterations, whichever came first. In many instances the maximum allowed error was not obtained, but the curve fit was still excellent. As a measure of the curve fit we therefore computed

$$E_{fit} = \frac{1}{L}\sum_{\ell=1}^{L}\left|F(\omega_\ell) - \frac{N_k(\omega_\ell)}{D_k(\omega_\ell)}\right|^2 \quad (5)$$

(c.f. (2)), where the polynomials are those obtained from the final iteration, and recorded this quantity. Due to the limited precision with which the data were stored, any value of E_{fit} less than 0.25×10^{-7} was shown to be zero. Since the curve fit was excellent in most cases, it was not unusual for this to occur.

All of the initial runs were carried out for $\theta = 0$ (for which $T_2 = T_1$). It was found almost immediately that numerical difficulties arise if N exceeds (about) 25, and if M = N, these problems can occur for M,N as small as 18. In either instance the exponential range of the computer (Amdahl 470/V8) was exceeded. We therefore chose M < N, and because of the restriction on N, limited the frequency span of the data to $\omega a/c \leq 4.0$ to allow for a reasonable number of curve fitting poles in addition to the SEM poles that were sought.

Figure 3.1 shows the curve fit to $|F(\omega_\ell)|$ for $\theta = 0$ and $\Delta\omega a/c = 0.1$ with M = 7 and N = 8. The criterion for E_{max} was met and $E_{fit} = 0.25 \times 10^{-3}$. The extracted pole locations are shown in Fig. 3.2, and we observe that three of the poles vaguely resemble the first three SEM poles, more closely as regards Im s_m than Re s_m. The agreement is better if M = 9 and N = 10, and better still if M and N are increased to 11 and 12 respectively (see Fig. 3.3). We are now beginning to pick up the fifth SEM pole of the first layer (which lies outside the range of Im s spanned by the data), as well as the first pole of the second layer. The convergence criterion was again met and

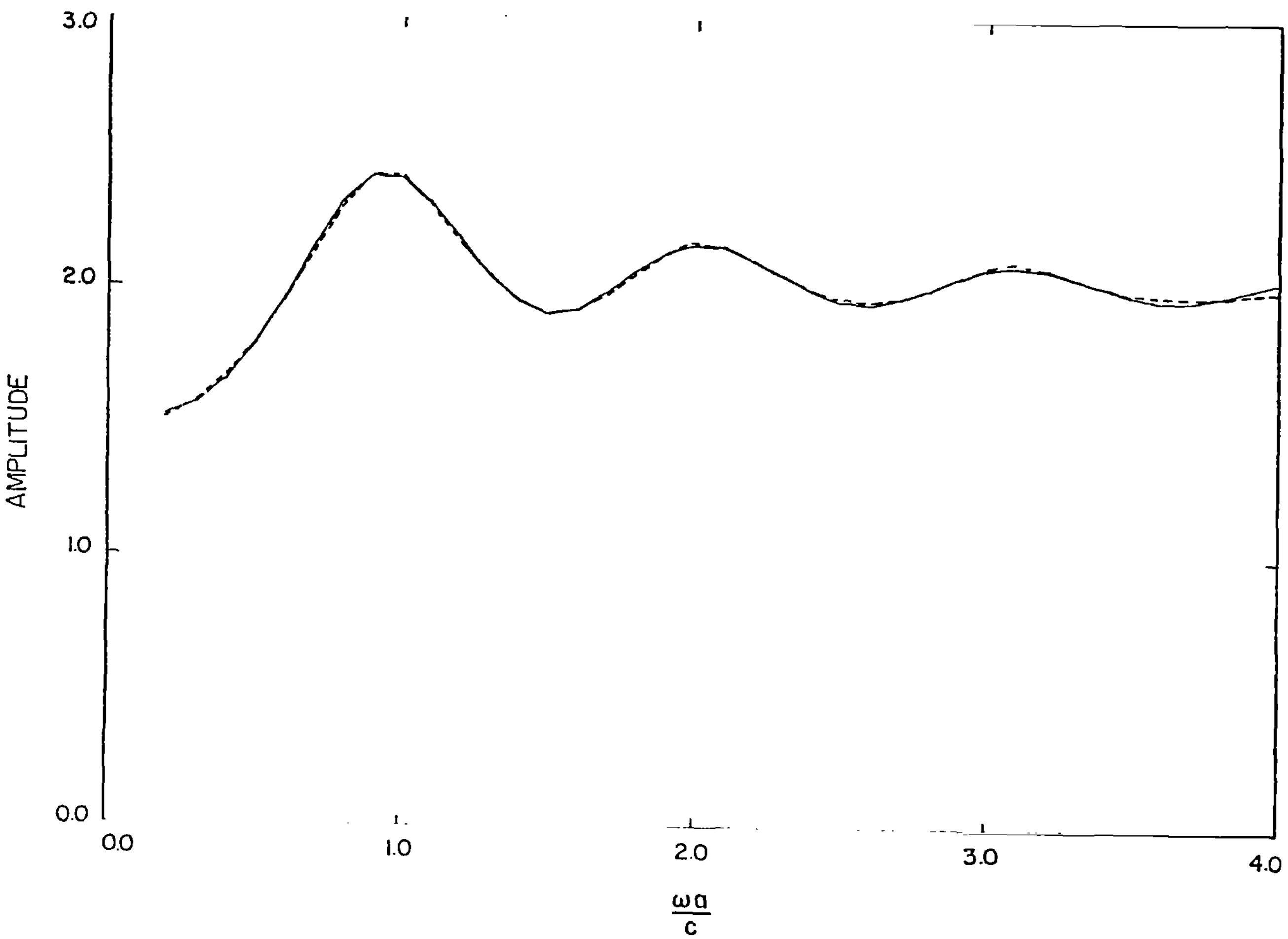

Fig. 3.1: Comparison of $T_2(0\ )$ (——) and the curve fit (----) obtained with $\omega a/c$ = 0.2(0.1)4.0, M = 7 and N = 8.

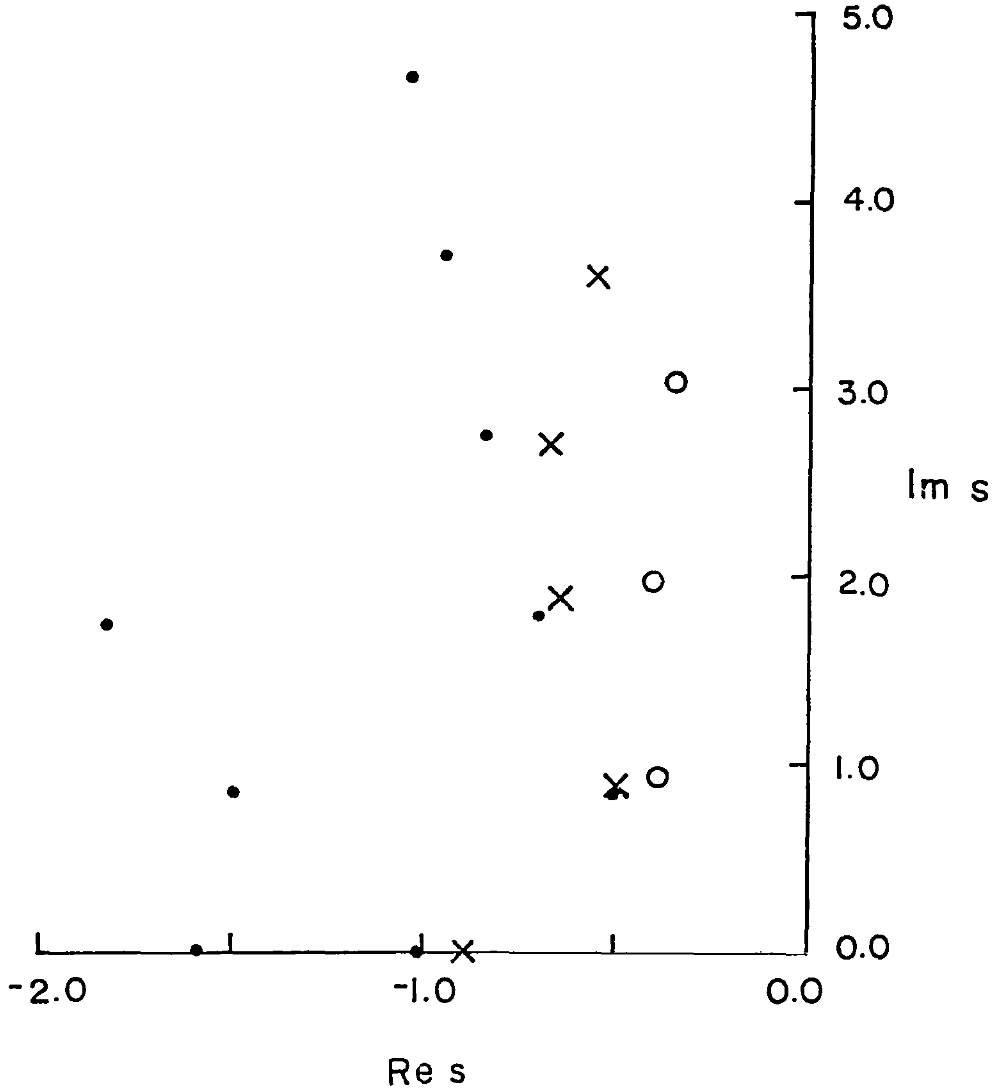

Fig. 3.2: Comparison of exact (• •) and fitted function poles for M = 7 and N = 8 (O O) and for M = 9 and N = 10 (X X).

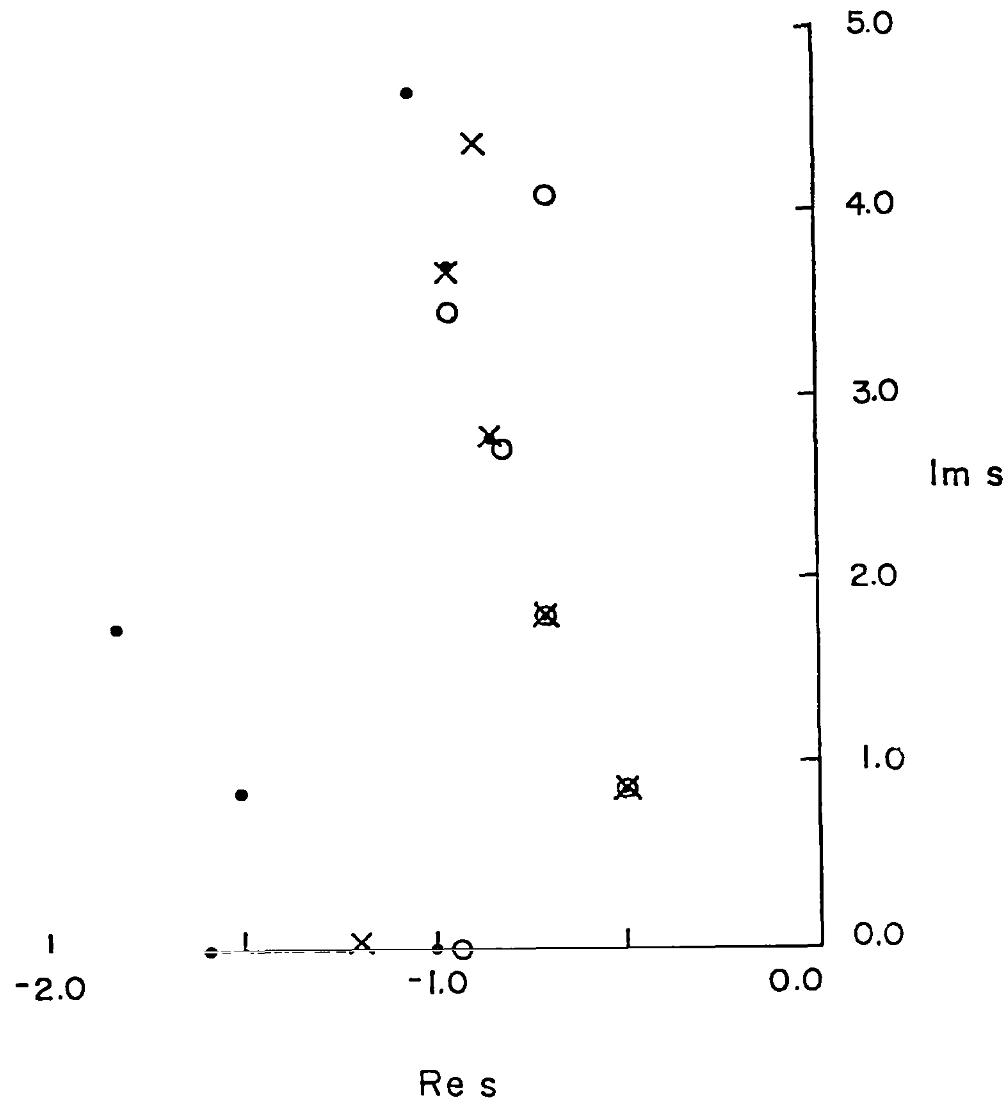

Fig. 3.3: Comparison of exact (• •) and fitted function poles for M = 11 and N = 12 (O O) and for M = 15 and N = 16 (X X).

$E_{fit} = 0.51 \times 10^{-7}$. In this case and in all others discussed, the modulus of the simulated response was graphically indistinguishable from the data within the frequency range spanned by the data, but as seen from Fig. 3.4, there are discrepancies outside the range.

Table 3.2 compares the locations of the first four SEM poles with those of the extracted poles for $\theta = 0$, $\Delta\omega a/c = 0.1$ and four M and N combinations. In each case $E_{fit} \simeq 0$ and the agreement in pole locations improves with increasing order of the polynomials. The best results are for M = 15 and N = 16 in the sense that a further increase in M and/or N gives no improvement. Similar comparisons for a variety of polynomial orders from 8 to 18 have shown that the accuracy of the extracted poles is best for M = N-1 and diminishes for $N \gtrsim 20$.

For given M and N a decrease in the sampling interval from 0.1 (39 data points) to 0.02 (191 data points) has no appreciable effect, as indicated in Table 3.3. The results of shifting the phase reference of the data to a plane through the center of the sphere are shown in Table 3.4 and, as expected, the accuracy of the pole locations is poorer.

The above data are all for $\theta = 0$, and for the cases considered in Tables 3.2 through 3.4 the accuracy of curve fit is extremely good. However, this does not imply a comparable accuracy in the extracted pole locations; and in a practical situation where the locations of the true poles are unknown, it is necessary to vary the illumination conditions, e.g., change θ, and use the positional invariance of the true poles as the criterion of accuracy. We also comment that E_{fit} is unrelated to E_{max}, and for the cases in Tables 3.2 through 3.4, the specified error 10^{-8} was never achieved prior to the completion of the allowed 20 iterations.

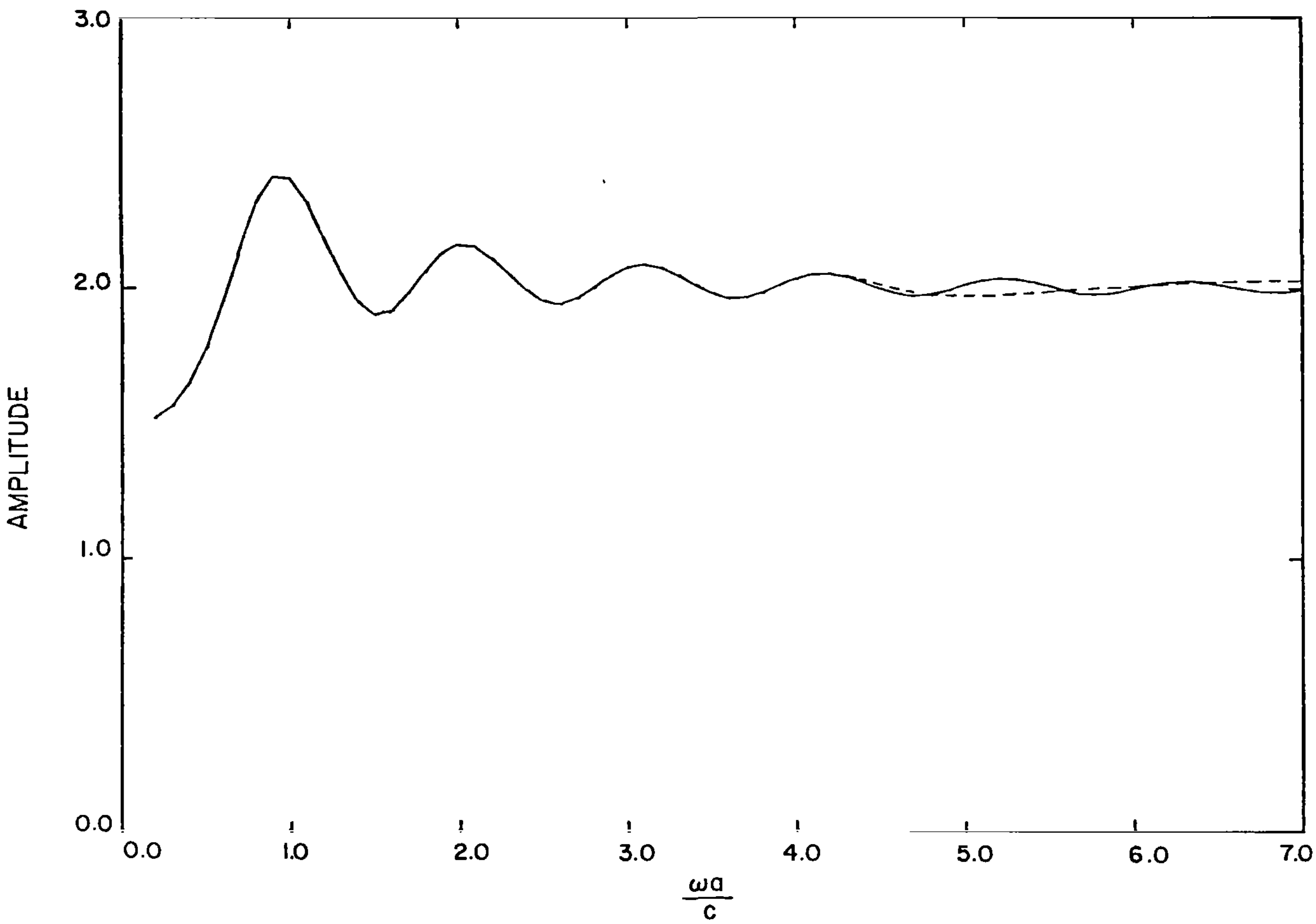

Fig. 3.4: Comparison of $T_2(0\ )$ (——) and the curve fit (----) obtained with $\omega a/c = 0.2(0.1)4.0$, $M = 11$ and $N = 12$.

Table 3.2: Comparison of exact and extracted pole locations for $\theta = 0$, $\Delta\omega a/c = 0.1$ and various M,N

Exact	Extracted			
	M=12, N=14	M=13, N=14	M=14, N=16	M=15, N=16
-0.500000 $\pm$i0.866025	-0.5010 $\pm$i0.8641	-0.5007 $\pm$i0.8659	-0.5007 $\pm$i0.8657	-0.5000 $\pm$i0.8658
-0.701964 $\pm$i1.80740	-0.6964 $\pm$i1.808	-0.7052 $\pm$i1.804	-0.7027 $\pm$i1.803	-0.7025 $\pm$i1.806
-0.842862 $\pm$i2.75786	-0.8436 $\pm$i2.739	-0.8334 $\pm$i2.762	-0.8408 $\pm$i2.766	-0.8399 $\pm$i.2.760
-0.954230 $\pm$i3.71478	-1.056 $\pm$i3.575	-0.9309 $\pm$i3.642	-0.9199 $\pm$i3.685	-0.9439 $\pm$i3.678

Table 3.3: Comparison of exact and extracted pole locations for $\theta = 0$, showing the effect of $\Delta\omega a/c$

Exact	Extracted			
	M = 13, N = 14		M = 15, N = 16	
	$\Delta\omega a/c = 0.02$	$\Delta\omega a/c = 0.1$	$\Delta\omega a/c = 0.02$	$\Delta\omega a/c = 0.1$
-0.500000 $\pm$i0.866025	-0.5003 $\pm$i0.8635	-0.5007 $\pm$i0.8659	-0.4999 $\pm$i0.8657	-0.5000 $\pm$i0.8658
-0.701964 $\pm$i1.80740	-0.6997 $\pm$i1.810	-0.7052 $\pm$i1.804	-0.7021 $\pm$i1.806	-0.7025 $\pm$i1.806
-0.842862 $\pm$i2.75786	-0.8364 $\pm$i2.752	-0.8334 $\pm$i2.762	-0.8407 $\pm$i2.760	-0.8399 $\pm$i2.760
-0.954230 $\pm$i3.71478	-0.9721 $\pm$i3.647	-0.9309 $\pm$i3.642	-0.9489 $\pm$i3.682	-0.9439 $\pm$i3.678

Table 3.4: Comparison of exact and extracted pole locations for $\theta = 0$ and $\Delta\omega a/c = 0.1$, showing the effect of phase reference

Exact	Extracted			
	M = 13, N = 14		M = 15, N = 16	
	center	surface	center	surface
-0.500000	-0.5010	-0.5007	-0.5009	-0.5000
±i0.866025	±i0.8655	±i0.8659	±i0.8650	±i0.8658
-0.701964	-0.6994	-0.7052	-0.6994	-0.7025
±i1.80740	±i1.801	±i1.804	±i1.804	±i1.806
-0.842862	-0.8600	-0.8334	-0.8522	-0.8399
±i2.75786	±i2.770	±i2.762	±i2.769	±i2.760
-0.954230	-0.8879	-0.9309	-0.8794	-0.9439
±i3.71478	±i3.797	±i3.642	±i3.785	±i3.678

The effect of changing θ is shown in Table 3.5, which gives the extracted pole locations for $\theta = 0(45)180°$ with $M = 15$, $N = 16$ and $\Delta\omega a/c = 0.1$. The accuracy does not vary significantly with θ, though we observe that at $\theta = 90°$ where the first and third poles are not excited, the accuracy of the second and fourth poles is better than before. The residues $R_2^m(\theta)$ of the first four poles for T_2 are plotted in Figs. 3.5 through 3.8, and the somewhat poorer accuracy with which the fourth pole is located, particularly for $\theta > 90°$, is reflected in its residue.

The fourth pole is fairly close to the upper limit of the frequencies spanned by the data. To improve its accuracy and, at the same time, locate the next pole or two, it is natural to increase max $\omega a/c$ to 5 or 6, and the results of doing so are shown in Table 3.6. The best agreement is obtained with $M = 17$ and $N = 18$. Although the curve fit is again excellent, as it was for $M = 15$ and $N = 16$ with the smaller data set (see Table 3.3), the first three poles are not quite as accurately located, but the fourth through sixth are in reasonable agreement. Unfortunately, to increase the data span still more and extract further poles requires the use of polynomials of higher order, and because of the numerical difficulties that occur when N exceeds (about) 25, this does not prove to be effective. An alternative approach is to retain the same span of data and 'window', i.e., shift the span to encompass those poles which are sought. This is illustrated in Table 3.7 for three different M and N combinations applied to the data for $2.0 \leq \omega a/c \leq 6.0$. In terms of the accuracy of the extracted poles, the case $M = 15$ and $N = 16$ is best. The fourth through sixth poles are located more accurately than with the larger frequency span, but the first pole is

Table 3.5: Comparison of exact and extracted pole locations for $\Delta\omega a/c = 0.1$, $M = 15$, $N = 16$ and $\theta = 0(45)180°$

Exact	Extracted				
	$\theta = 0°$	$\theta = 45°$	$\theta = 90°$	$\theta = 135°$	$\theta = 180°$
-0.500000	-0.5000	-0.5000	not excited	-0.4997	-0.5001
$\pm i0.866025$	$\pm i0.8658$	$\pm i0.8661$		$\pm i0.8661$	$\pm i0.8660$
-0.701964	-0.7025	not excited	-0.7020	not excited	-0.7008
$\pm i1.80740$	$\pm i1.806$		$\pm i1.807$		$\pm i1.808$
-0.842862	-0.8399	-0.8418	not excited	-0.8419	-0.8410
$\pm i2.75786$	$\pm i2.760$	$\pm i2.760$		$\pm i2.759$	$\pm i2.751$
-0.954230	-0.9439	-0.9490	-0.9565	-0.9341	-0.9310
$\pm i3.71478$	$\pm i3.678$	$\pm i3.698$	$\pm i.3716$	$\pm i3.732$	$\pm i3.622$

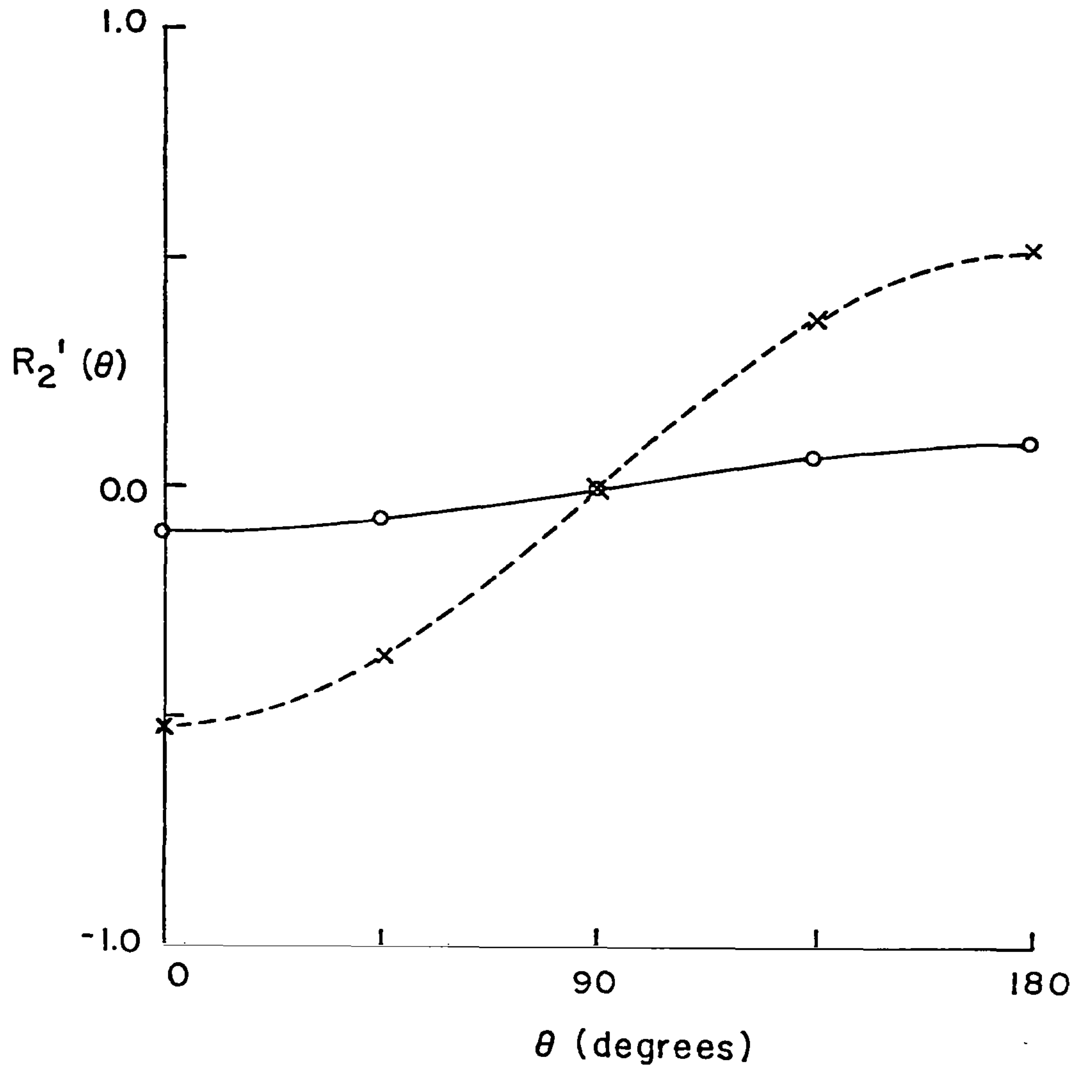

Fig. 3.5: Real (——) and imaginary (- - -) parts of the residue, $R_2'(\theta)$, of the first pole of the first layer and the extracted real (O O) and imaginary (X X) parts.

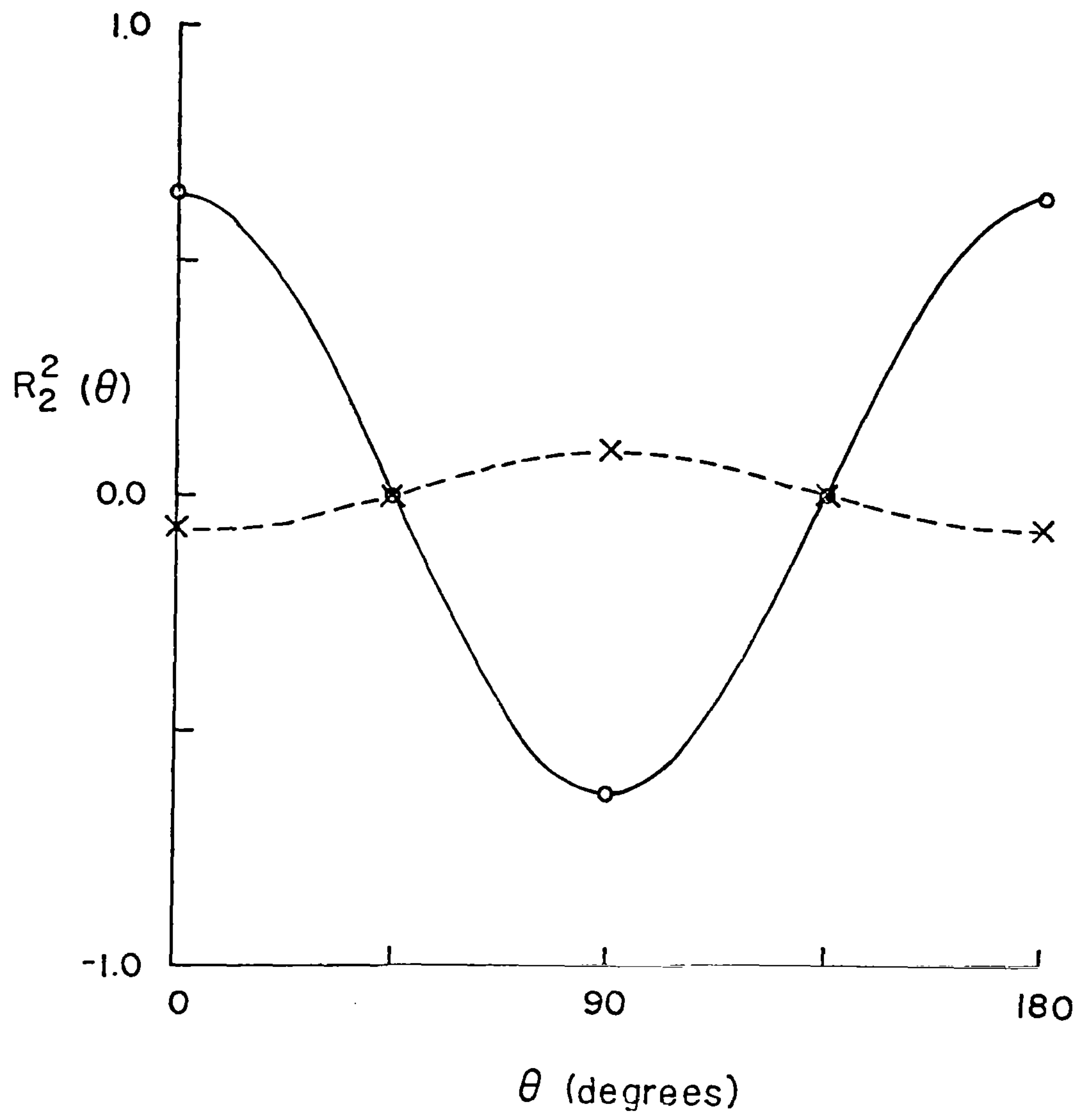

Fig. 3.6: Real (——) and imaginary (- - -) parts of the residue, $R_2^2(\theta)$, of the second pole of the first layer and the extracted real (O O) and imaginary (X X) parts.

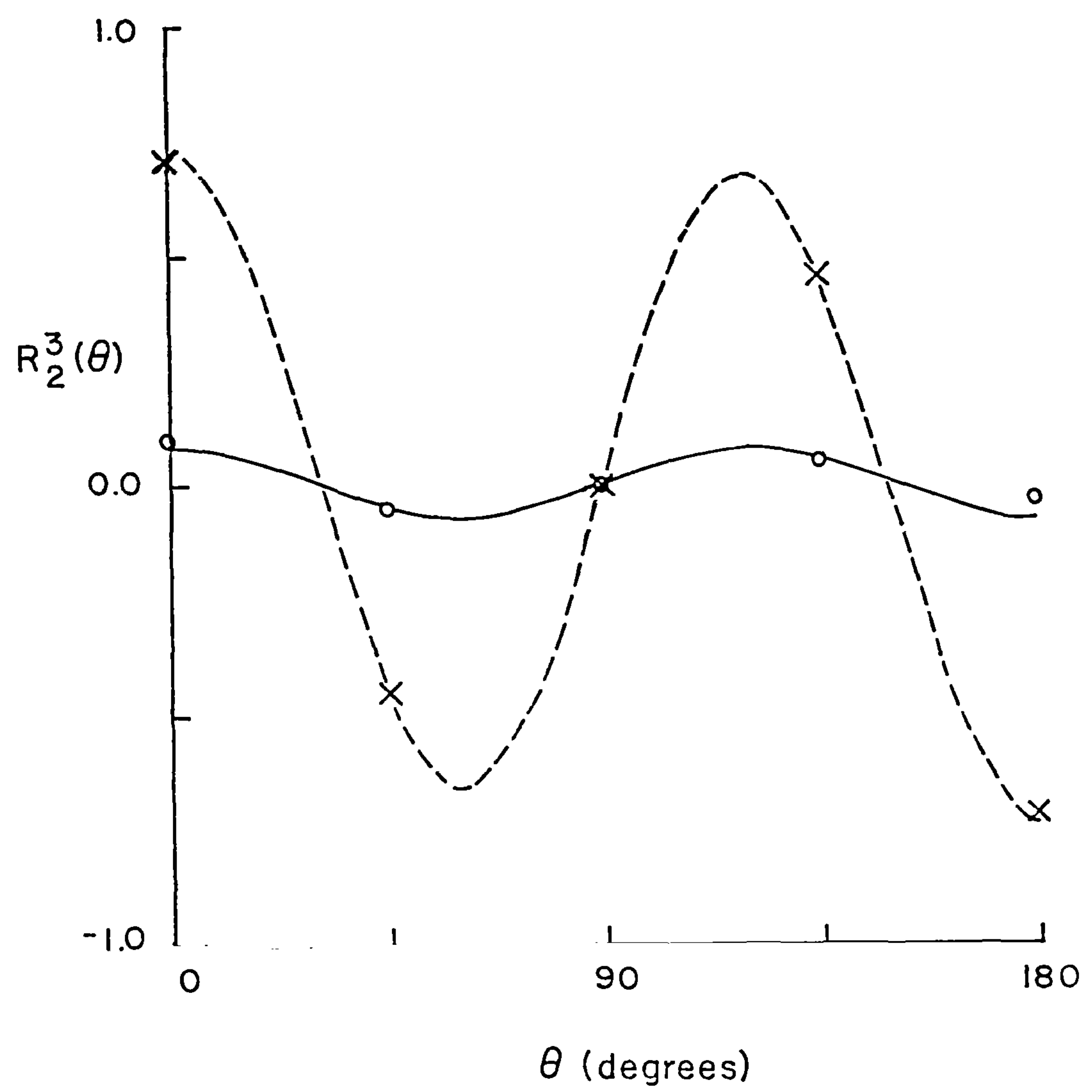

Fig. 3.7: Real (——) and imaginary (- - -) parts of the residue, $R_2^3(\theta)$, of the third pole of the first layer and the extracted real (○ ○) and imaginary (× ×) parts.

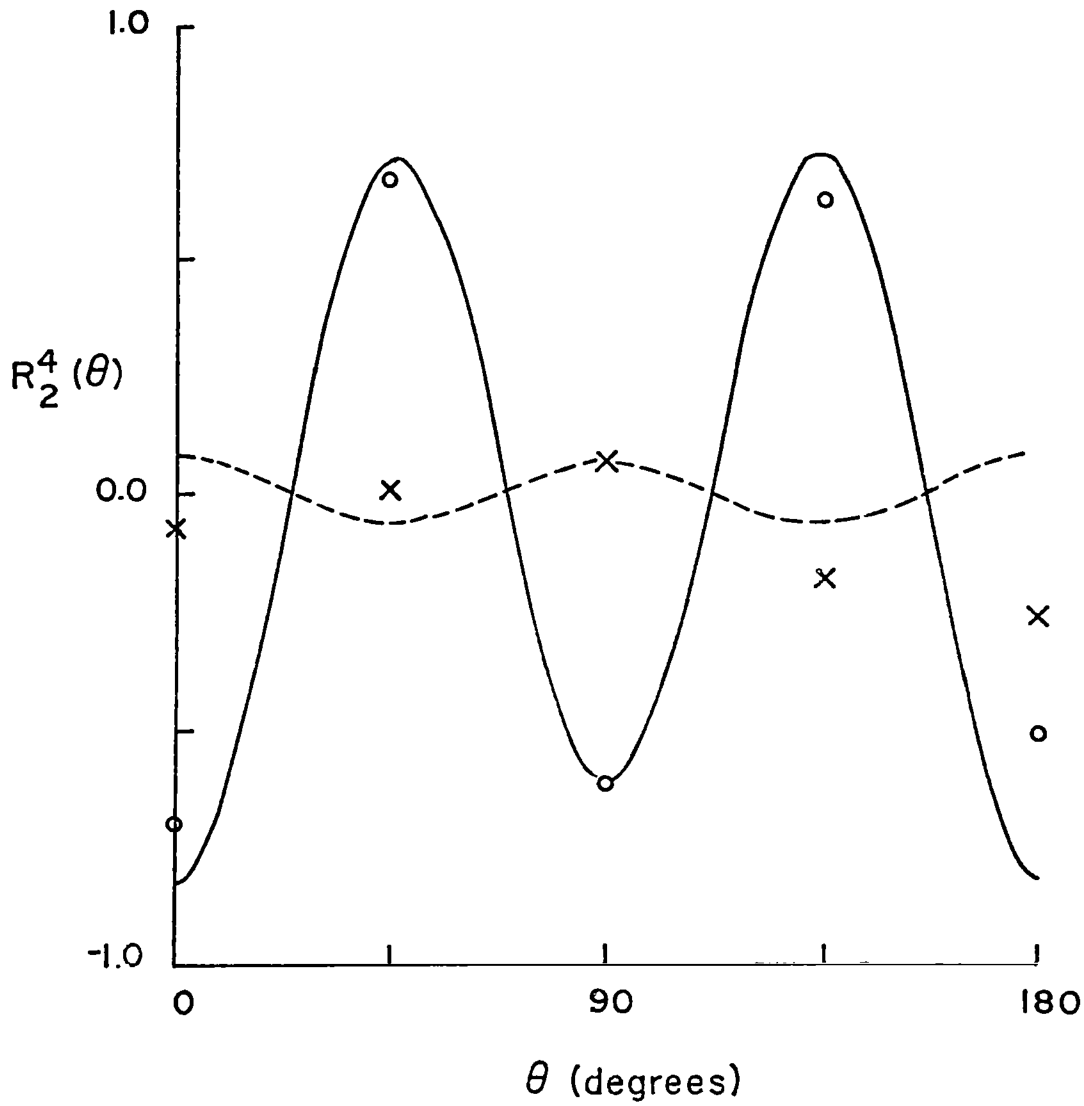

Fig. 3.8: Real (——) and imaginary (- - -) parts of the residue, $R_2^4(\theta)$, of the fourth pole of the first layer and the extracted real (○ ○) and imaginary (× ×) parts.

Table 3.6: Comparison of exact and extracted pole locations for $\theta = 0$, and $\omega a/c = 0.2(0.1)6.0$

Exact	Extracted		
	M = 15, N = 16	M = 17, N = 18	M = 19, N = 20
-0.500000	-0.5020	-0.5007	-0.5008
±i0.866025	±i0.8643	±i0.8637	±i0.8638
-0.701964	-0.6935	-0.6986	-0.6980
±i1.80740	±i1.812	±i1.810	±i1.809
-0.842862	-0.8252	-0.8370	-0.8369
±i2.75786	±i2.742	±i2.753	±i2.751
-0.954230	-0.9472	-0.9532	-0.9567
±i3.71478	±i3.649	±i3.697	±i3.693
-1.04764	-1.061	-1.073	-1.090
±i4.67641	±i4.464	±i.4.622	±i4.619
-1.12891	-0.9781	-1.161	-0.8810
±i5.64163	±i5.183	±i5.372	±i6.046

Table 3.7: Comparison of exact and extracted pole locations for $\theta = 0$, and $\omega a/c = 2.0(0.1)6.0$

Exact	Extracted		
	M = 15, N = 16	M = 17, N = 18	M = 19, N = 20
-0.500000 $\pm$i0.866025	not located	not located	not located
-0.701964 $\pm$i1.80740	-0.6365 $\pm$i1.802	-0.7005 $\pm$i1.730	-0.6025 $\pm$i1.816
-0.842862 $\pm$i2.75786	-0.8449 $\pm$i2.746	-0.8558 $\pm$i2.765	-0.8536 $\pm$i2.730
-0.954230 $\pm$i3.71478	-0.9582 $\pm$i3.714	-0.9422 $\pm$i3.728	-0.9787 $\pm$i3.738
-1.04764 $\pm$i4.67641	-1.041 $\pm$i4.656	-1.011 $\pm$i4.658	-1.011 $\pm$i4.728
-1.12891 $\pm$i5.64163	-1.079 $\pm$i5.467	-1.054 $\pm$i5.497	-0.9399 $\pm$i5.658

not picked up at all, and the second is considerably in error. This is hardly surprising since the first two poles are no longer spanned by the data.

As a result of the above investigation, the following conclusions can be drawn. In the first place, the data should fully span the imaginary parts of the poles to be located. If n SEM poles are spanned, N should be in the range 3n to 4n with M = N-1, but N should not exceed (about) 25 to avoid numerical difficulties. This upper limit decreases with increasing max $\omega a/c$ and is almost certainly machine dependent as well. For a greater span of data and/or to extract more than a handful of SEM poles, it may be necessary to process the data in batches (perhaps overlapping), i.e., use windowing.

3.4 Effect of Noise

In most practical applications of the pole extraction method, the data for the frequency response have been obtained by measurement or by the numerical solution of a less than perfect model of the scatterer. Inevitably such data are subject to noise and other uncertainties, and it is important to see how the accuracy of both the curve fit and the SEM pole extraction are affected. For this purpose, two types of noise were considered: numerical inaccuracies in the form of data limited to k decimal places, and added Gaussian white noise of various amplitudes.

For the first study, the real and imaginary parts of $T_2(0)$ which were originally accurate to six decimal places were rounded to k decimals with k progressively reduced. The data used spanned $0.2 \leq \omega a/c \leq 4.0$ in increments of 0.1 and 0.02, and since a rational function with M = 15 and N = 16 had proved to be effective in the absence of noise (i.e., when k = 6), this function was chosen. For $\Delta\omega a/c = 0.1$ and 0.02 the curve fits were equally good; but because the accuracy of the extracted poles was slightly better for the closer sampling, we used this in all of the noise studies.

As k was reduced down to 1, the extracted poles became increasingly inaccurate as shown in Table 3.8, and for k = 2 even the dominant pole was substantially in error. In spite of this, the curve fit remained good. Figure 3.9 shows the loci of the extracted poles as functions of k. As k decreases, each pole moves closer to the imaginary s axis, and the general behavior is similar to that found when fitting the exact data with rational functions of progressively lower order. This suggests that by increasing M and N we might be able to overcome some of the noise effects and thereby improve the accuracy of the extracted poles. Because of the numerical difficulties referred to earlier, the largest N that could easily be handled was 24, and the results of using M = 23 and N = 24 with data having k = 3 and 2 are presented in Table 3.9. The increased order of polynomials produces only a slight improvement, primarily for the data with k = 2.

In the second study Gaussian distributed white noise was added to the exact data for the real and imaginary parts of $T_2(0)$, $\omega a/c$ = 0.2(0.02)4.0. The noise was produced by a random number generator for which the mean and standard deviation could be specified. In all cases the mean was chosen to be zero and the standard deviation varied to change the noise level. For noise with standard deviations 10^{-5} and 10^{-4}, the values of E_{fit} and the pole locations provided by a

Table 3.8: Comparison of exact and extracted poles for $\theta = 0$, $\omega a/c = 0.2(0.02)4.0$, $M = 15$ and $N = 16$, with data sets rounded to k decimal places

Exact	Extracted				
	$k = 6$	$k = 4$	$k = 3$	$k = 2$	$k = 1$
-0.500000 $\pm i0.866025$	-0.5000 $\pm i0.8658$	-0.5011 $\pm i0.8639$	-0.5140 $\pm i0.8577$	-0.4081 $\pm i0.8369$	-0.3764 $\pm i0.9174$
-0.701964 $\pm i1.80740$	-0.7025 $\pm i1.806$	-0.6957 $\pm i1.811$	-0.7005 $\pm i1.861$	-0.4924 $\pm i1.643$	-0.2961 $\pm i1.939$
-0.842862 $\pm i2.75786$	-0.8399 $\pm i2.760$	-0.8323 $\pm i2.732$	-0.7548 $\pm i2.842$	-0.4727 $\pm i2.516$	-0.1581 $\pm i2.964$
-0.954230 $\pm i3.71478$	-0.9439 $\pm i3.678$	-0.9614 $\pm i3.517$	-0.6875 $\pm i3.784$	-0.3981 $\pm i3.924$	-0.04094 $\pm i3.257$
E_{fit}	$<0.25 \times 10^{-7}$	0.27×10^{-1}	0.27×10^{-1}	0.27×10^{-1}	0.31×10^{-1}

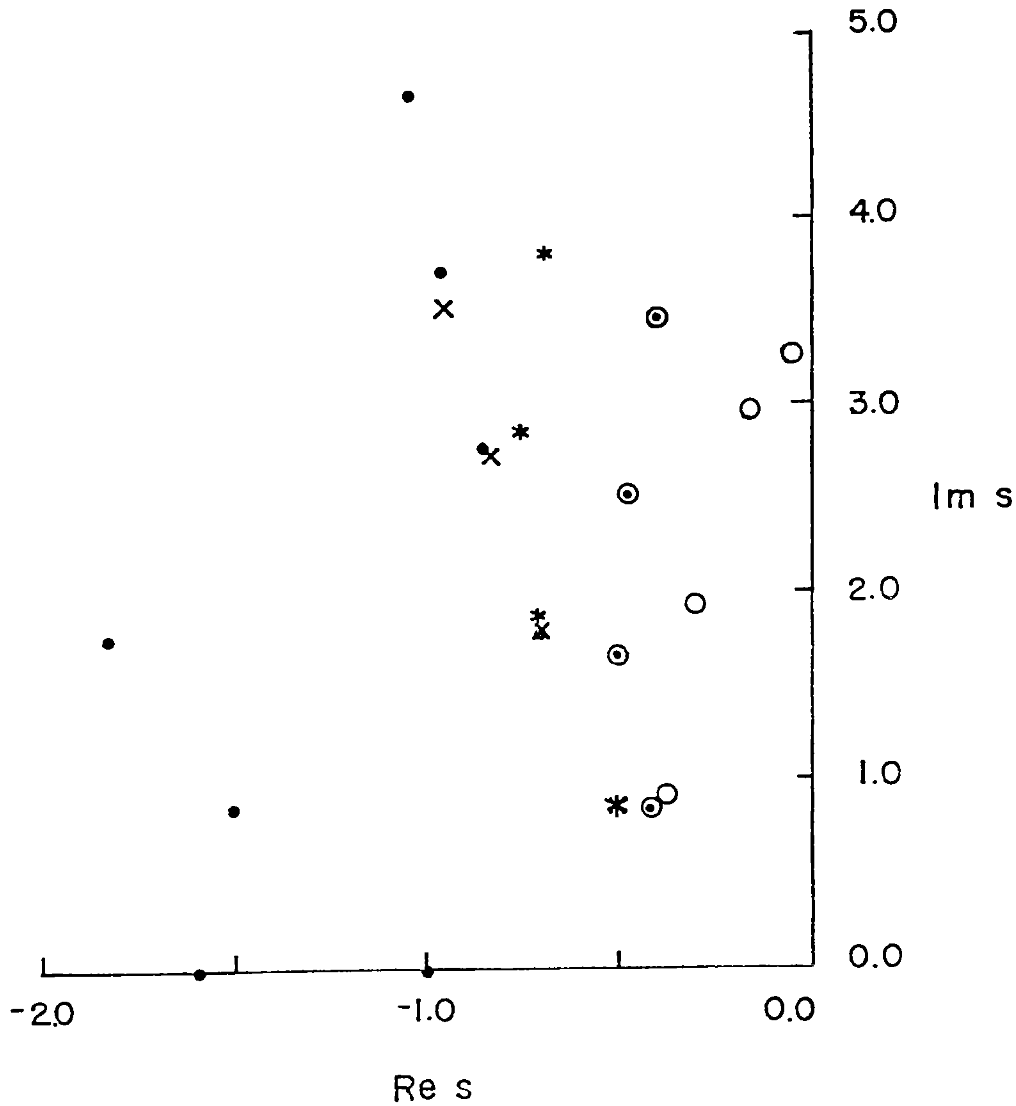

Fig. 3.9: Comparison of exact (• •) and extracted poles for $\theta = 0$, $\omega a/c = 0.2(0.1)4.0$, M = 15 and N = 16 with data rounded to k = 1 (○ ○), k = 2 (⊙ ⊙), k = 3 (✱ ✱), and k = 4 (× ×) decimal places.

Table 3.9: Comparison of exact and extracted pole locations for $\theta = 0$, and $\omega a/c = 0.2(0.02)4.0$ for various decimal places k of data accuracy

Exact	Extracted			
	$k = 3$		$k = 2$	
	$M = 15, N = 16$	$M = 23, N = 24$	$M = 15, N = 16$	$M = 23, N = 24$
-0.500000 $\pm i0.866025$	-0.5140 $\pm i0.8577$	-0.5054 $\pm i0.8648$	-0.4081 $\pm i0.8369$	-0.4824 $\pm i0.8051$
-0.701964 $\pm i1.80740$	-0.7005 $\pm i1.861$	-0.6873 $\pm i1.827$	-0.4924 $\pm i1.643$	-0.6564 $\pm i1.676$
-0.842862 $\pm i2.75786$	-0.7548 $\pm i2.842$	-0.7488 $\pm i2.753$	-0.4727 $\pm i2.516$	-0.6578 $\pm i2.643$
-0.954230 $\pm i3.71478$	-0.6875 $\pm i3.784$	-0.6607 $\pm i3.670$	-0.3981 $\pm i3.924$	-0.5721 $\pm i3.620$
E_{fit}	0.27×10^{-1}	0.27×10^{-1}	0.27×10^{-1}	0.27×10^{-1}

rational function having $M = 15$ and $N = 16$ are listed in Table 3.10; and even in the former case, the extracted poles differ substantially from the exact ones. Figure 3.10 shows the curve fit to the magnitudes of the noisy data for the standard deviation 10^{-4}.

As a final test the curve fitting and pole extraction algorithm was applied to measured data for the field component T_2 at the front ($\theta = 0$) of a metallic sphere 6 inches in diameter. The data were obtained in an anechoic chamber over the frequency range 0.118 to 4.4 GHz, corresponding to $0.2 \leq \omega a/c \leq 7.0$, but only the data for $0.2 \leq \omega a/c \leq 4.0$ were used. Since prior studies using measured data for the fields at the surface of a thick cylinder had shown that filtering could remove some of the experimental noise, the measured data were also processed using a seventh order digital filter. For both the unfiltered and filtered data, the results of pole extraction with a rational function having $M = 15$ and $N = 16$ are given in Table 3.11, and are comparable to those in Table 3.10 for Gaussian noise with standard deviations 10^{-4} and 10^{-5} respectively. Although filtering gives some slight improvement in the accuracy with which the second, third and fourth poles are located, it does so at the expense of a decrease in the accuracy of the first pole. Figure 3.11 shows the curve fit to the magnitudes of the experimental data.

As a result of these studies it appears unlikely that the curve fitting and pole extraction algorithm can accurately locate more than (at most) the first (dominant) SEM pole using measured data for the frequency response.

Table 3.10: Comparison of exact and extracted pole locations for $\theta = 0$, $\omega a/c = 0.2(0.02)4.0$, $M = 15$ and $N = 16$ for different levels of Gaussian distributed white noise

Exact	Extracted	
	std. dev. = 10^{-5}	std. dev. = 10^{-4}
-0.500000 $\pm i0.866025$	-0.4492 $\pm i0.8313$	-0.3907 $\pm i0.9026$
-0.701964 $\pm i1.80740$	-0.6022 $\pm i1.700$	-0.4235 $\pm i1.855$
-0.842862 $\pm i2.75786$	-0.5819 $\pm i2.625$	-0.3092 $\pm i2.849$
-0.954230 $\pm i3.71478$	-0.4773 $\pm i3.582$	-0.06515 $\pm i3.436$
E_{fit}	0.27×10^{-4}	0.38×10^{-3}

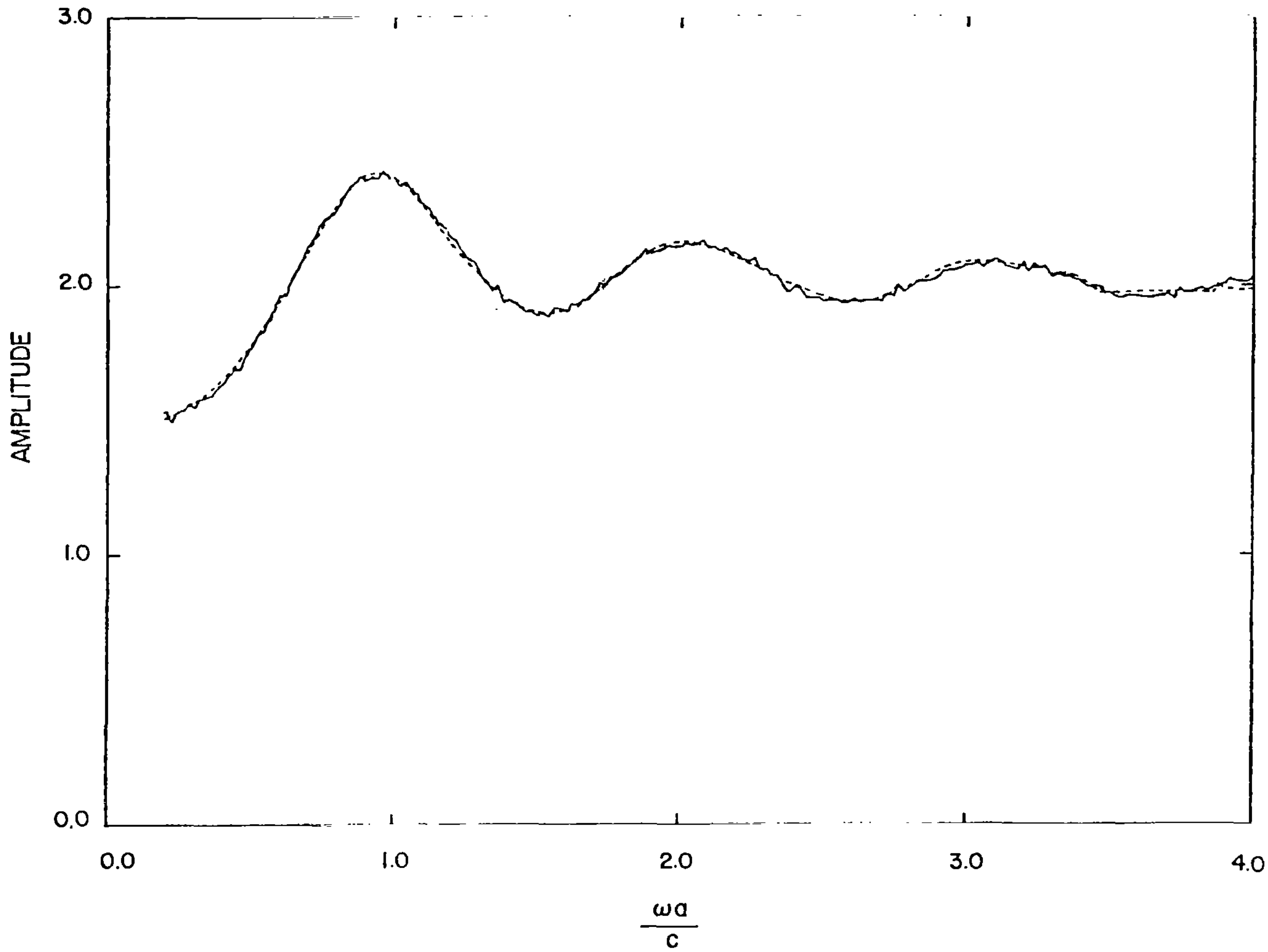

Fig. 3.10: Comparison of $T_2(0)$ with additive noise level of std. dev. = 10^{-4} (——) and the curve fit (----) obtained with $\omega a/c$ = 0.2(0.02)4.0, M = 15 and N = 16.

Table 3.11: Comparison of exact and extracted pole locations for measured data at $\theta = 0$ with $0.2 \leq \omega a/c \leq 4.0$, $M = 15$ and $N = 16$

Exact	Extracted	
	Experimental	Filtered Experimental
-0.500000 $\pm i0.866025$	-0.3920 $\pm i0.8575$	-0.3709 $\pm i0.8014$
-0.701964 $\pm i1.80740$	-0.3530 $\pm i1.927$	-0.4101 $\pm i1.872$
-0.842862 $\pm i2.75786$	-0.2764 $\pm i3.066$	-0.4258 $\pm i2.662$
-0.954230 $\pm i3.71478$	not located	-0.3332 $\pm i3.764$
E_{fit}	0.77×10^{-1}	0.78×10^{-1}

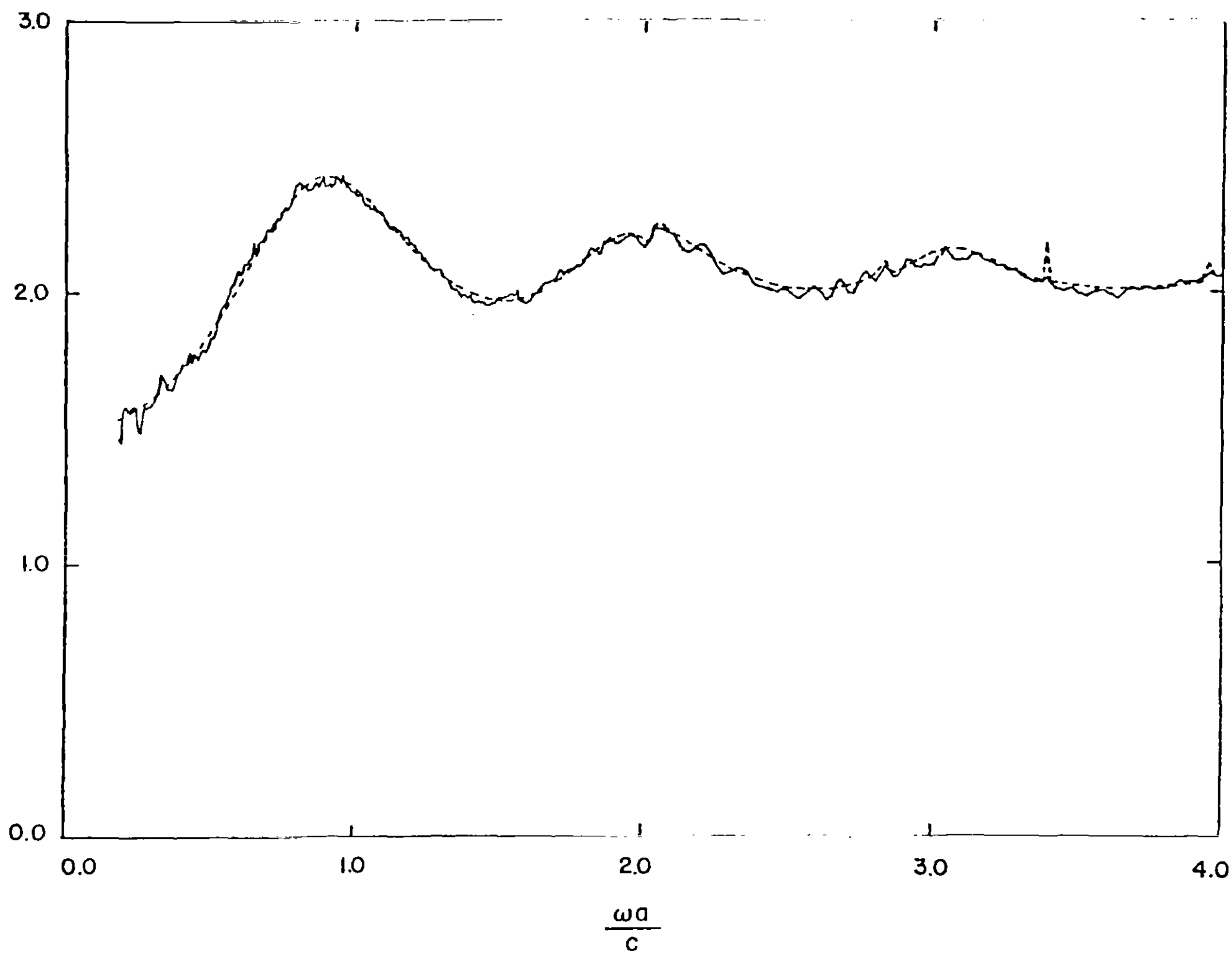

Fig. 3.11: Comparison of experimental data at $\theta = 0$ (——) and the curve fit (- - - -) obtained with $0.2 \leq \omega a/c \leq 4.0$, $M = 15$ and $N = 16$.

3.5 Conclusions

Using rational functions a curve fitting and pole extraction algorithm has been developed and applied to exact frequency domain data for the surface fields on a sphere. The data are fitted extremely closely and for at least a handful of the lowest order SEM poles, the extracted poles and their residues are in good agreement with their known values. It is possible that the method could be further refined to yield a few more poles, but the performance is already close to the limits of the computer. Overall, the success is comparable to that achieved by Brittingham et al.(1980) using a frequency domain Prony's method.

Unfortunately, the situation is very different if the frequency response is noisy or degraded in accuracy in a manner typical of measured data. Although the curve fit is still good, even a small amount of noise is sufficient to produce considerable discrepancies between the extracted and true (SEM) poles; and for noise levels characteristic of the best experimental data, it is impossible to locate more than (at most) the dominant SEM pole to any degree of accuracy.

CHAPTER 4: APPLICATION TO MEASURED SURFACE FIELDS ON A B-52G

The ultimate objective of the project was to determine the poles for a B-52G aircraft using data for the surface fields measured on a small scale model, and then deduce the dependence of the residues on the excitation, i.e., polarization and angle of illumination. Because it was expected that the noise levels in the data would be similar to those which precluded the extraction of all pole pairs other than the dominant one for a sphere (Chapter 3) and a circular cylinder (Appendix A), it seemed unlikely that the project would be successful unless the more resonant character of the aircraft response were to have a drastic effect.

Currents and charges were measured at several locations on a 1:100 scale model of the aircraft, and we present data for one component of the current at each of two locations. The measurement procedures and the manner in which the test points are defined are described in a report by Liepa (1980). The first point, W667T(R), was on the top of the right wing on the bisector of the leading and trailing edges approximately half way along, i.e., at midwing, and the second, F562T, was on the top of the fuselage between the wings. The currents flowing along the bisector and across, i.e., transverse to, the fuselage were measured using a surface-mounted probe. At the first location the major current paths are from wing tip to wing tip, from the wing tip to the fuselage tail, and from the wing tip to the aircraft's nose, whereas on the fuselage only the first of these paths is expected to be significant. Because of the symmetry of the fuselage location, only the odd order modes can be detected.

Data were recorded for seven different roll angles θ about the axis of the fuselage, where $\theta = 90°$ corresponds to topside illumination with the incident plane wave having the electric vector transverse to the fuselage. Each recording consisted of 437 data points spanning the frequency range 0.118 to 4.4 GHz. The radius L of the minimum circumscribing sphere for the model was determined to be 0.284 m, and for purposes of analysis and presentation of the data the frequencies were subsequently normalized to this value.

At the midwing location the major current paths are from one wing tip to the other, from the wing tip to the tail of the fuselage, and from the wing tip to the nose. At the fuselage location, it seems probable that the first current path will be dominant. When $\theta = 0$ or 180° the currents are only minimally excited, and at $\theta = 90°$ symmetry indicates that only odd order modes can exist. It therefore appears that the most general responses having the largest numbers of modes with signficant excitations are those measured at the midway location for $\theta = 30, 60, 120$ and 150°, and our initial attention was directed at these.

The more resonant features of the frequency responses occur for $f < 1.0$ GHz. We therefore concentrated on the frequency range $0.118 \leq f \leq 1.0$ GHz; and since there was no a priori knowledge of the number of poles in this range, it was first necessary to choose the polynomial orders M and N in the Sharpe-Roussi program for the best fit to the data. After some exploration it was found that $M = N-1 = 23$ was optimum, and Fig. 4.1 illustrates the resulting fit to the data. For the midwing response with $\theta = 0(30)180°$, the locations of the extracted poles in the third quadrant of the complex s plane are shown in Fig. 4.2. The poles have no clear subsets which are positionally (i.e., θ) invariant, and though there are several groupings which are suggestive of approximations to true poles, the spread (or wandering) is too great for any meaningful analysis of their residues.

One simplification is to eliminate those poles which do not contribute significantly; but because of the wandering, it is not sufficient to do so based on the residues alone. The contribution of a pole is primarily determined by $|A_m|/\mathrm{Re}\ s_m$ where s_m and A_m are the computed pole location and residue respectively. For each θ the maximum value of this ratio was obtained and only those poles having factors greater than 10 percent of this were deemed to contribute significantly to the response. Their locations in the complex s plane are shown in Fig. 4.3. The groupings which were previously regarded as approximations to true poles are now more evident, and are still further enhanced when we eliminate the poles associated with the responses for $\theta = 0$ and $180°$ for which the currents are only minimally excited (see Fig. 4.4). The two pole groups at $\omega L/\pi c \simeq 0.4$ are consistent with the first order wing tip to fuselage tail and wing tip to wing tip modes. The pole group at $\omega L/\pi c \simeq 0.7$ is consistent with the dominant wing tip to nose mode where the current path crosses from wing to fuselage at the leading edge of the wing. The pole group at $\omega L/\pi c \simeq 0.97$ is consistent with a second order mode.

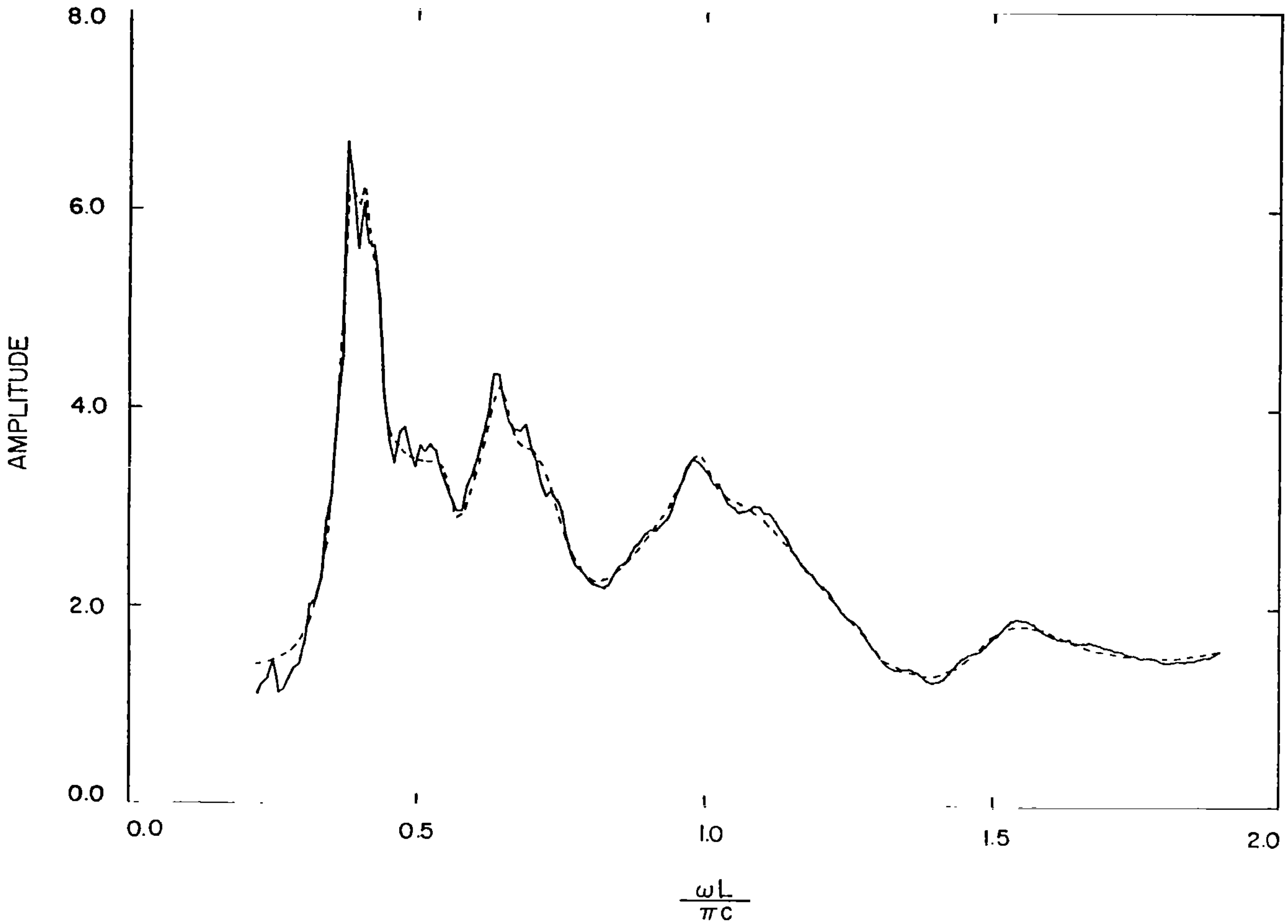

Fig. 4.1: Example of the fit (---) obtained with a rational function (M = 23, N = 24) to the measured surface currents (——) at midwing. This fit is for θ = 150°.

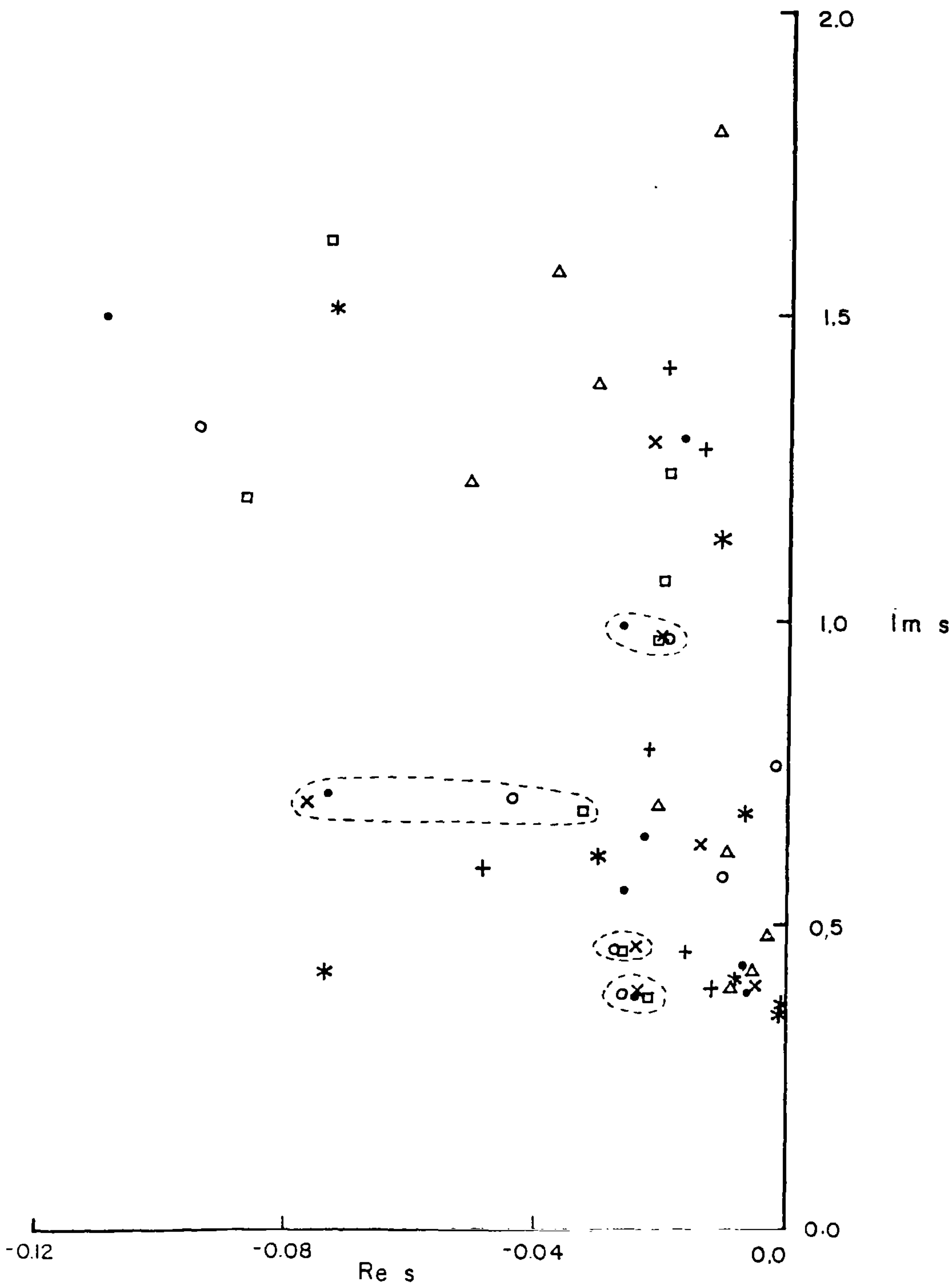

Fig. 4.2: Third quadrant poles of the rational functions (M = 23, N = 24) obtained by fiting the measured surface currents at midwing for θ = 0° (△), 30° (□), 60° (○), 90° (∗), 120° (×), 150° (•) and 180° (+).

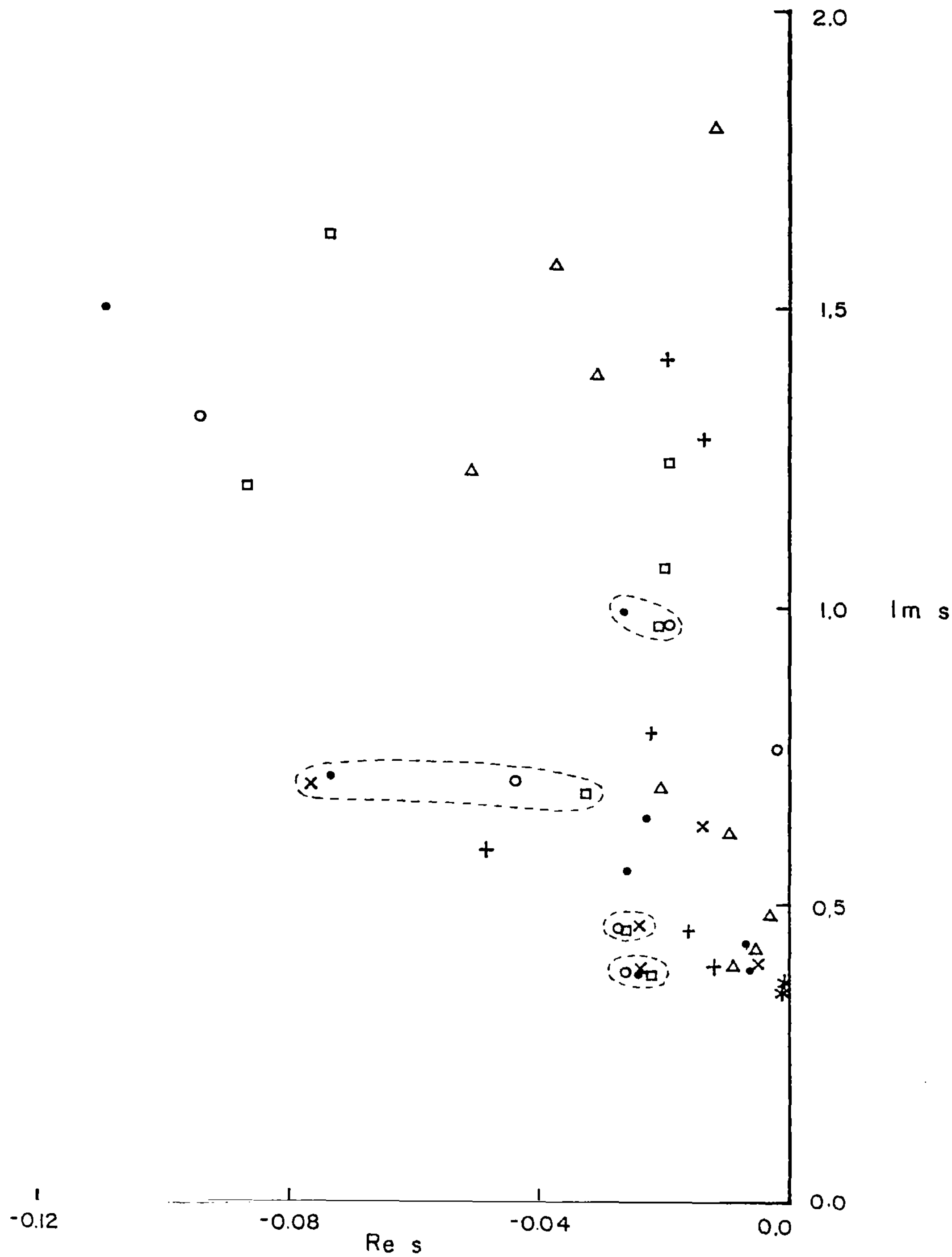

Fig. 4.3: Dominant third quadrant poles of the rational function (M = 23, N = 24) obtained by fitting the measured surface current at midwing for θ = 0° (Δ), 30° (□), 60° (○), 90° (*), 120° (×), 150° (•) and 180° (+).

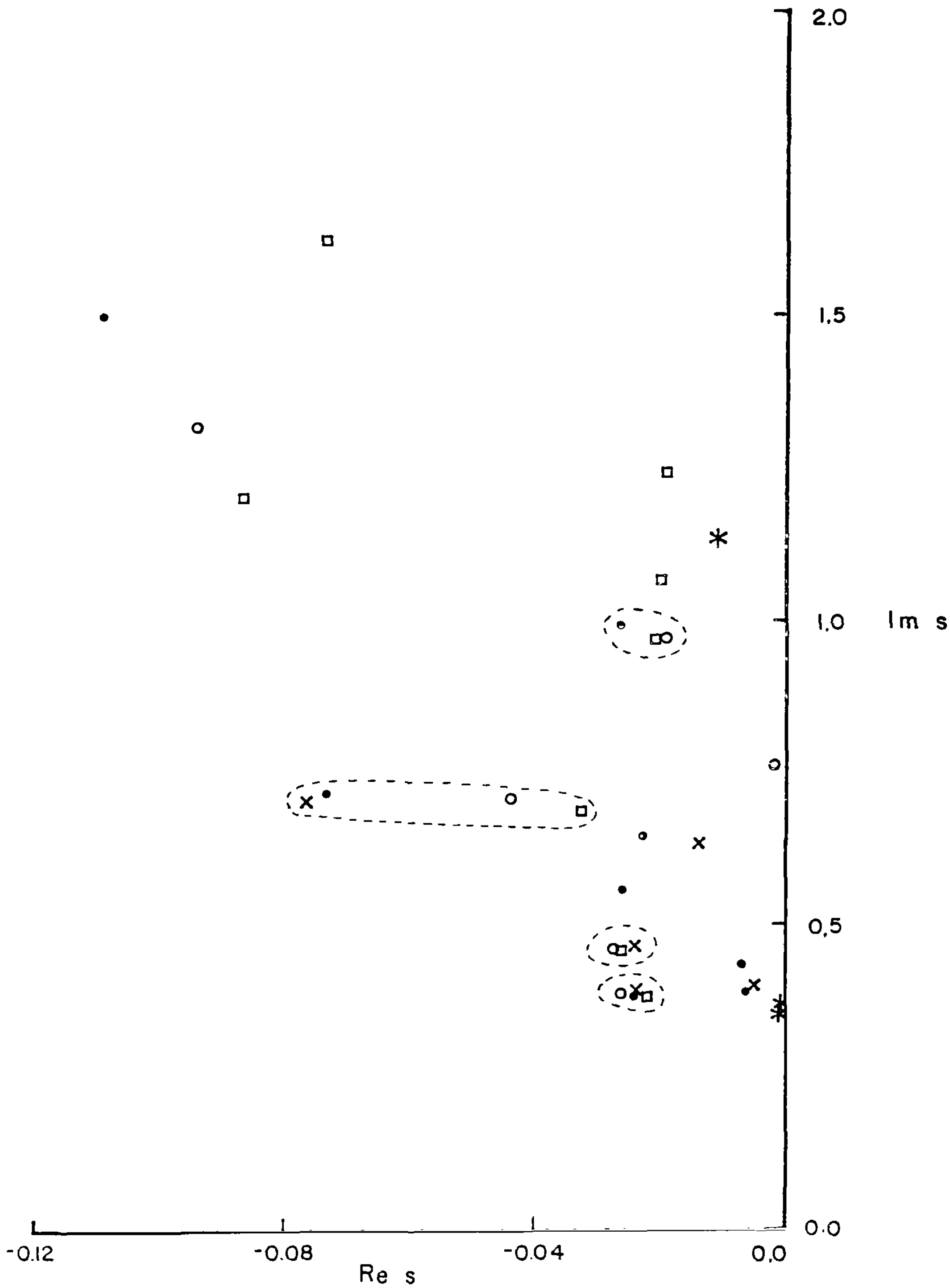

Fig. 4.4: Dominant third quadrant poles of the rational functions (M = 23, N = 24) obtained by fitting the measured surface currents at midwing (omitting those angles where the dominant modes are not excited) for θ = 30° (□), 60° (○), 90° (*), 120° (×) and 150° (•).

Several other procedures were tried in an attempt to concentrate the poles still further. Different combinations of M and N did not produce as good a fit to the measured data and the resulting poles were more spread out. This was true also when reduced ranges of frequency were used; and since digital filtering had produced, at best, only marginal improvements in the case of the sphere and cylinder, it was not felt to be appropriate for the B-52G data whose high frequency structure may not be entirely noise.

Similar analyses were also applied to the data measured on top of the fuselage at station F562T. It was found that the best fit was obtained with $M = N-1 = 19$, and Fig. 4.5 illustrates the type of fit that was achieved. Figure 4.6 shows the extracted poles in the third quadrant of the complex s plane for $\theta = 0(30)180°$ and we note that clustering is less evident than for the wing data. If we use the above-mentioned criterion to eliminate those poles which do not contribute significantly and, in addition, ignore the results for $\theta = 0$ and 180° for which there is minimal excitation, we are left with the poles shown in Fig. 4.7. There is no clear specification of any true poles and we have been unsuccessful in all attempts to localize the poles still further. Indeed, polynomials of other orders and/or reductions in the frequency range used increased the apparent randomness of the pole locations.

Because of our inability to accurately locate the SEM poles, it is impossible to give credence to the residues; and there is no point in pursuing further the dependence of the residues on the polarization and direction of the illumination, etc. The failure

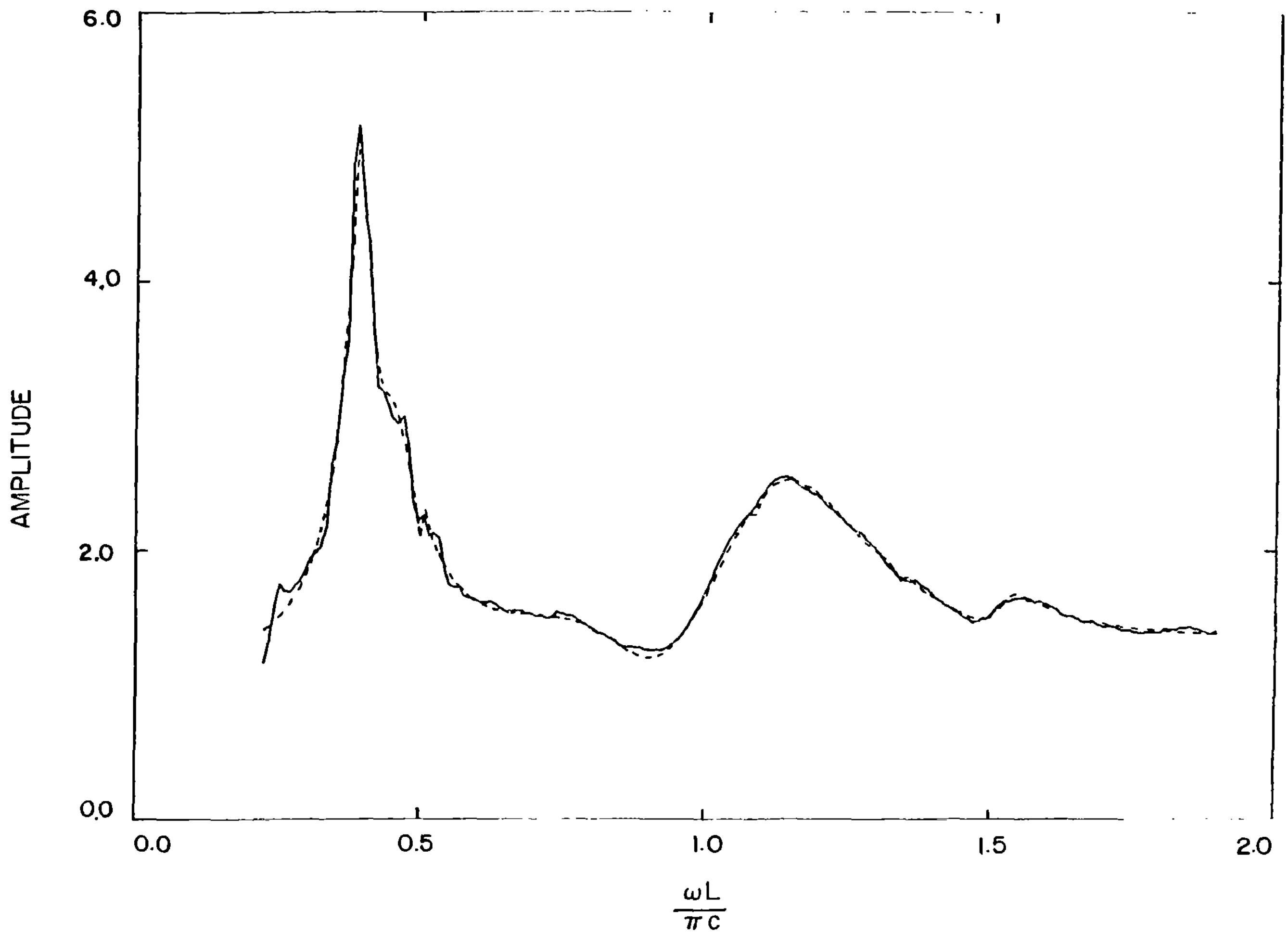

Fig. 4.5: Example of the fit (---) obtained with a rational function ($M = 19$, $N = 20$) to the measured surface currents (——) at the fuselage. This fit is for $\theta = 150°$.

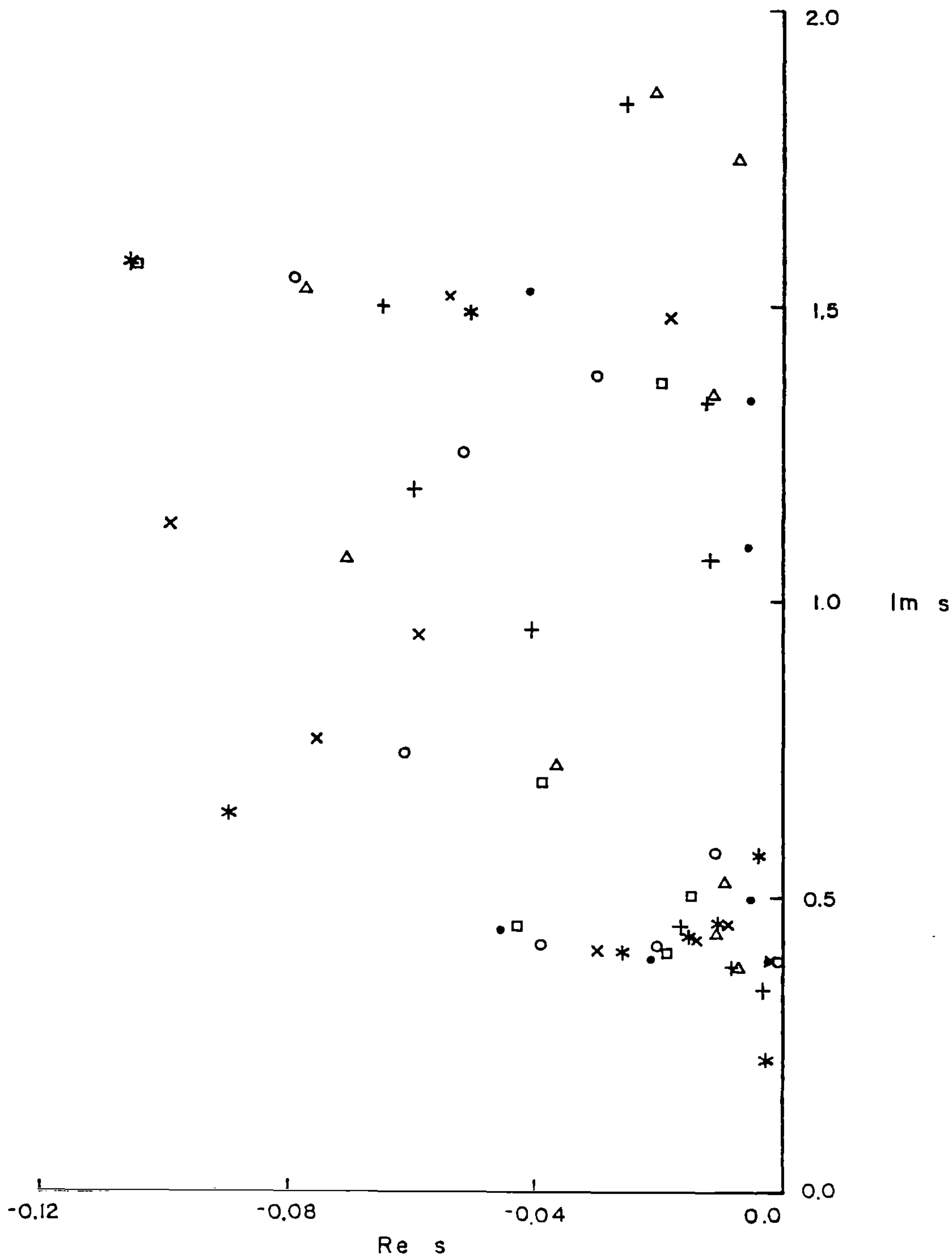

Fig. 4.6: Third quadrant poles of the rational functions (M = 19, N = 20) obtained by fitting the measured surface currents at the fuselage for θ = 0° (△), 30° (□), 60° (○), 90° (*), 120° (×), 150° (•) and 180° (+).

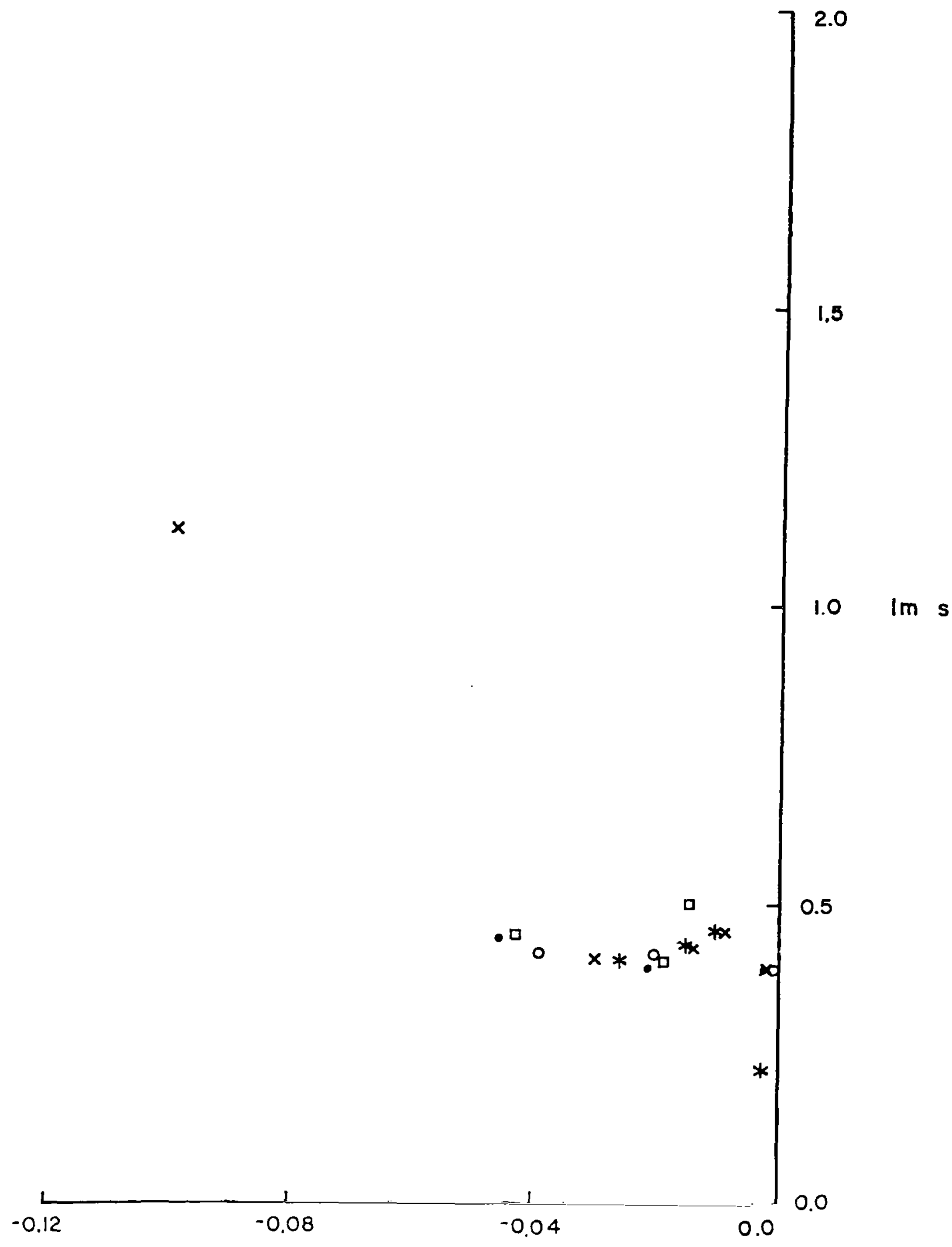

Fig. 4.7: Dominant third quadrant poles of the rational functions (M = 19, N = 20) obtained by fitting the measured surface currents at the fuselage (omitting those angles where the dominant modes are not excited) for θ = 30° (□), 60° (○), 90° (*), 120° (×) and 150° (•).

was not surprising in view of the results of our previous studies of sphere and cylinder data, and the effects of noise and other data degradations on the accuracy of pole extraction. This is in spite of the continued success of the Sharpe-Roussi program at curve fitting using a rational function--the task that it was actually designed to do. It is therefore unlikely that any other similar procedure would be more effective; but since this is always a possibility, it may be helpful to present the entire frequency responses that were measured at the midwing and fuselage stations. These are shown for all seven orientations of the aircraft in Figs. 4.8 through 4.21.

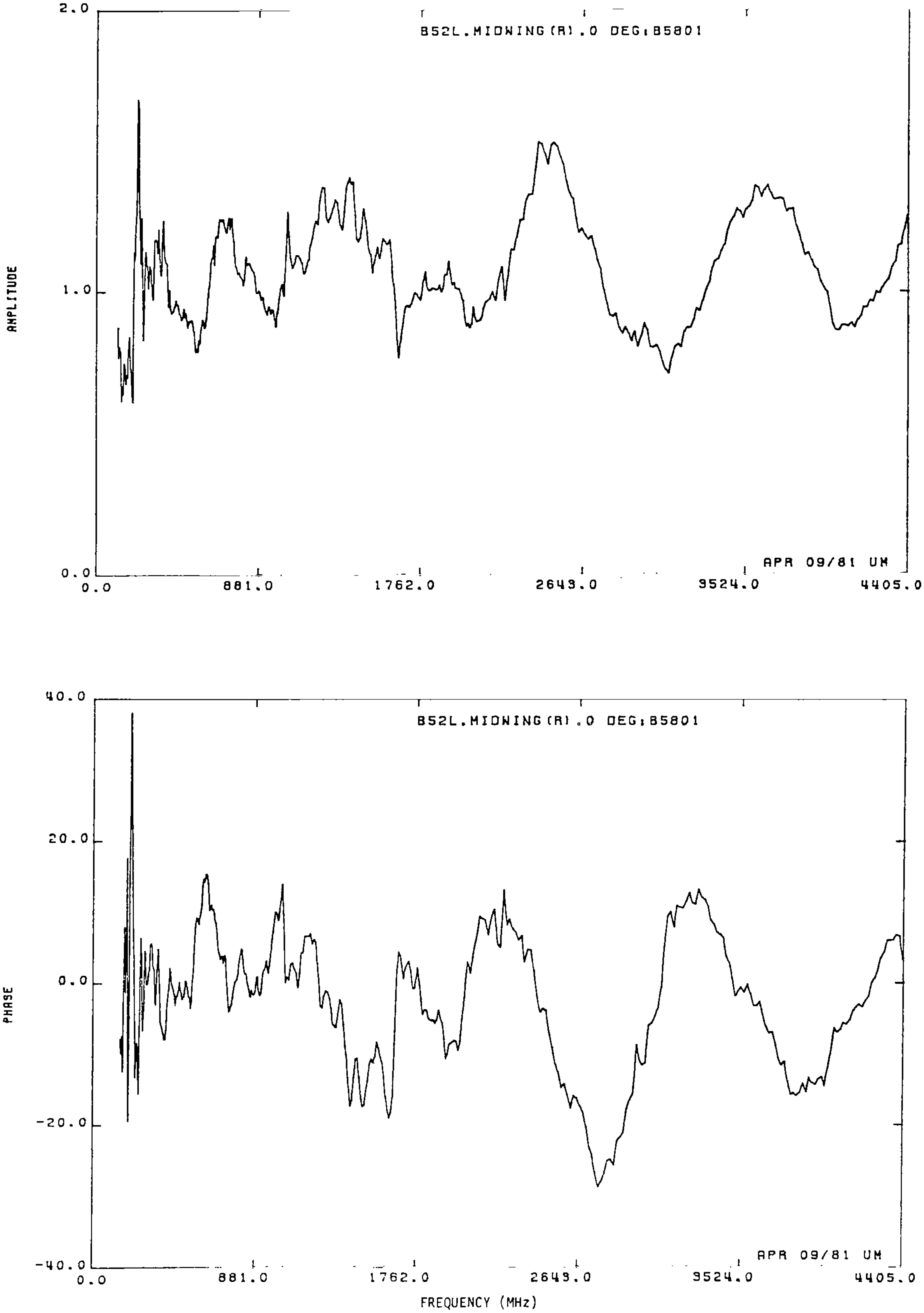

Fig. 4.8: Measured response of the surface current at midwing for $\theta = 0°$.

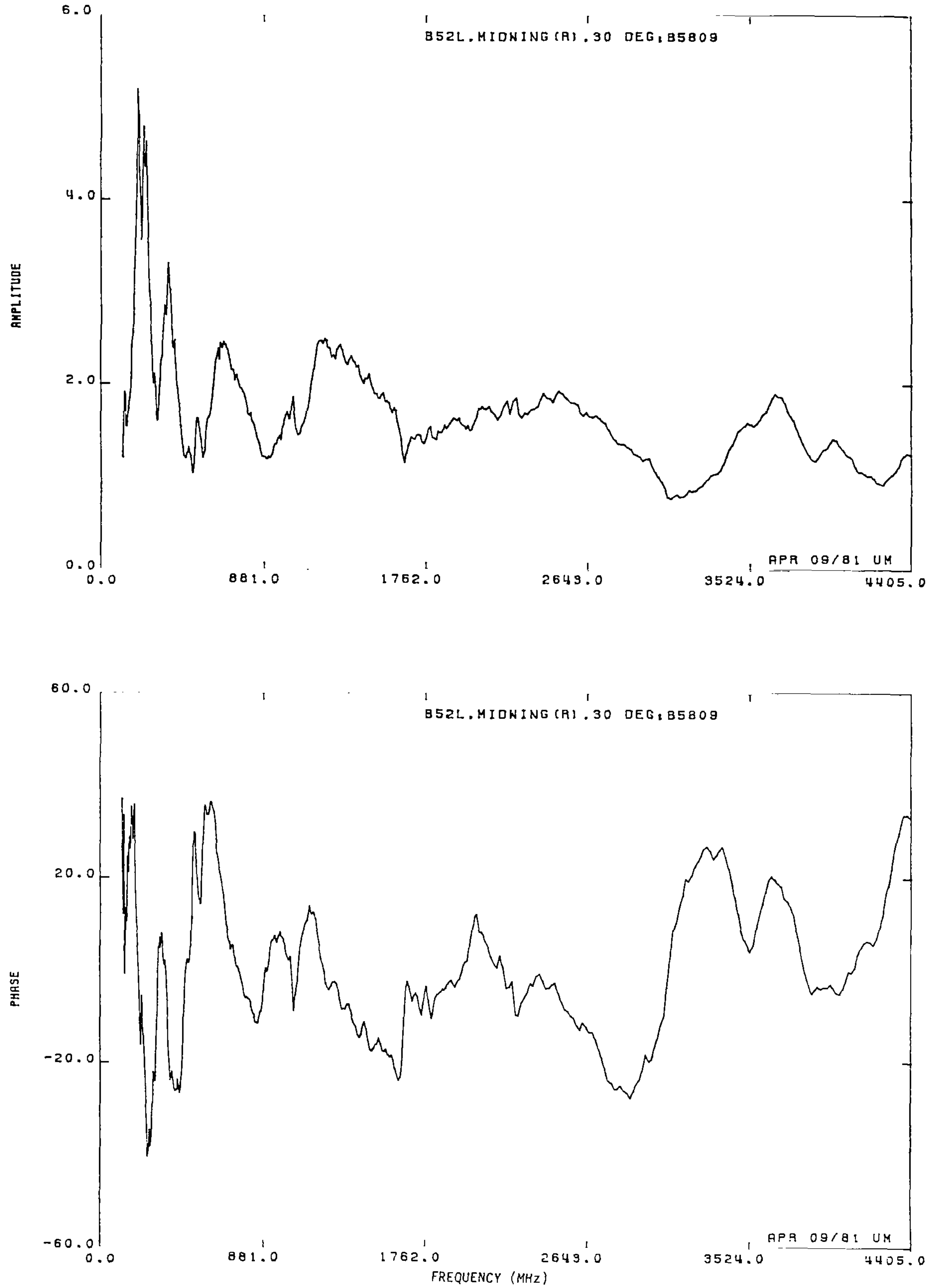

Fig. 4.9: Measured response of the surface current at midwing for $\theta = 30°$.

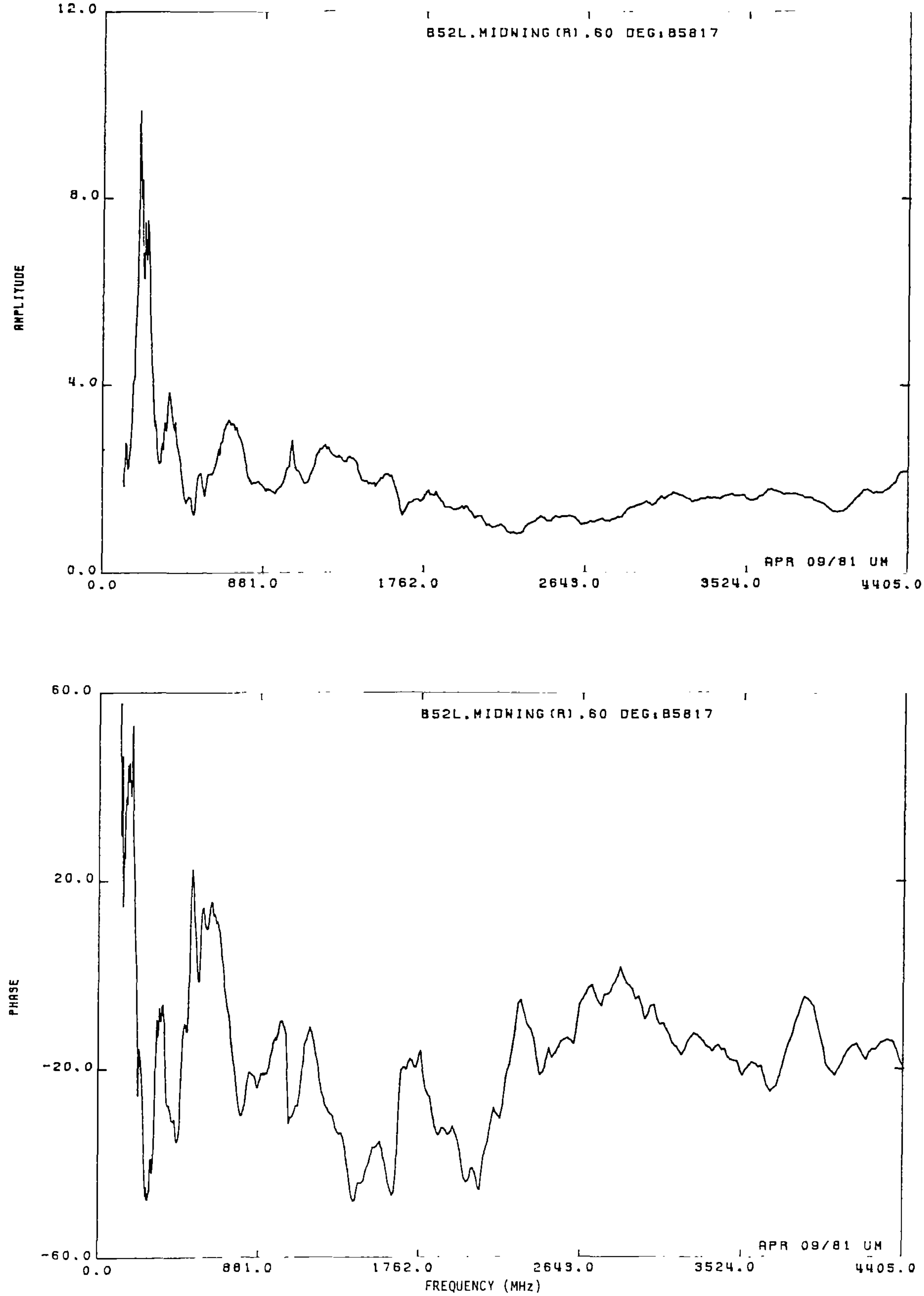

Fig. 4.10: Measured response of the surface current at midwing for $\theta = 60°$.

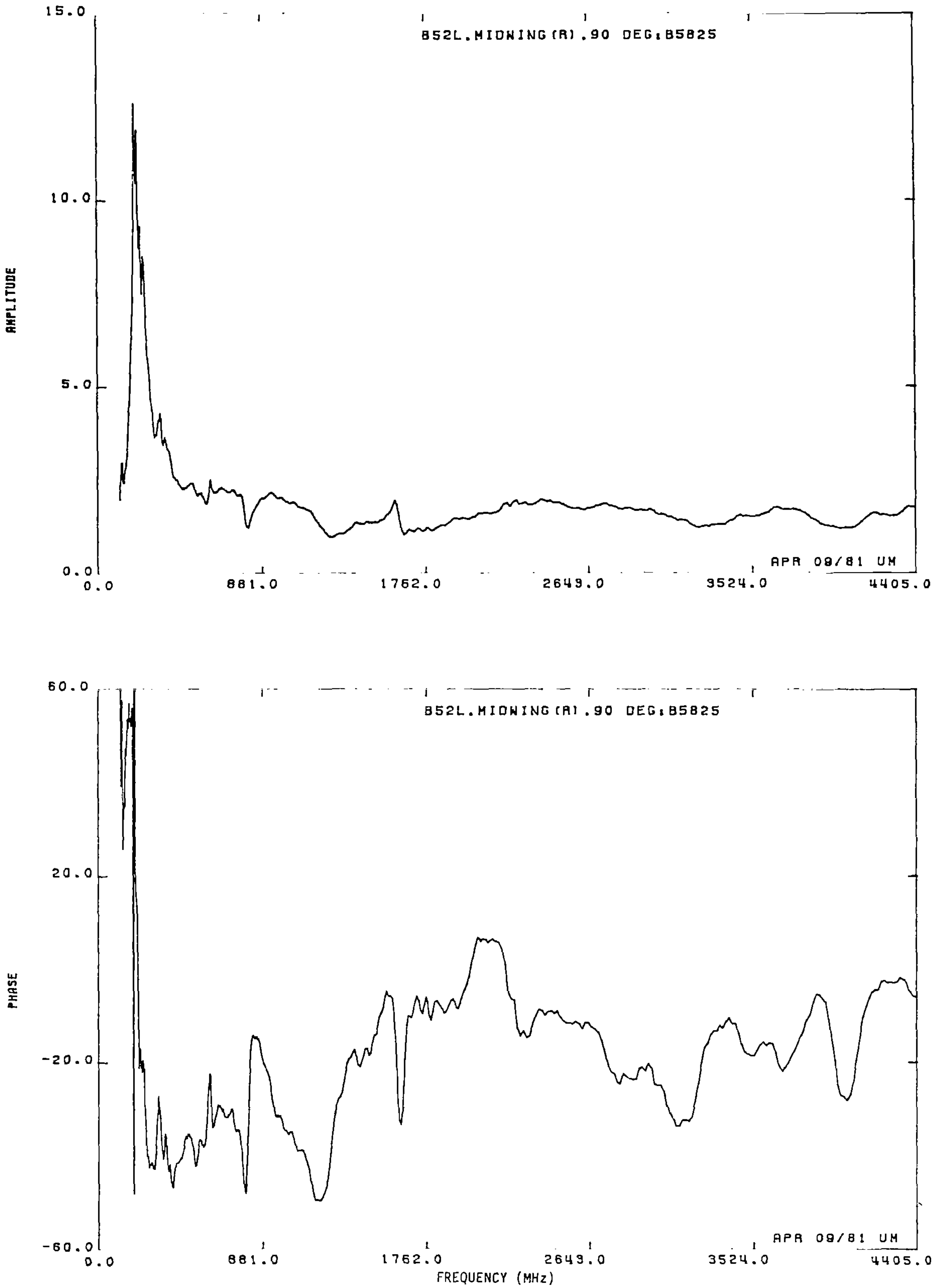

Fig. 4.11: Measured response of the surface current at midwing for $\theta = 90°$.

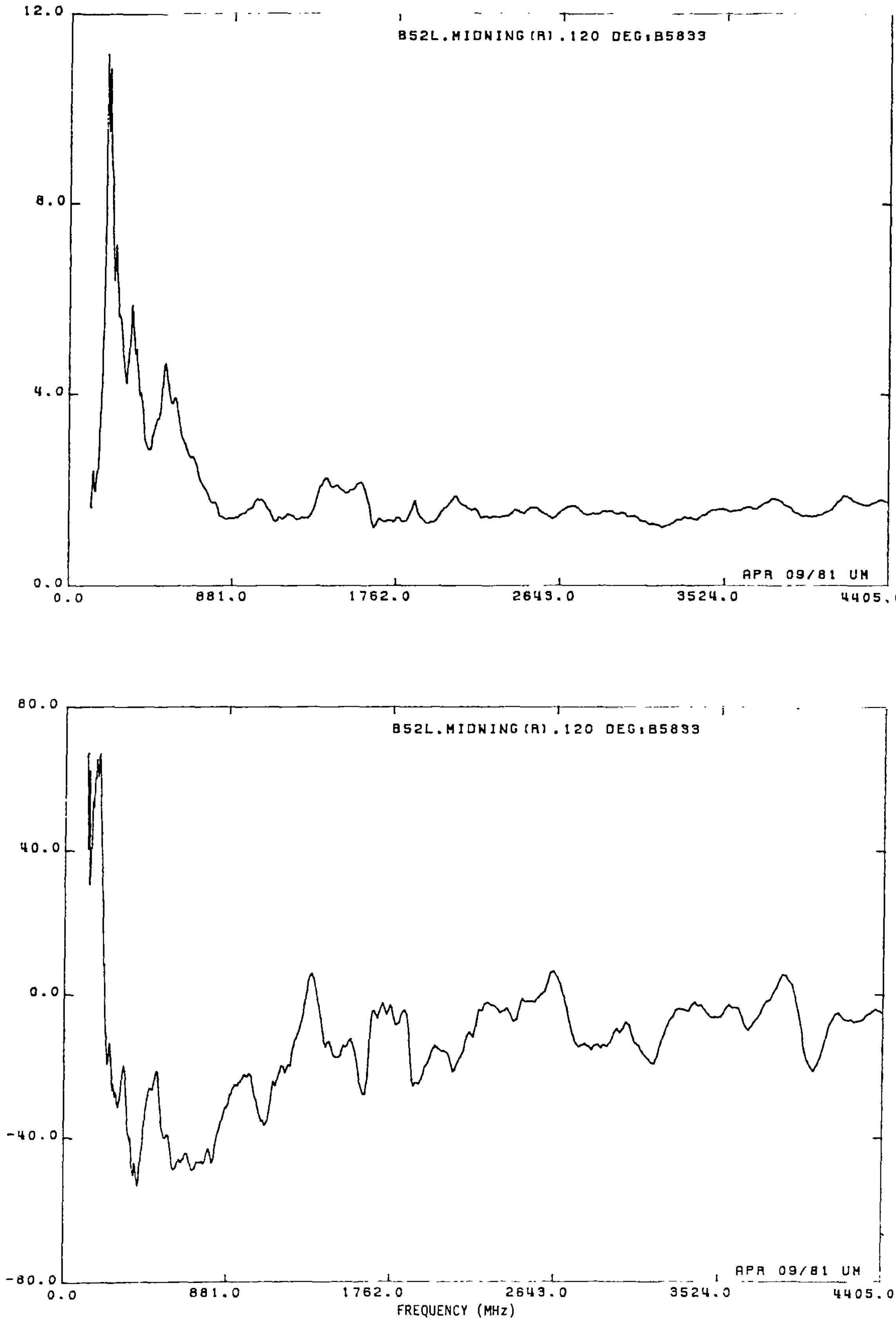

Fig. 4.12: Measured response of the surface current at midwing for $\theta = 120°$

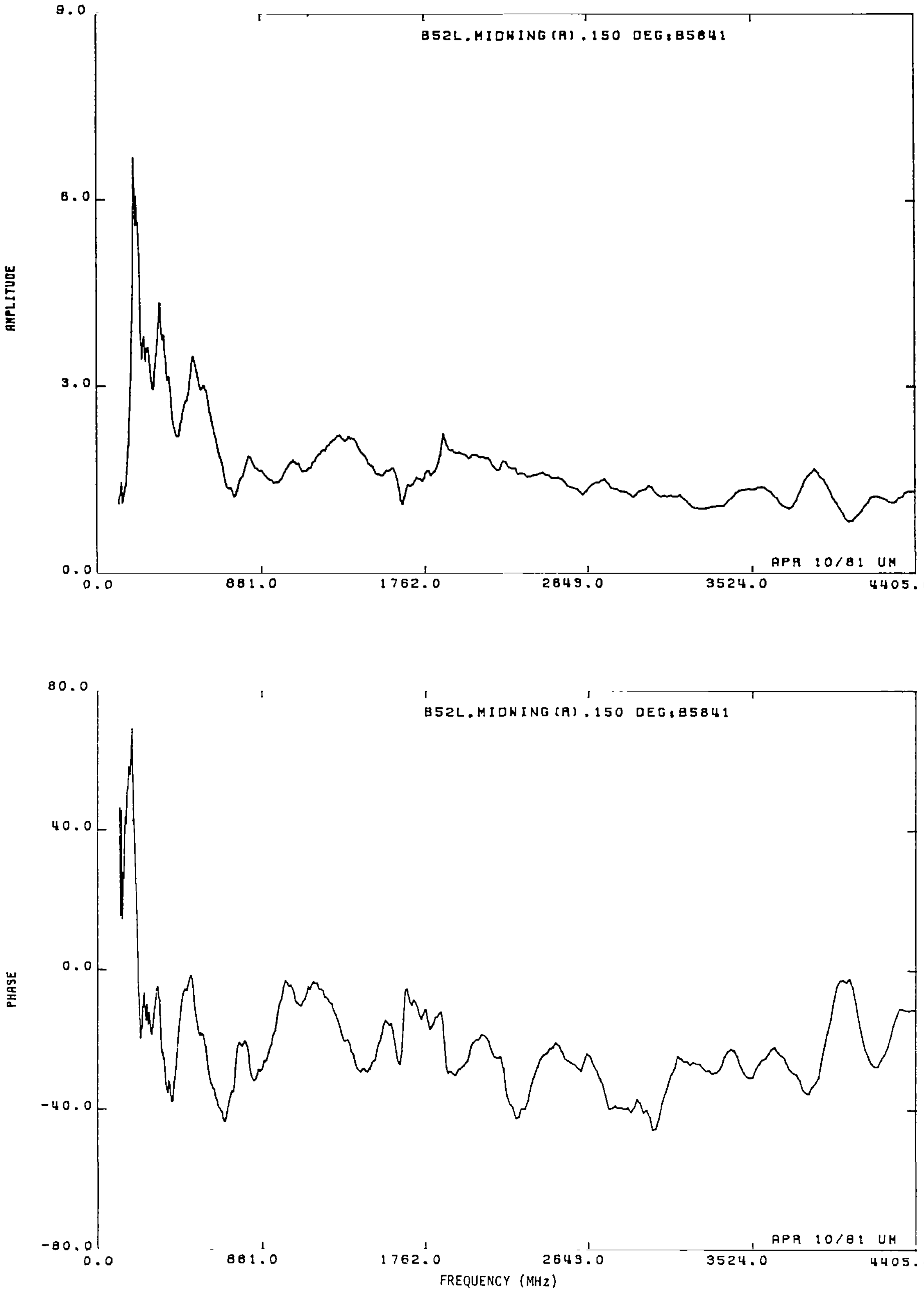

Fig. 4.13: Measured response of the surface current at midwing for $\theta = 150°$.

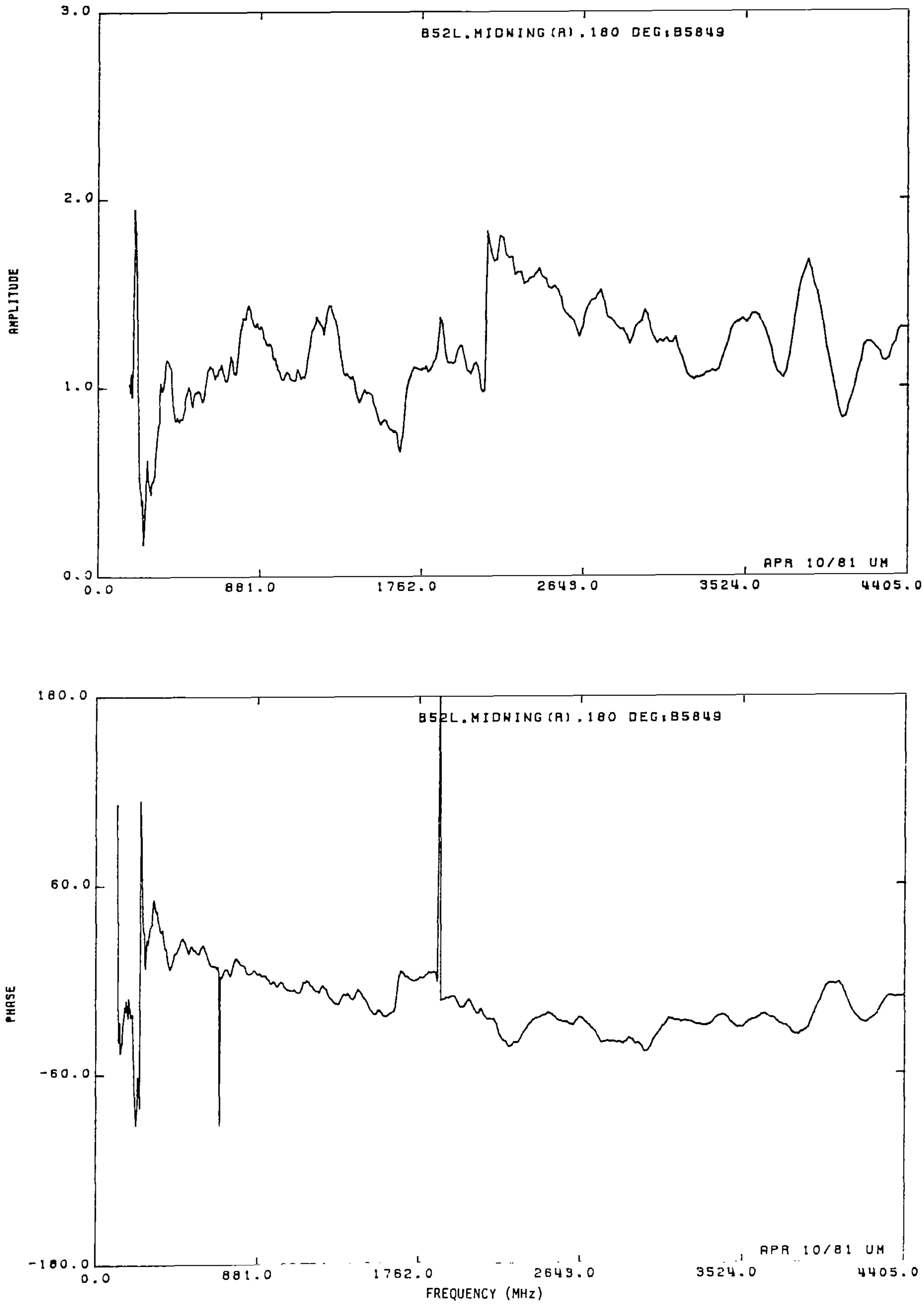

Fig. 4.14: Measured response of the surface current at midwing for θ = 180°.

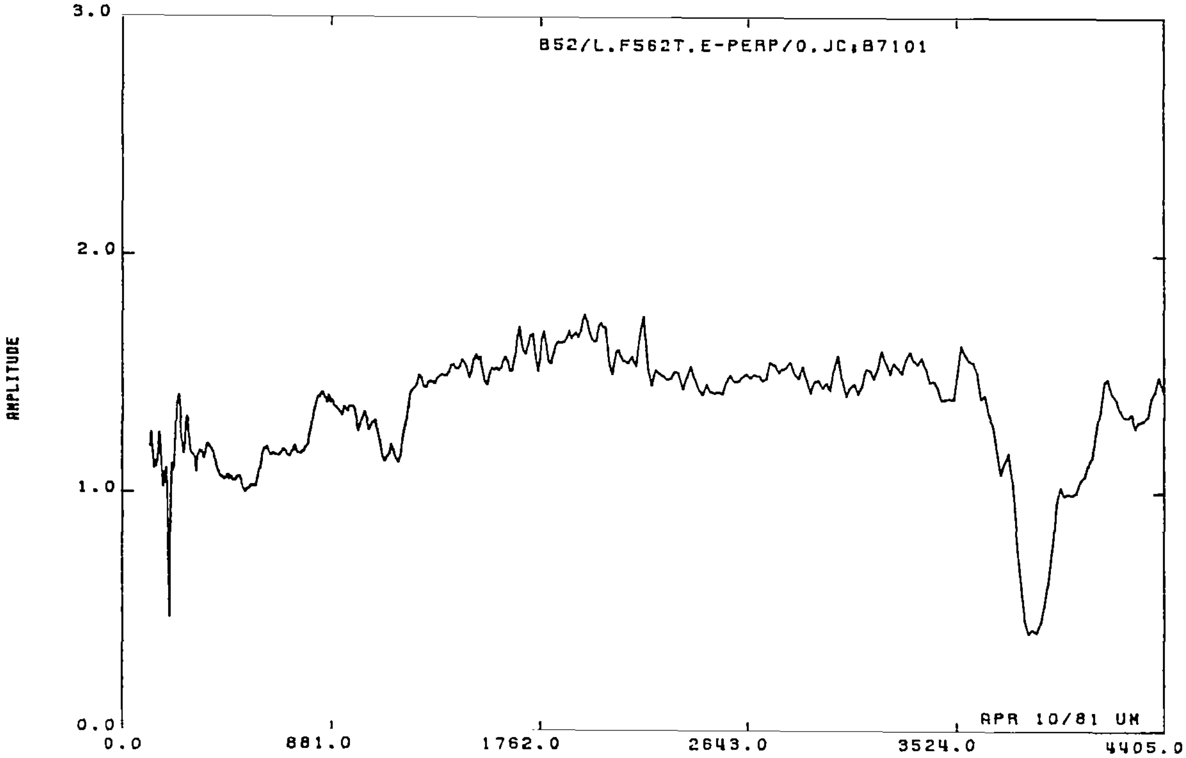

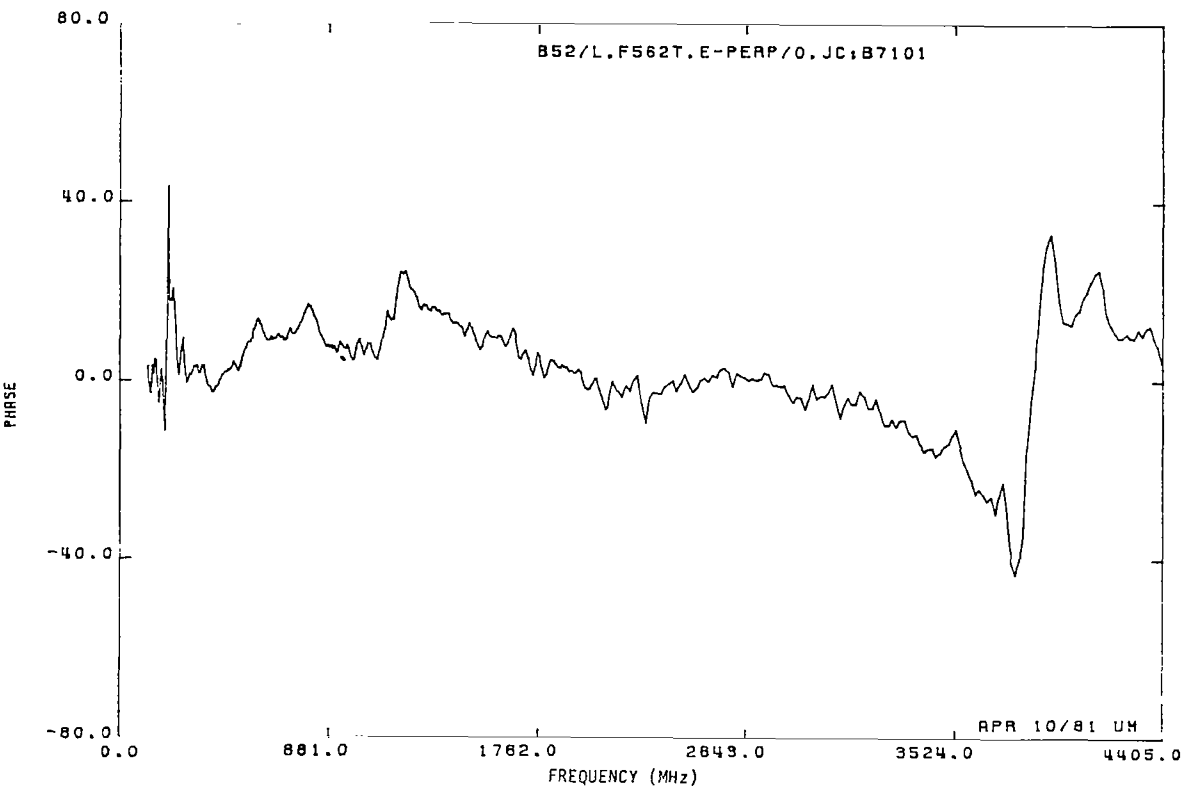

Fig. 4.15: Measured response of the surface current at the fuselage for $\theta = 0°$

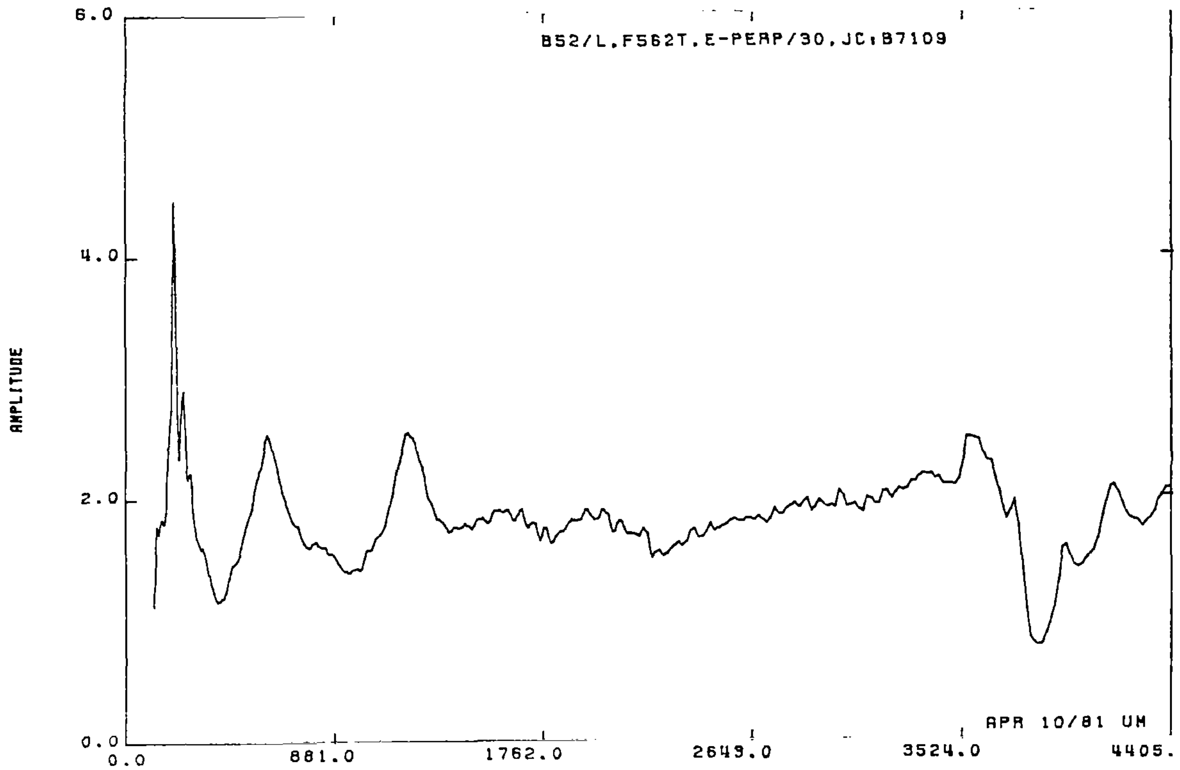

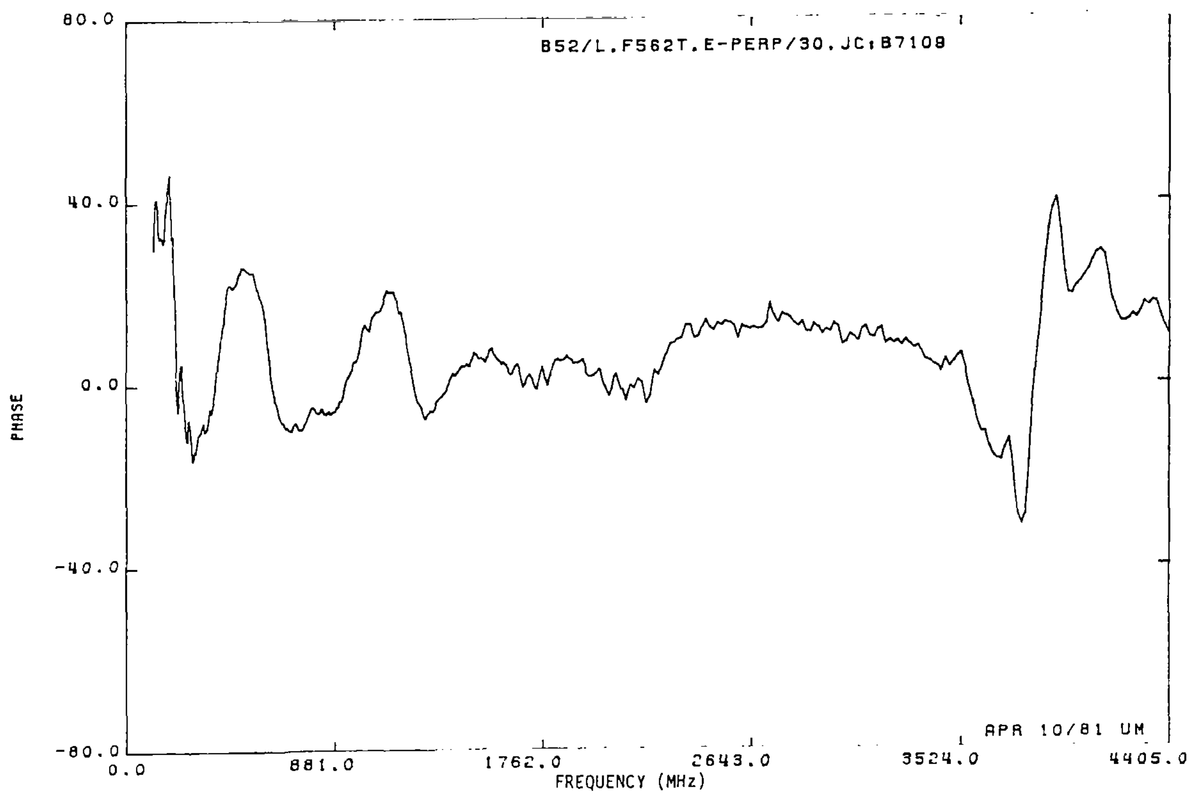

Fig. 4.16: Measured response of the surface current at the fuselage for $\theta = 30°$.

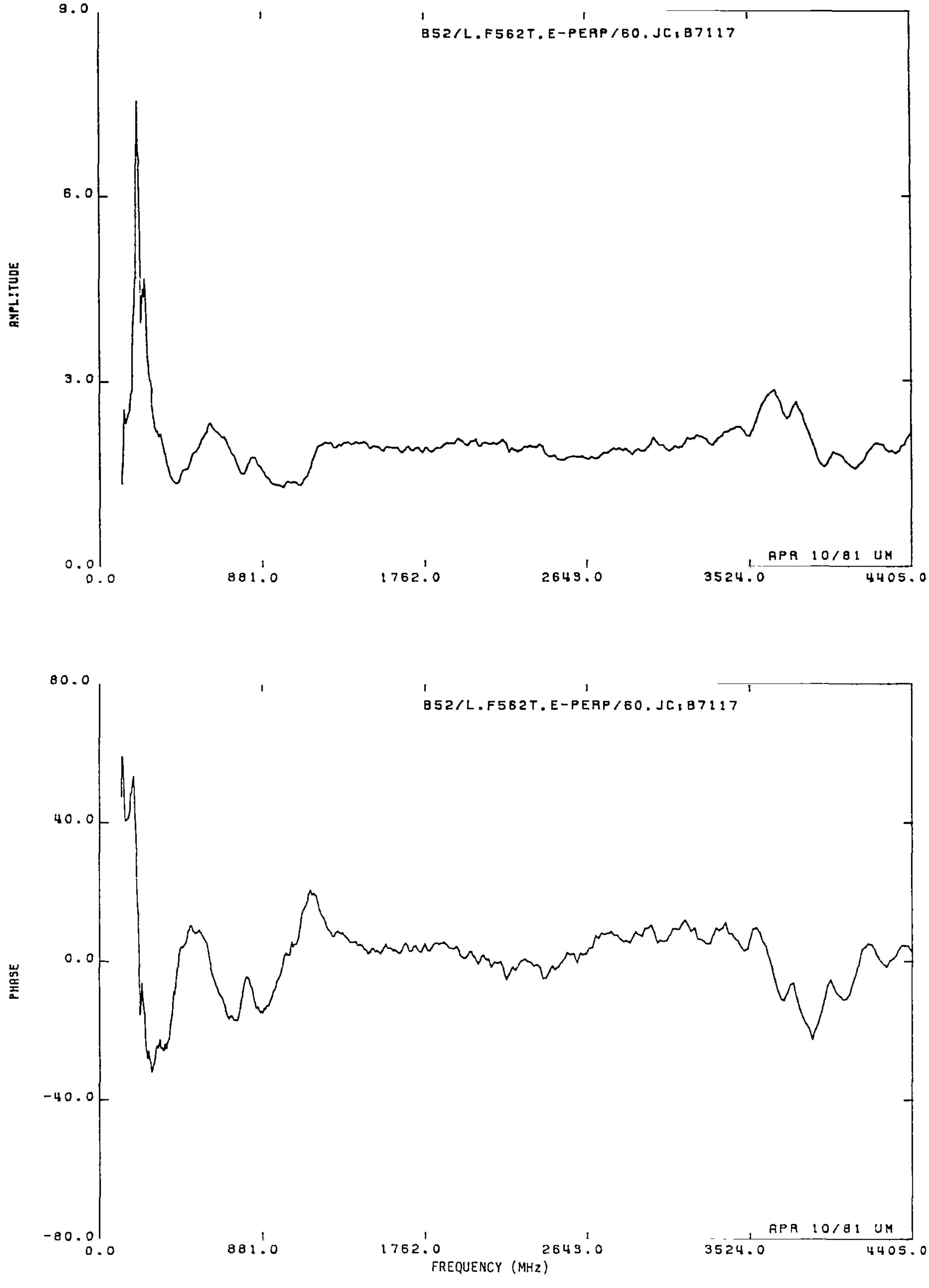

Fig. 4.17: Measured response of the surface current at the fuselage for $\theta = 60°$.

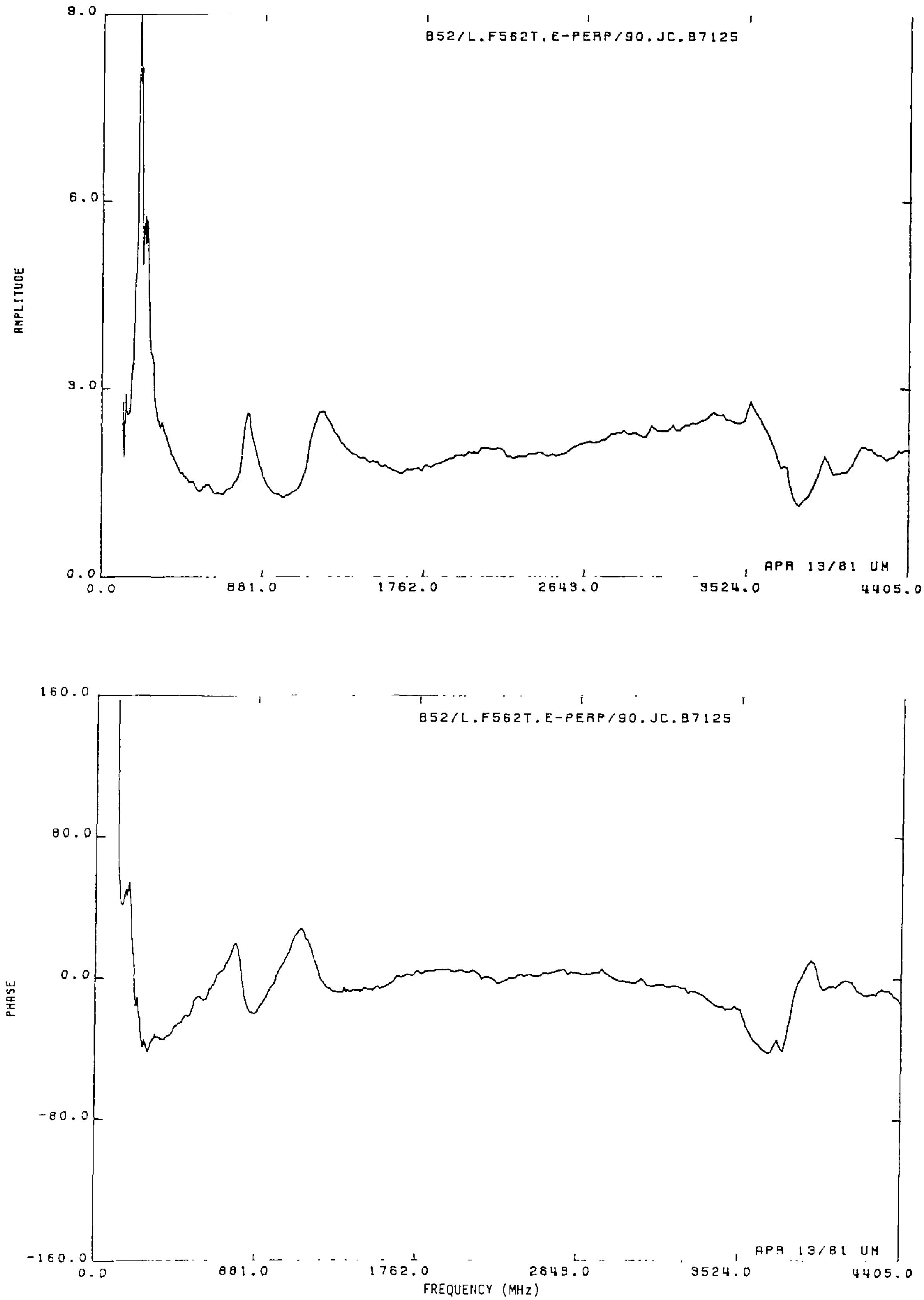

Fig. 4.18: Measured response of the surface current at the fuselage for θ = 90°.

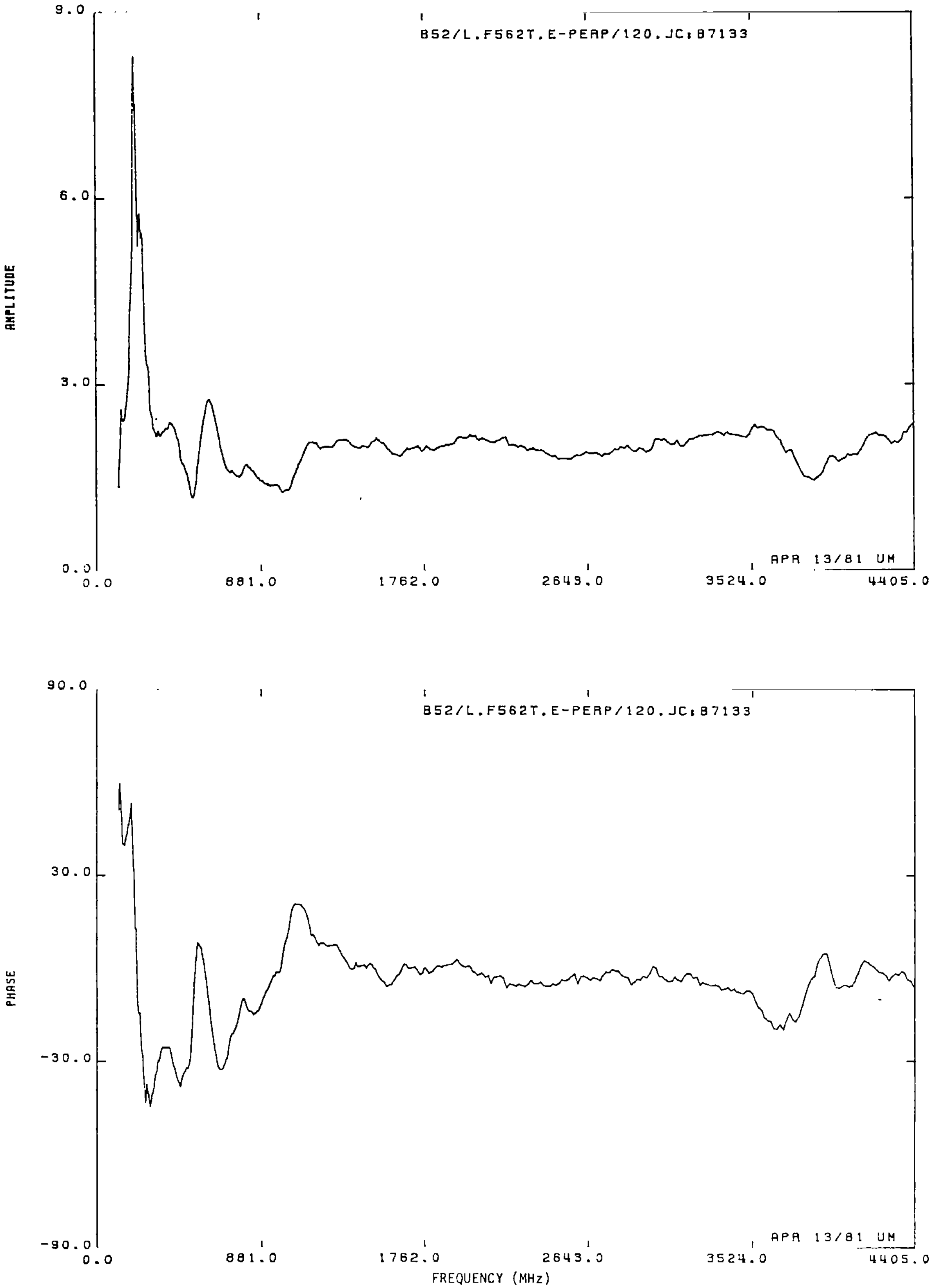

Fig. 4.19: Measured response of the surface current at the fuselage for θ = 120°.

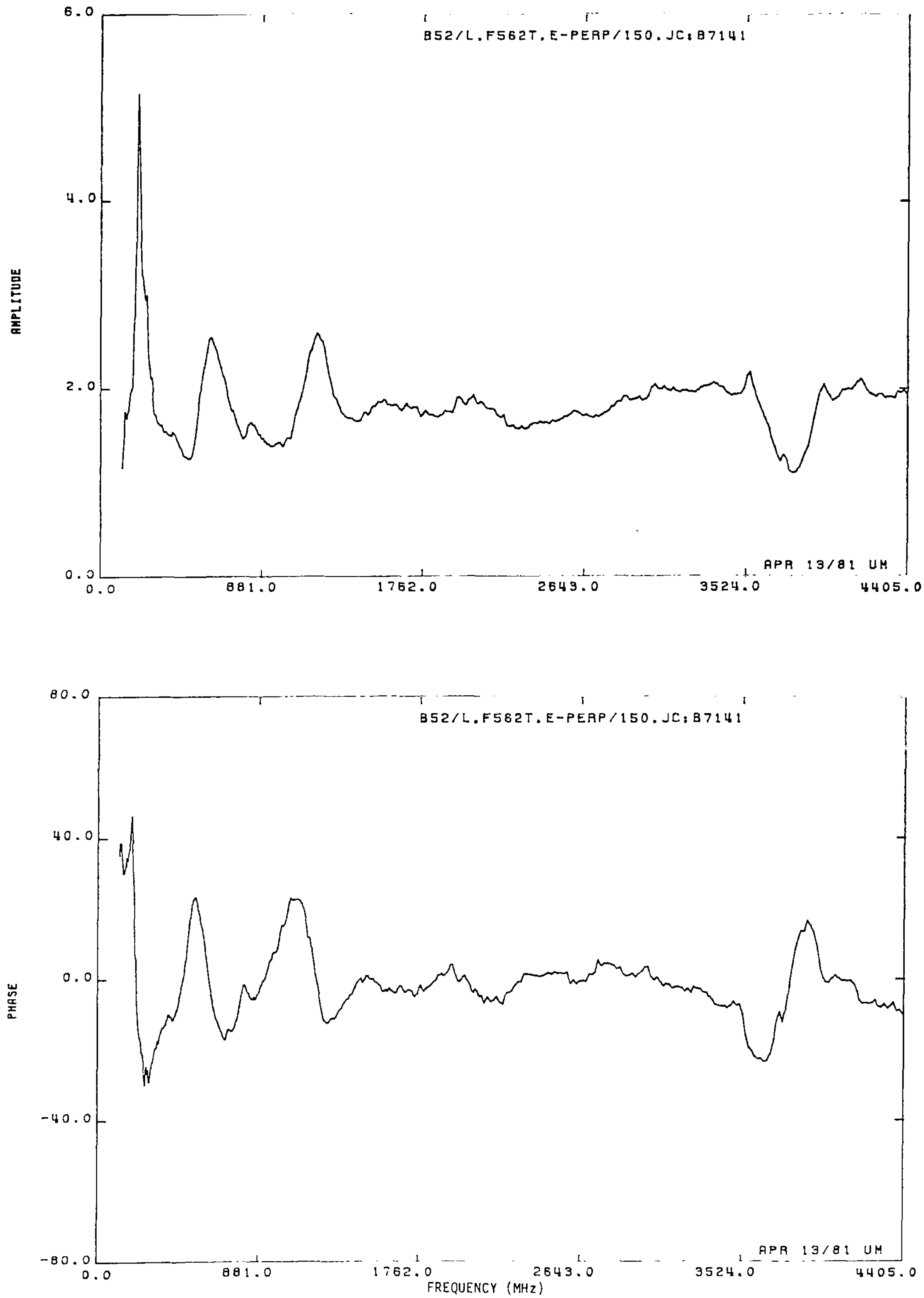

Fig. 4.20: Measured response of the surface current at the fuselage for $\theta = 150°$.

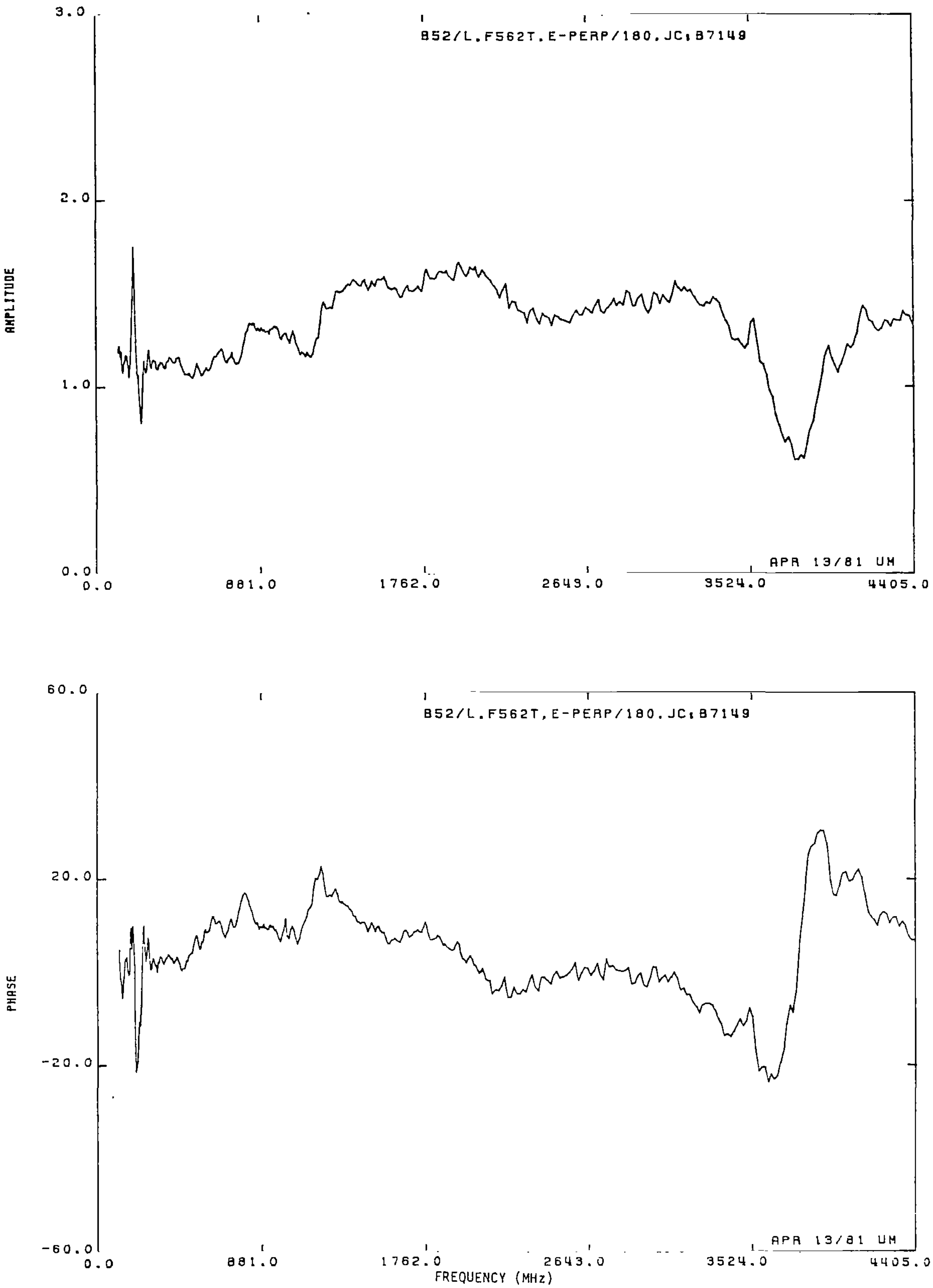

Fig. 4.21: Measured response of the surface current at the fuselage for $\theta = 180°$.

CHAPTER 5: CONCLUSIONS

A numerical technique has been developed which accurately fits a rational function to the frequency domain response of a body. The algorithm has been applied to data for the surface fields on a scatterer to extract the dominant SEM poles.

The algorithm is one of three curve fitting techniques that were investigated, and was selected because of its superior ability to fit a response and correctly determine the poles and residues. It was then applied to measured data for the longitudinal current on a circular cylinder. Although the resulting curve fits were excellent, only the dominant pole pair could be accurately located; and all of the other poles produced showed considerable movement in the complex s plane with changes in illumination. Because of this wandering, it was impossible to separate the true (but unknown) poles from those generated by the curve fitting process.

To optimize the choice of parameters involved in the program, we made a detailed study of the application of the algorithm to data for the surface fields on a perfectly conducting sphere. To extract a handful (M, say) of the pole pairs within a given frequency range it was necessary to adequately sample the response over the frequency range of interest, and to use a rational function with polynomials of orders 4M-1 and 4M (approximately) in the numerator and denominator respectively. When applied to 'exact' data for the sphere, five pole pairs could be located and their residues determined. Unfortunately, noise and/or other data degradation dramatically decreased the poles and residues that could be found. Several noise models were investigated; and for a noise level of about one percent, only the dominant pole could be extracted. Some of the other extracted poles were grouped in a manner that suggested approximations to a true pole, but their accuracy was no longer sufficient to provide meaningful information about the residues. With measured data, it was difficult to locate even the dominant pole pair in spite of the continued accuracy with which the data were fitted.

As a final test, the program was applied to data for the currents on a B-52G aircraft measured using a small scale model. Data were measured for several angles of incidence at a number of locations on the aircraft including the middle of a wing and on the top of the fuselage between the wings, and care was taken to achieve the best possible accuracy. The fits to the resulting curves were again excellent, but none of the SEM poles could be accurately located. Several groupings of extracted poles were suggestive of approximations to true poles, but the dispersion was too great either to separate true from curve fitting poles based on their positional invariance, or to warrant an analysis of the residues.

It is, of course, possible that some other algorithm could have more success, but the one that we used is reasonably sophisticated and was eminently successful in that which it was designed to do, namely, to fit a data set with a rational function. Unfortunately, accuracy of curve fitting is not itself a measure of the accuracy with which the true poles are extracted.

Appendix A. Application to the Surface Field on a Circular Cylinder

Prior to the present study some measurements had been made of the longitudinal current on a circular cylinder with hemispherical end caps. The brass cylinder had an overall length of 15.20 inches and a diameter of 2.005 inches and was illuminated by a plane wave incident in a plane perpendicular to the axis with its electric vector parallel to the axis. The current was measured in a plane 3.80 inches from an end at the five positions specified by $\theta = 0(45)180°$, where $\theta = 0$ corresponds to the front and in each case the phase was normalized to that of the incident field at the point of measurement. Because of the probe location it was anticipated that only the odd order modes could be detected. The frequency was stepped over the range 0.250 to 4.325 GHz to provide 816 values of the complex frequency response, and in the graphs which follow the current is shown as a function of the normalized frequency $2fL/c$ where L is the length of the cylinder and c is the velocity of light in vacuo.

These data were used to test the ability of each computer program to extract the SEM poles from measured values of the frequency response. As the study progressed, the MRC1, MRC2 and Sharpe-Roussi programs were applied in turn; and since none of them were successful, it is sufficient to summarize the results obtained with the best of the three, namely, the Sharpe-Roussi program.

Our initial efforts were directed at fitting the response over the entire frequency range using a single rational function, and it was found that a function with $M = 13$ and $N = 14$ was optimum. The extracted pole locations are shown in Fig. A-1 and it is seen that all poles except the lowest order (dominant) one varied with θ. In each case, however, the rational function provided an excellent fit to the data, and Fig. A-2 is an example of the curve fit obtained. With lower order polynomials the poles wandered more, and higher order polynomials produced a splitting of the dominant pole and no better clustering of the others.

We also tried a variety of other approaches to improve the accuracy of the extracted SEM poles. Reducing the frequency range of the data did not significantly affect the positional stability of the poles. For that portion of the response curve corresponding to $0.250 \leq f \leq 2.745$ GHz (the first 500 data points), the optimum fit was obtained with $M = 9$ and $N = 10$, and the resulting poles are shown in Fig. A-3. Once again the curve fits were excellent (see, for example, Fig. A-4) and polynomials of lower and higher order had the same effect as before.

Measured data are inevitably subject to noise and other types of experimental error. In the belief that noise was one factor limiting the accuracy of the extracted poles, digital filtering was applied to the data. From an examination of the data it was felt that a seventh order filter would be best at remvoing the small ripples without distorting the rest of the curves. Prior to application of the filter, the data were smoothly continued to higher and lower frequencies to eliminate ringing, and after filtering the extrapolated portions were eliminated. In an effort to pinpoint the second pole

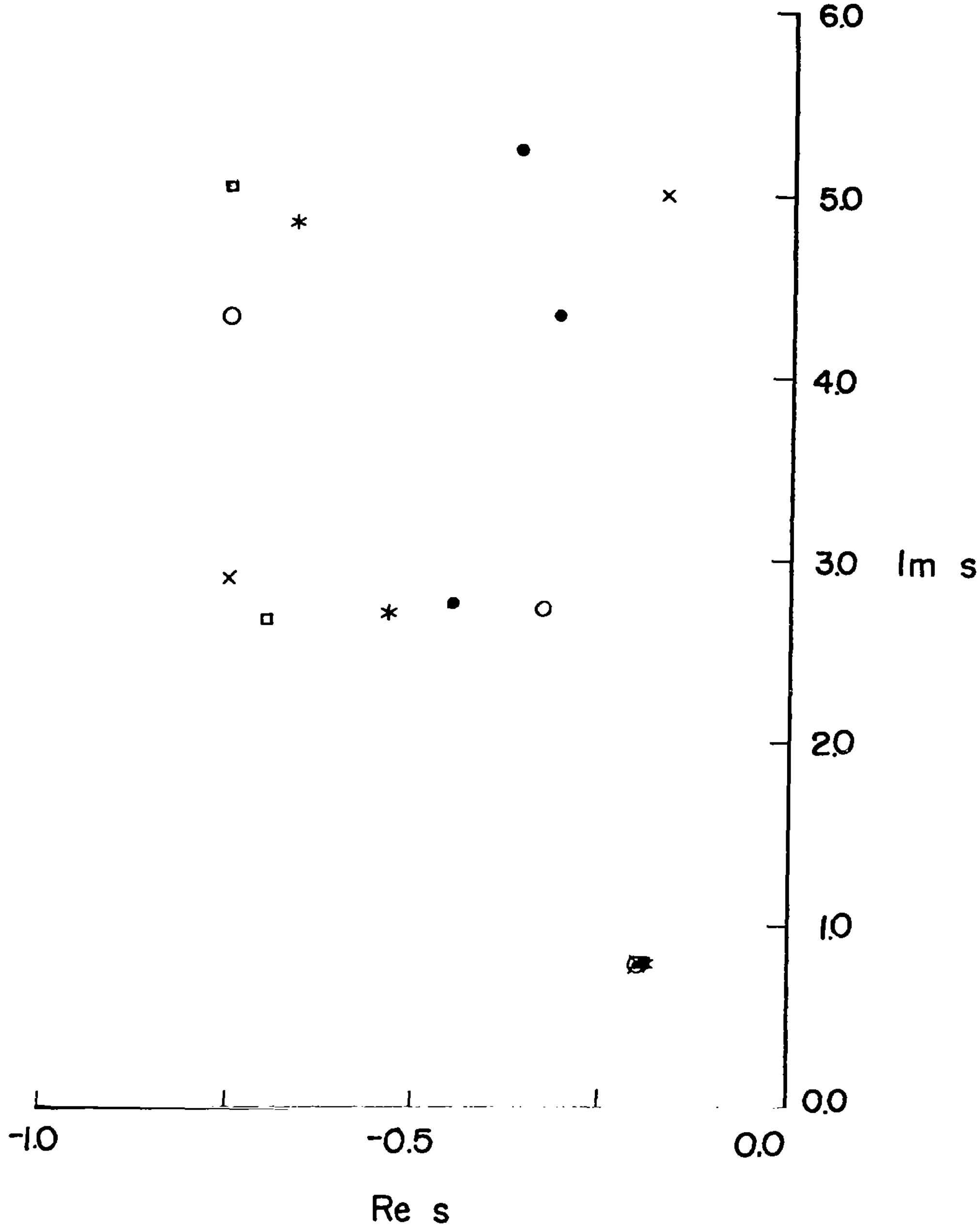

Fig. A-1: Dominant poles of the fitted rational functions for θ = 0° (•), 45° (×), 90° (o), 135° (*), 180° (□) and $0.643 \leq f_{norm} \leq 11.129$ for unfiltered data with M = 13 and N = 14.

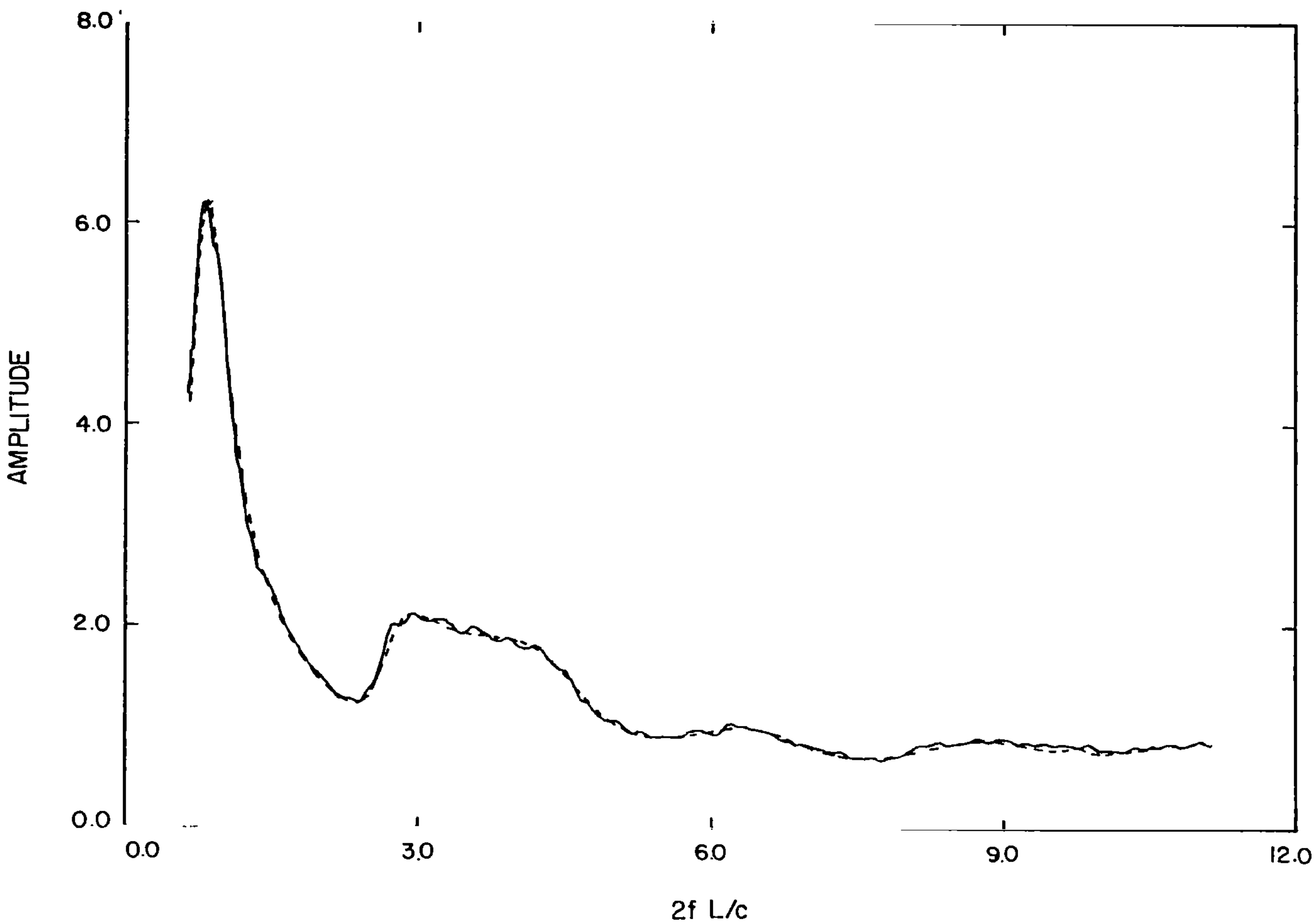

Fig. A-2: Amplitudes of the rational function with M = 13 and N = 14 (----) fitted to the longitudinal current (——) for $0.643 \leq f_{norm} \leq 11.129$ and $\theta = 90°$.

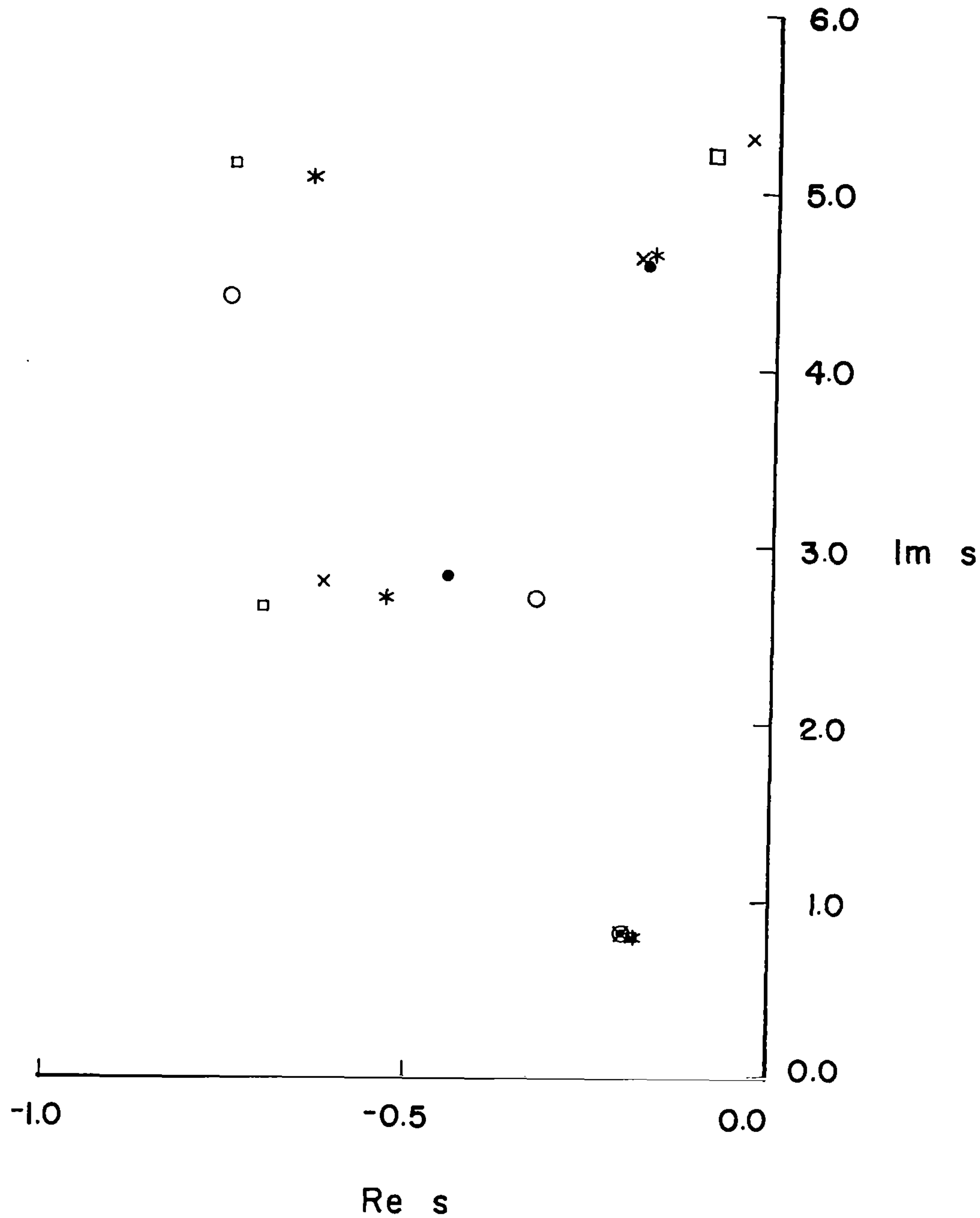

Fig. A-3: Dominant poles of the fitted rational functions for θ = 0° (•), 45° (×), 90° (o), 135° (*), 180° (□) and $0.643 \leq f_{norm} \leq 7.064$ for unfiltered data with M = 9 and N = 10.

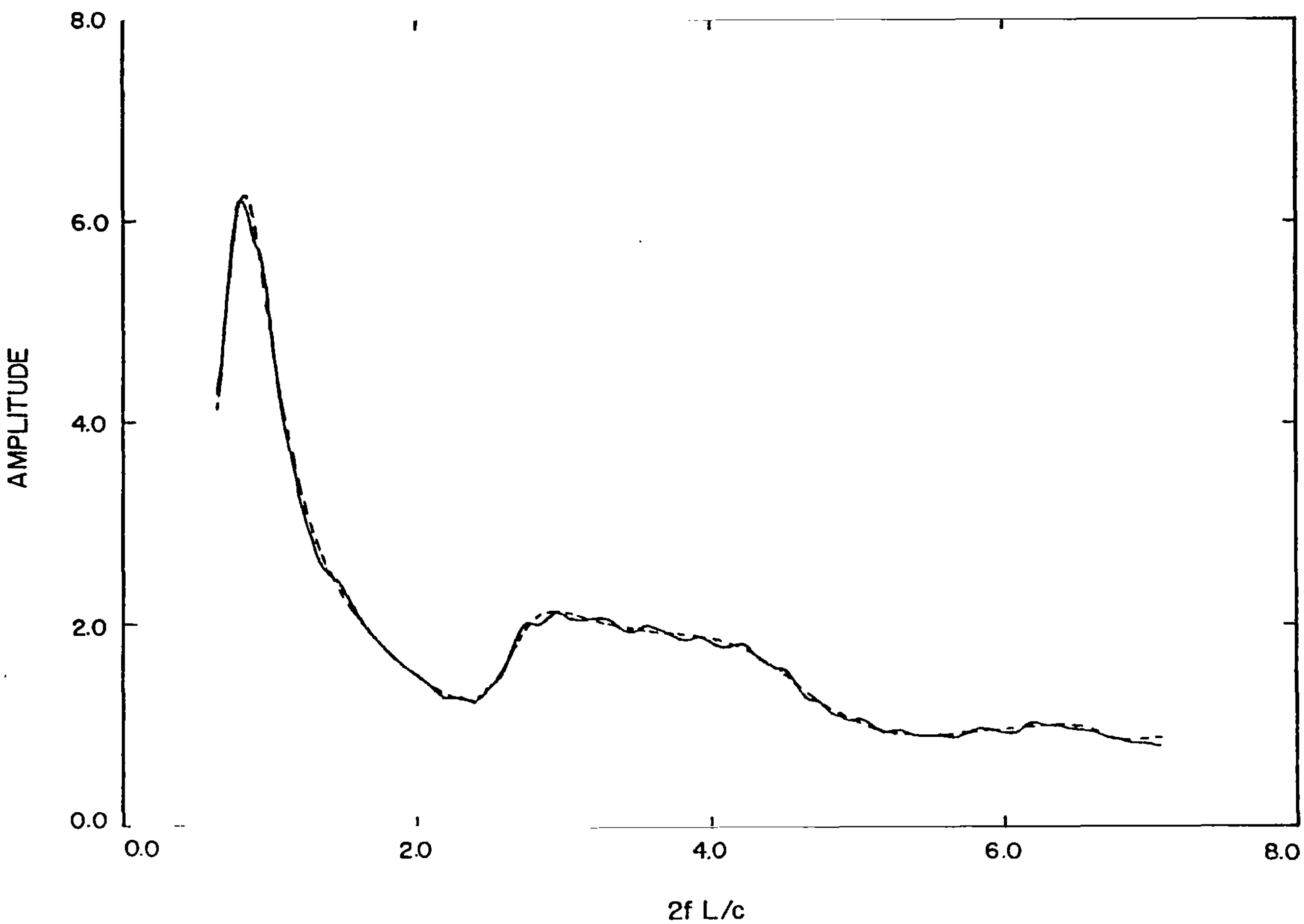

Fig. A-4: Amplitudes of the rational function with M = 9 and N = 10 (----) fitted to the longitudinal current (——) for $0.643 \leq f_{norm} \leq 7.064$ and $\theta = 90°$.

(which is actually the third order pole), we now used only the data spanning the frequency range from 0.250 to 2.745 GHz. The least wandering of this pole was obtained with M = 9 and N = 10 (Fig. A-5), but the results are not much better than with the unfiltered data and are achieved at the expense of a splitting of the dominant pole for several values of θ. In every case the curve fit was again excellent (Fig. A-6).

Another approach that was tried was to subtract the dominant pole contribution from each data set and to fit the remainder. To our disappointment this made little difference in the accuracy with which the second pole was located in spite of its new role as the 'dominant' pole. We also modified the program to allow a pole to be constrained after each iteration to 'encourage' the convergence of the second pole to a location which was the average of that produced by other data sets. To the credit of the program it rebelled; and after each such constraint, the next iteration restored the pole to the location which it would have had if freely chosen.

Our lack of success should not obscure the fact that the program does achieve that which it is mathematically designed to do, namely, to best fit a rational function of specified order to a data set. It would appear that the best fit is absolute rather than local; and provided the orders of the rational function polynomials are sufficient, the curve fits that are obtained are remarkably good. Unfortunately, the same cannot be said for the accuracy with which the poles other than the dominant one approximate the SEM poles.

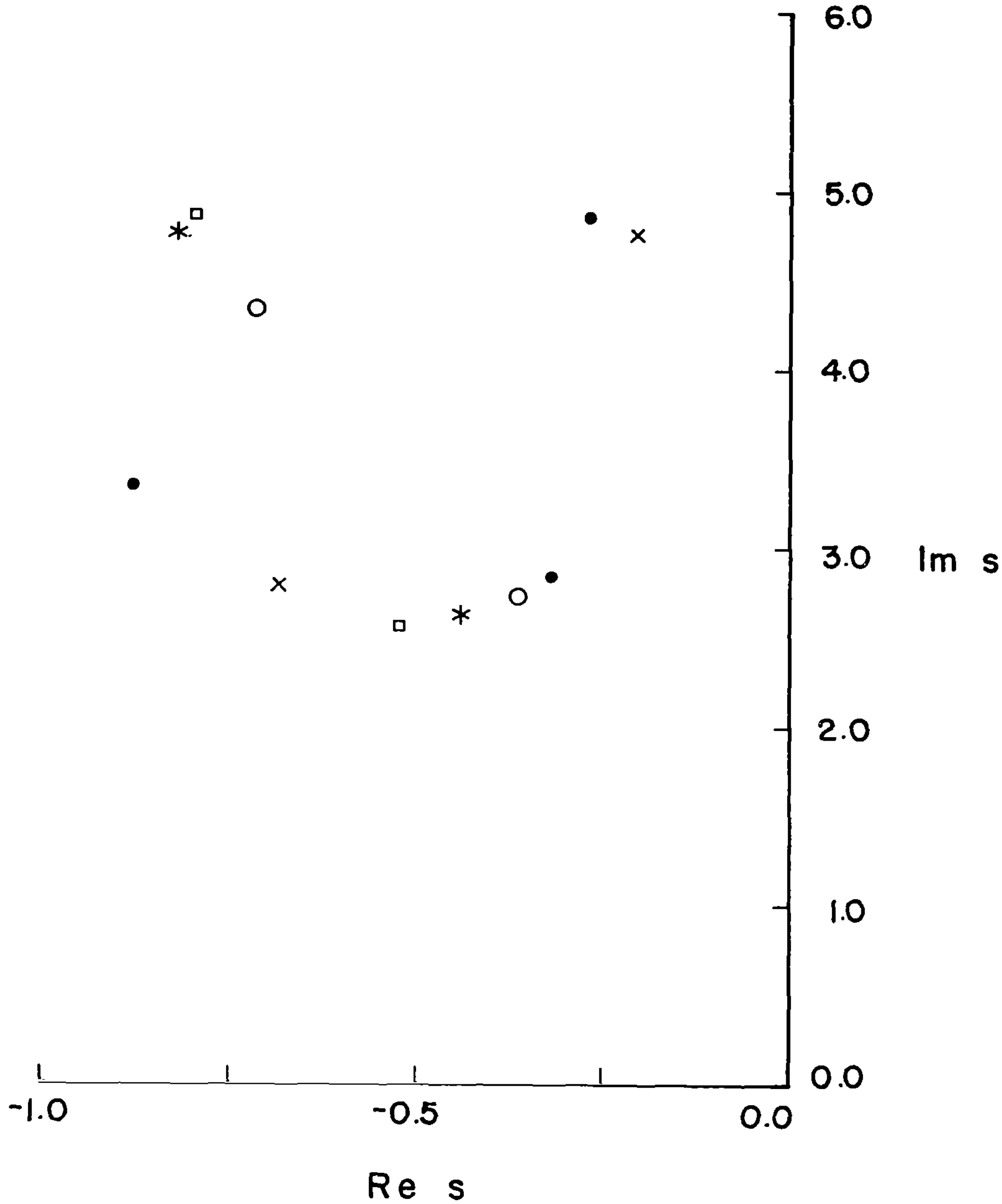

Fig. A-5: Dominant poles of the fitted rational functions for $\theta = 0°$ (●), 45° (×), 90° (○), 135° (∗), 180° (□) and $0.643 \leq f_{norm} \leq 7.064$ for filtered data with M = 9 and N = 10.

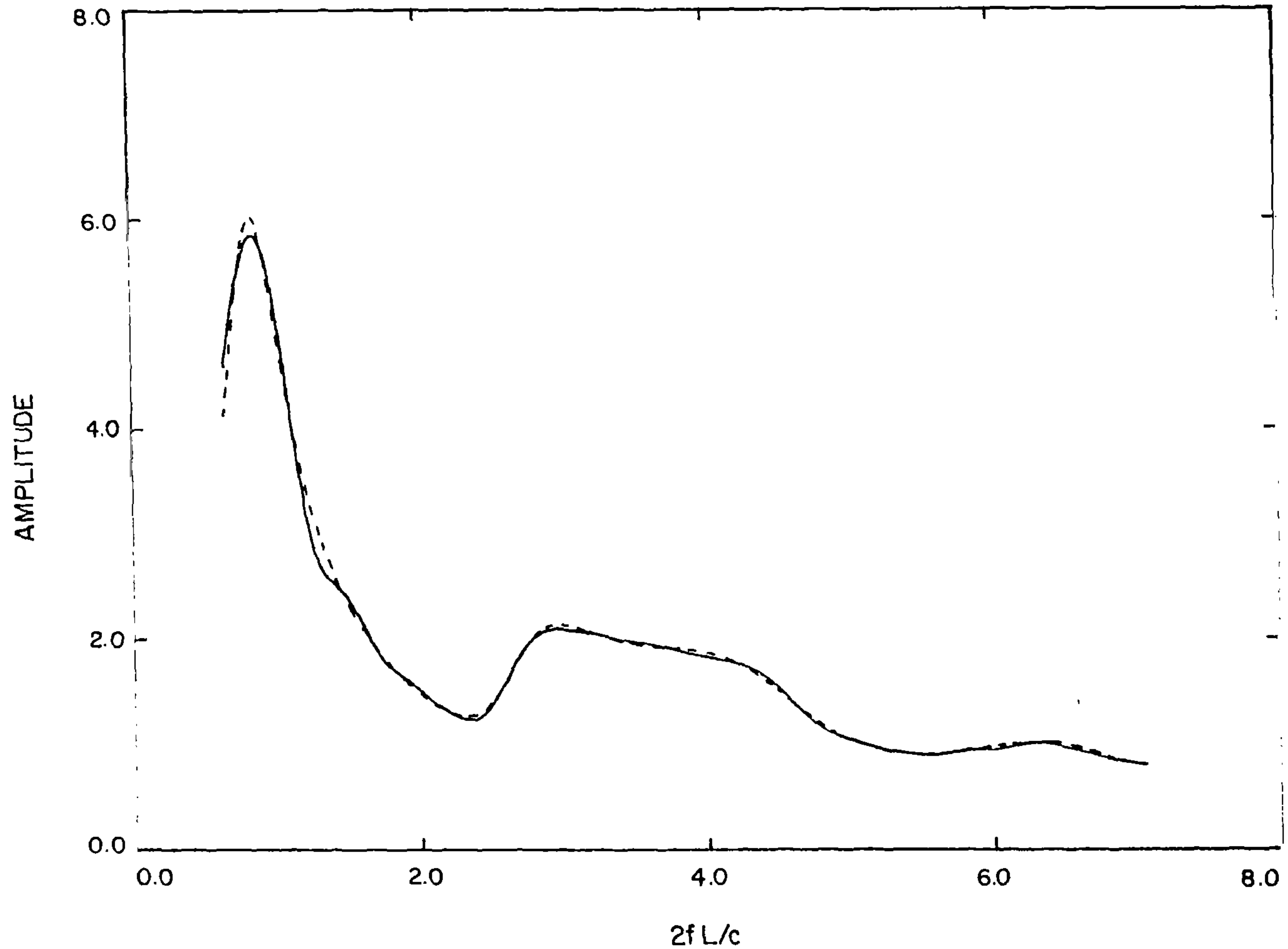

Fig. A-6: Amplitudes of the rational function with M = 0 and N = 10 (– – –) fitted to the filtered longitudinal current (——) for $0.643 \leq f_{norm} \leq 7.064$ and $\theta = 90°$.

APPENDIX B. EFFECT OF AN ERROR IN POLE LOCATION ON THE RESIDUE

Our study of pole extraction from frequency domain data has led to the conclusion that in a practical situation where the given data are subject to experimental noise and/or other data inaccuracies, no SEM pole other than (perhaps) the dominant one can be extracted with sufficient accuracy to specify the manner in which the residues depend on the polarization and the incident field direction. Indeed, the separation of the true poles from those introduced by the curve fitting process can no longer be carried out with certainty; but even in those cases where it is believed that a cluster of poles extracted from the various data sets are all approximations to a single SEM pole, the variation in position is too large to justify a meaningful analysis of their residues.

In order to quantify this statement it is necessary to relate the error in a residue determination to the error in the location of the corresponding pole. If the correct location of a pole were known, the positional error of the extracted pole could be defined as the radius of the smallest circle which encompasses the positions found from all of the data sets. In practice, however, the SEM poles are not known; but it is generally true that the main error in the location of the extracted pole is in the real part of the complex frequency s, i.e., the 'wandering' is roughly parallel to the real axis in the s plane. An illustration is provided by the second (actually, third order) pole in Fig. A-3. A rough estimate of the effect on the residue can now be obtained as follows. Let the actual contribution of a pole to the frequency response be $A/(s - s_m)$, and let the approximation provided by the curve fitting process be $A'/(s - s_m')$. At the resonant frequency $\omega = \mathrm{Im}\ s$ where the pole has most effect on the frequency response, a precise curve fit would now yield

$$A' = A \frac{\mathrm{Re}\ s_m}{\mathrm{Re}\ s_m'} ,$$

showing that a given percent error in the real part of the pole location translates into the same error in the determination of the residue. In the case of the second pole in Fig. A-3, the wandering as a function of the aspect angle θ implies ± 40 percent error in the computed residue.

To establish a criterion for a computed residue to be useful, it is convenient to consider a perfectly conducting sphere for which the residues are known precisely. Assuming the dominant dependence of a residue on the angle θ (position on the sphere) to be $A_n \cos n\theta$, it was found necessary for the residue of an extracted pole to lie within the bounds $A_n(\cos n\theta \pm 0.5)$ in order to be able to discern the true θ dependence. In general this was satisfied only if $|s_m' - s_m| \leq 0.1$ where s_m and s_m' are the true and extracted pole locations expressed in terms of the normalized (complex) frequency, and for at least the first four poles, the criterion was the same independently of m. An error of less than (about) 10 percent in the pole location is therefore necessary for any meaningful analysis of the residues.

APPENDIX C: COMPUTER PROGRAM

We present here a listing of the computer algorithm used in this study, along with appropriate documentation for its use. The program is in IBM Fortran for use in an interactive mode to facilitate the curve fitting process. It has been run on an AMDAHL 470/V8.

The program was written to accept in two different formats the input data for the frequency response which is to be fitted with a rational function. The first format is approprate for experimental data, and is:

```
Line 1    FILENAME (4A4)
     2    Comments (18A4)
     3    Comments (18A4)
     4    TITLE (18A4)
     5    FMIN, FMAX, AMPMIN, AMPMAX, PHASEMIN, PHASEMAX, NN
          (4F8.3, 2F8.2, I5)
     6    F(1), AMP(1), PHASE(1), F(2), AMP(2), PHASE(2), F(3)
          AMP(3), PHASE(3)  3(2F8.3, F8.2)
     ↑
   data
     ↓
          ...............F(NN), AMP(NN), PHASE(NN)
```

where all frequencies are in MHz and NN is the number of sample frequencies. AMP(I) and PHASE(I) are the amplitude and phase respectively of the response at F(I) in MHz. The second data format is appropriate for numerically generated data of high precision; and this Numerical Format is:

Line 1	FILENAME (4A4)
2	Comments (18A4)
3	Comments (18A4)
4	TITLE (18A4)
5	WMIN, WMAX, NN (2F8.3, 32X, I5)
6	W(1), REAL(1), IMAG(1) (3F12,6)
7	W(2), REAL(2), IMAG(2) (3F12.6)
↑	
data	
↓	
NN+5	W(NN), REAL(NN), IMAG(NN) (3F12.6)

where all frequencies are in M rad/sec and NN is the number of sample frequencies. REAL(I) and IMAG(I) are the real and imaginary parts respectively of the response at W(I) in M rad/sec.

The program uses data from two different sources for input and has four different outputs. The following is a list of the inputs and outputs, where the number in parentheses is the data set reference number for the various inputs and outputs. The program requires the following inputs:

Terminal (5): interactively the user supplies M,N,R (radius of minimum circumscribing sphere), number of iterations, maximum allowed convergence error, and type of frequency response data supplied.

Frequency Response: Data (9)	frequency response data in either Experimental or Numerical Format.

The following outputs are available:

Terminal (6):	iteration number and convergence error value at each iteration, poles and residues.
Normalized Frequency: Response (7)	the frequency response of the input data with frequency normalized by $F_{norm} = F \times 2 \times R/c$ where R = radius of minimum circumscribing sphere and c = speed of light in vacuo. Data are given in the Experimental Format.
Rational Function: Response (8)	the frequency response of the fitted rational function over the same frequency range in normalized frequency. Data are given in the Experimental Format.
Poles and Residues: (10)	a tabulation of the poles and residues of the rational function in terms of normalized frequency. The zero frequency value of the rational function is also given.

A sample run follows. This is an attempt to fit, with a rational function having M = 19, N = 20, the surface current on a 1/100.60 scale model B52 aircraft over the frequency range 118.4 MHz to 100.6 MHz. The sample consists of: the interactive process, experimental frequency response (Data Set 9), normalized experimental data (Data Set 7), rational function approximation (Data Set 8), and poles and residues list (Data Set 10). Following the sample run is a listing of the computer program in Fortran.

Sample Run:

Interactive Process:

```
#RUN PROGRAM 7=B5809.030.N 8=B5809,030.C 9=B5809.030 10=B5809.030.L
#EXECUTION BEGINS



 ENTER THE DEGREE OF THE NUMERATOR POLYNOMIAL
 AS A TWO DIGIT INTEGER
 19

 ENTER THE DEGREE OF THE DENOMINATOR POLYNOMIAL
 AS A TWO DIGIT INTEGER
 20

 B5809
 B52L,MIDWING(R),30 DEG;B5809

 IS DATA IN THE FORM OF FREQ(MRAD),REAL,IMAG. ?
 NO

 ENTER RADIUS OF MINIMUM CIRCUMSCRIBING SPHERE
 .284

 ENTER THE MAXIMUM NUMBER OF ITERATIONS
 ALLOWED WITH A TWO DIGIT INTEGER
 20

 ENTER THE CONVERGENCE ERROR VALUE
 IN DOUBLE PRECISION FORMAT
 1.D-8,

   IT=  1      ERR=0.460197E+01
   IT=  2      ERR=0.383788E+00
   IT=  3      ERR=0.702864E-02
   IT=  4      ERR=0.258376E-01
   IT=  5      ERR=0.630893E-01
   IT=  6      ERR=0.489766E-01
   IT=  7      ERR=0.116682E-01
   IT=  8      ERR=0.322956E-02
   IT=  9      ERR=0.231244E-01
   IT= 10      ERR=0.192095E-02
   IT= 11      ERR=0.293791E-02
   IT= 12      ERR=0.145043E-01
   IT= 13      ERR=0.110082E-01
   IT= 14      ERR=0.371138E-02
   IT= 15      ERR=0.671837E-04
   IT= 16      ERR=0.360689E-02
   IT= 17      ERR=0.600027E-02
   IT= 18      ERR=0.596786E-02
   IT= 19      ERR=0.700338E-03
   IT= 20      ERR=0.212555E-03
```

ROOTS OF DENOMINATOR ARE:

-0.4664E-01	-0.6879E+00
-0.4664E-01	0.6879E+00
-0.3017E-01	-0.4524E+00
-0.3017E-01	0.4524E+00
-0.9809E-02	-0.8033E+00
-0.9809E-02	0.8033E+00
-0.8290E-02	-0.1217E+01
-0.8290E-02	0.1217E+01
-0.2192E-01	-0.3874E+00
-0.2192E-01	0.3874E+00
-0.1247E-01	-0.9768E+00
-0.1247E-01	0.9768E+00
0.2585E+00	-0.8358E+00
0.2585E+00	0.8358E+00
-0.9319E-01	-0.1204E+01
-0.9319E-01	0.1204E+01
-0.8649E-01	-0.1559E+01
-0.8649E-01	0.1559E+01
0.3099E+00	-0.3075E+01
0.3099E+00	0.3075E+01

RESIDUES ARE, RESPECTIVELY:

0.8242E-01	0.1361E-01
0.8242E-01	-0.1361E-01
0.8080E-01	0.2689E-01
0.8080E-01	-0.2689E-01
0.7844E-03	0.4094E-02
0.7844E-03	-0.4094E-02
-0.2182E-02	0.1408E-02
-0.2182E-02	-0.1408E-02
0.5808E-01	0.1566E-01
0.5808E-01	-0.1566E-01
0.3618E-02	-0.5775E-02
0.3618E-02	0.5775E-02
-0.1380E+00	0.8804E-01
-0.1380E+00	-0.8804E-01
0.7695E-01	-0.9471E-01
0.7695E-01	0.9471E-01
0.4928E-02	0.4267E-01
0.4928E-02	-0.4267E-01
0.3732E+00	0.1579E+01
0.3732E+00	-0.1579E+01

#EXECUTION TERMINATED

Data Set 9: Experimentally measured data for a scale model B52 aircraft. Data is in Experimental Format.

```
 1      B5809
 2      B52,L,30DEG,-2.2CM,2,C/J3,JA,JX,10/23/80,RW...BAND 1
 3      SF=1
 4      B52L,MIDWING(R),30 DEG;B5809
 5       118.4001001.600      .781    5.191   -40.42    36.99  185
 6       118.400     1.212    36.99 123.200    1.450    12.12 128.000    1.908    33.35
 7       132.800     1.874     -.81 137.600    1.545    13.22 142.400    1.538    10.56
 8       147.200     1.722    24.49 152.000    1.808    21.13 156.800    1.894    28.56
 9       161.600     1.966    26.30 166.400    2.387    35.34 171.200    2.535    32.97
10       176.000     2.743    28.31 180.800    3.239    32.65 185.600    3.393    35.69
11       190.400     3.817    20.93 195.200    4.064    10.47 200.000    5.191     7.71
12       204.800     4.903     3.55 209.600    4.312    -1.71 214.400    4.130   -10.67
13       219.200     3.558   -16.13 224.000    3.886    -5.68 228.800    4.784   -12.64
14       233.600     4.468   -14.30 238.400    4.349   -19.05 243.200    4.621   -26.51
15       248.000     4.276   -33.66 252.800    3.519   -40.42 257.600    2.998   -39.27

60       896.000     1.192      .39 900.800    1.206     -.35 905.600    1.218     -.20
61       910.400     1.208      .65 915.200    1.209     2.00 920.000    1.226     3.65
62       924.800     1.244     5.89 929.600    1.268     6.43 934.400    1.316     6.47
63       939.200     1.350     7.11 944.000    1.353     7.44 948.800    1.363     6.27
64       953.600     1.398     5.80 958.400    1.421     6.62 963.200    1.425     7.15
65       968.000     1.445     7.57 972.800    1.399     8.09 977.600    1.464     7.21
66       982.400     1.537     7.02 987.200    1.572     6.64 992.000    1.605     6.15
67       996.800     1.634     5.561001.600    1.663     4.87
```

Data Set 7: Experimentally measured data for a scale model B52 aircraft in normalized frequency. Data is in Experimental Format.

1	B5809								
2	NORMAILIZED EXPERIMENTAL DATA								
3									
4	B52L,MIDWING(R),30 DEG$B5809								
5	0.224	1.896	0.781	5.191	-40.42	36.99	185		
6	0.224	1.212	36.99	0.233	1.450	12.12	0.242	1.908	33.35
7	0.251	1.874	-0.81	0.261	1.545	13.22	0.270	1.538	10.56
8	0.279	1.722	24.49	0.288	1.808	21.13	0.297	1.894	28.56
9	0.306	1.966	26.30	0.315	2.387	35.34	0.324	2.535	32.97
10	0.333	2.743	28.31	0.342	3.239	32.65	0.351	3.393	35.69
11	0.360	3.817	20.93	0.370	4.064	10.47	0.379	5.191	7.71
12	0.388	4.903	3.55	0.397	4.312	-1.71	0.406	4.130	-10.67
13	0.415	3.558	-16.13	0.424	3.886	-5.68	0.433	4.784	-12.64
14	0.442	4.468	-14.30	0.451	4.349	-19.05	0.460	4.621	-26.51
15	0.470	4.276	-33.66	0.479	3.519	-40.42	0.488	2.998	-39.27
60	1.696	1.192	0.39	1.706	1.206	-0.35	1.715	1.218	-0.20
61	1.724	1.208	0.65	1.733	1.209	2.00	1.742	1.226	3.65
62	1.751	1.244	5.89	1.760	1.268	6.43	1.769	1.316	6.47
63	1.778	1.350	7.11	1.787	1.353	7.44	1.796	1.363	6.27
64	1.805	1.398	5.80	1.815	1.421	6.62	1.824	1.425	7.15
65	1.833	1.445	7.57	1.842	1.399	8.09	1.851	1.464	7.21
66	1.860	1.537	7.02	1.869	1.572	6.64	1.878	1.605	6.15
67	1.887	1.634	5.56	1.896	1.663	4.87			

Data Set 8: Frequency response of a fitted rational function with M = 19, N = 20, in terms of normalized frequency. Data is in Experimental Format.

```
B5809
RATIONAL FUNCTION RESPONSE WITH NORMAILIZED FREQUENCY

B52L,MIDWING(R),30 DEG;B5809
  0.224   1.896   1.211   4.901  -42.26   38.84  185
  0.224   1.753   18.93   0.233   1.786   19.90   0.242   1.824   20.90
  0.251   1.867   21.91   0.261   1.915   22.95   0.270   1.971   24.01
  0.279   2.035   25.08   0.288   2.109   26.15   0.297   2.197   27.21
  0.306   2.302   28.24   0.315   2.429   29.19   0.324   2.584   30.01
  0.333   2.780   30.57   0.342   3.030   30.67   0.351   3.357   29.95
  0.360   3.783   27.75   0.370   4.309   22.92   0.379   4.805   14.13
  0.388   4.901    2.22   0.397   4.443   -7.15   0.406   3.908   -9.72
  0.415   3.668   -7.69   0.424   3.746   -5.52   0.433   4.037   -6.26
  0.442   4.375  -11.12   0.451   4.531  -19.45   0.460   4.354  -28.71
  0.470   3.927  -36.11   0.479   3.440  -40.54   0.488   3.009  -42.26


  1.696   1.323    1.06   1.706   1.329    1.89   1.715   1.337    2.66
  1.724   1.344    3.37   1.733   1.352    4.02   1.742   1.361    4.63
  1.751   1.369    5.20   1.760   1.378    5.73   1.769   1.386    6.23
  1.778   1.395    6.71   1.787   1.404    7.16   1.796   1.412    7.59
  1.805   1.421    8.00   1.815   1.430    8.39   1.824   1.439    8.77
  1.833   1.448    9.14   1.842   1.456    9.50   1.851   1.465    9.85
  1.860   1.474   10.19   1.869   1.483   10.52   1.878   1.492   10.84
  1.887   1.501   11.16   1.896   1.511   11.48
```

Date Set 10: List of normalized pole locations and residues of a rational function with M = 19, N = 20.

B5809

NORMALIZED POLE LOCATIONS AND RESIDUES

M N

19 20

B52L,MIDWING(R),30 DEG;B5809

-0.4664E-01	-0.6879E+00	0.8242E-01	0.1361E-01
-0.4664E-01	0.6879E+00	0.8242E-01	-0.1361E-01
-0.3017E-01	-0.4524E+00	0.8080E-01	0.2689E-01
-0.3017E-01	0.4524E+00	0.8080E-01	-0.2689E-01
-0.9809E-02	-0.8033E+00	0.7844E-03	0.4094E-02
-0.9809E-02	0.8033E+00	0.7844E-03	-0.4094E-02
-0.8290E-02	-0.1217E+01	-0.2182E-02	0.1408E-02
-0.8290E-02	0.1217E+01	-0.2182E-02	-0.1408E-02
-0.2192E-01	-0.3874E+00	0.5808E-01	0.1566E-01
-0.2192E-01	0.3874E+00	0.5808E-01	-0.1566E-01
-0.1247E-01	-0.9768E+00	0.3618E-02	-0.5775E-02
-0.1247E-01	0.9768E+00	0.3618E-02	0.5775E-02
0.2585E+00	-0.8358E+00	-0.1380E+00	0.8804E-01
0.2585E+00	0.8358E+00	-0.1380E+00	-0.8804E-01
-0.9319E-01	-0.1204E+01	0.7695E-01	-0.9471E-01
-0.9319E-01	0.1204E+01	0.7695E-01	0.9471E-01
-0.8649E-01	-0.1559E+01	0.4928E-02	0.4267E-01
-0.8649E-01	0.1559E+01	0.4928E-02	-0.4267E-01
0.3099E+00	-0.3075E+01	0.3732E+00	0.1579E+01
0.3099E+00	0.3075E+01	0.3732E+00	-0.1579E+01

DC TERM IS:

0.1482E+01

Program Listing:

```
C=====================================================================
C......
C......USING THE REAL AND IMAGINARY PARTS OF A
C......FREQUENCY RESPONSE AS INPUT, THIS PROGRAM
C......GENERATES THE COEFFICIENTS OF THE RATIONAL
C......FUNCTION WHICH APPROXIMATES THE KNOWN
C......FREQUENCY RESPONSE.  THE NUMERATOR IS A
C......POLYNOMIAL IN POWERS OF S
C......OF DEGREE M.  THE DENOMINATOR IS OF DEGREE
C......N,(M<=N). THE POLES AND RESIDUES OF THE
C......RATIONAL FUNCTION ARE THEN COMPUTED.
C......
C=====================================================================
      IMPLICIT REAL*8 (A-H,O-Z)
      DIMENSION ACOF(40),BCOF(40),AACOF(40),BBCOF(40)
      DIMENSION XCOF(40),COF(40),BBCO(40)
      DIMENSION ROOTR(40),ROOTI(40),ROOTRN(40),ROOTIN(40)
      DIMENSION B(100),BDA(100),S(100),T(100),U(100),A(100,100)
      DIMENSION R(1000),X(1000),W(1000),FNEW(1000),AVEC(1000)
      DIMENSION PVEC(1000)
      COMMON FREQ(1000),OMEGA(1000),NFREQ
      COMPLEX RES(40)
      COMPLEX*16 S1,D,DJ,CDEXP,DCMPLX,DCONJG
      COMPLEX*16 SS(1000)
      INTEGER FNAME(4),TITLE(18)
      INTEGER YES/'Y'/
      WRITE(6,94)
      WRITE(6,94)
      WRITE(6,94)
      WRITE(6,94)
94    FORMAT(' ')
C......
C......READ DEGREE OF NUMERATOR AND DENOMINATOR POLYNOMIALS
C......
      WRITE(6,219)
219   FORMAT(' ENTER THE DEGREE OF THE NUMERATOR POLYNOMIAL',/
     1,' AS A TWO DIGIT INTEGER')
      READ(5,99)M
99    FORMAT(I2)
      WRITE(6,94)
      WRITE(6,98)
98    FORMAT(' ENTER THE DEGREE OF THE DENOMINATOR POLYNOMIAL',/
     2,' AS A TWO DIGIT INTEGER')
      READ(5,99)N
      WRITE(6,94)
C......
C......READ IN THE DATA TO BE CURVE FIT BY CALLING
C......SUBROUTINE DATA2
C......
      CALL DATA2(R,X,OMEGA,NFREQ,FREQ,FLO,FMAX,FNORM,AMPMIN
```

```
     4,AMPMAX,PHAMIN,PHAMAX,AVEC,PVEC,FNAME,TITLE,IANSW)
C......
C......MAKE A DATA FILE CONTAINING THE DATA TO BE
C......FIT BUT WITH F(NORM)=F(EXP)*2*R/C , WHERE
C......R=RADIUS OF MINIMUM CIRCUMSCRIBING SPHERE,
C......C=SPEED OF LIGHT
C......
      CALL NORMA(NFREQ,AMPMIN,AMPMAX,PHAMIN,PHAMAX,
     3FREQ,AVEC,PVEC,FNAME,TITLE,ALENG)
C......
C......COMPUTE THE SIZE OF THE MATRIX TO BE USED
C......FOR MINIMIZING THE ERROR TO OBTAIN THE LEAST
C......SQUARES ERROR FIT
C......
8810  MN1=M+N+1
      IER=0
C......
C......INITIALIZE THE MATRIX SO THAT ALL
C......THE ELEMENTS ARE SET TO ZERO
C......
      DO 7 I=1,MN1
      DO 7 J=1,MN1
7     A(I,J)=0.D0
      NDIM=50
      IT=0
C......
C......READ NUMBER OF ALLOWED ITERATIONS BY WHICH
C......THE RATIONAL FUNCTION MUST CONVERGE
C......
      WRITE(6,111)
111   FORMAT(' ENTER THE MAXIMUM NUMBER OF ITERATIONS',/
     3,' ALLOWED WITH A TWO DIGIT INTEGER')
      READ(5,113) ITMAX
113   FORMAT(I2)
      WRITE(6,1111)
1111  FORMAT(' ')
      DJ=DCMPLX(0.D0,1.D0)
C......
C......READ THE CONVERGENCE ERROR CRITERION VALUE WHICH
C......DETERMINES TERMINATION OF THE ITERATIVE PROCESS
C......
      WRITE(6,222)
222   FORMAT(' ENTER THE CONVERGENCE ERROR VALUE',/
     4,' IN DOUBLE PRECISION FORMAT')
      READ(5,221) EPS
221   FORMAT(D10.0)
      WRITE(6,921)
921   FORMAT(' ')
C......
C......INITIALIZE THE NUMERATOR AND DENOMINATOR COEFFICIENTS
```

```
C.......TO ZERO. SET W(I) TO ONE WHERE W(I) IS THE DENOMINATOR
C.......SQUARED OF THE K-1 ITERATION, FOR K=1.
C.......
        DO 4 I=1,NFREQ
 4      W(I)=1.D0
        DO 11 I=1,N
        ACOF(I)=0.D0
        AACOF(I)=0.D0
        BBCOF(I)=0.D0
 11     BCOF(I)=0.D0
        ACOF(N+1)=0.D0
        AACOF(N+1)=0.D0
        GOTO 3
C.......
C.......CALCULATE W(I) FOR THE K ITERATION
C.......WHERE K>1
C.......
 1      DO 8 I=1,MN1
        DO 8 J=1,MN1
 8      A(I,J)=0.D0
        DO 5 I=1,NFREQ
        S1=DJ*OMEGA(I)
        D=BCOF(N-1)+BCOF(N)*S1
        NM2=N-2
        DO 10 J=1,NM2
 10     D=BCOF(N-J-1)+D*S1
        D=1.D0+D*S1
 5      W(I)=1.D0/(CDABS(D))**2
C.......
C.......CALCULATE THE ELEMENTS OF THE MATRIX ARRIVED AT
C.......BY TAKING THE DERIVATIVES OF THE ERROR WITH
C.......RESPECT TO THE POLYNOMIAL COEFFICIENTS
C.......
 3      BD0=0.D0
        S0=0.D0
        N2=N+N
        DO 15 I=1,N2
        BDA(I)=0.D0
        S(I)=0.D0
        T(I)=0.D0
 15     U(I)=0.D0
        DO 16 K=1,NFREQ
        BD0=BD0+W(K)
 16     S0=S0+R(K)*W(K)
        DO 20 I=1,N2
        DO 20 K=1,NFREQ
        BDA(I)=BDA(I)+OMEGA(K)**I*W(K)
        S(I)=S(I)+OMEGA(K)**I*R(K)*W(K)
        T(I)=T(I)+OMEGA(K)**I*X(K)*W(K)
 20     U(I)=U(I)+OMEGA(K)**I*(R(K)**2+X(K)**2)*W(K)
```

```
      X1=1.0D0
      BD0=BD0*X1
      S0=S0*X1
      DO 21 K=1,N2
      BDA(K)=BDA(K)*X1
      S(K)=S(K)*X1
      T(K)=T(K)*X1
21    U(K)=U(K)*X1
C......
C......LOAD PARTITIONED MATRIX
C......
      MP1=M+1
C......
C......LOAD UPPER LEFT PARTITION
C......
      A(1,1)=BD0
      DO 30 I=1,MP1,2
      P=-1
      DO 40 J=1,MP1,2
      IF(I.EQ.1.AND.J.EQ.1)GOTO 35
      A(I,J)=BDA((I-1)+(J-1))*P*(-1)
      J1=J+1
      I1=I+1
      IF(J1.GT.MP1.OR.I1.GT.MP1)GOTO 40
35    A(I+1,J+1)=BDA((I-1)+(J-1)+2)*P*(-1)
40    P=P*(-1)
30    CONTINUE
C......
C......LOAD LOWER RIGHT PARTITION
C......
      DO 50 I=1,N,2
      P=-1
      DO 55 J=1,N,2
      A(MP1+I,MP1+J)=U(I+J)*P*(-1)
      MPI=MP1+I+1
      MPJ=MP1+J+1
      IF(MPI.GT.MN1.OR.MPJ.GT.MN1)GOTO 55
      A(MPI,MPJ)=U(I+J+2)*P*(-1)
55    P=P*(-1)
50    CONTINUE
C......
C......LOAD UPPER RIGHT AND LOWER LEFT MATRICES
C......
      DO 60 I=1,N,2
      P=-1
      DO 60 J=1,N,2
      IF(I.LE.MP1)A(I,MP1+J)=T(I+J-1)*P*(-1)
      IF(J.LE.MP1)A(I+MP1,J)=T(I+J-1)*P*(-1)
      I1=I+1
      J1=J+1
```

```
      IF(I1.LE.MP1.AND.J1.LE.N)A(I1,J1+MP1)=T(I+J+1)*P*(-1)
      IF(J1.LE.MP1.AND.I1.LE.N)A(I1+MP1,J1)=T(I+J+1)*P*(-1)
60    P=P*(-1)
      DO 65 I=1,N,2
      P=-1
      DO 65 J=2,N,2
      IF(I.LE.MP1)A(I,MP1+J)=S(I-1+J)*P*(-1)
      IF(J.LE.MP1)A(I+MP1,J)=S(I-1+J)*P
      I1=I+1
      J1=J+1
      MPI=MP1+1
      IF(I1.LE.N.AND.J.LE.MPI)A(I+MP1+1,J-1)=S(I-1+J)*P*(-1)
      IF(I1.LE.N)A(I1,J+MP1-1)=S(I-1+J)*P
      IF(I1.LE.N.AND.J1.LE.MP1)A(I1+MP1,J1)=S(I+J+1)*P
      IF(I1.LE.MP1.AND.J1.LE.N)A(I1,J1+MP1)=S(I+J+1)*P*(-1)
65    P=P*(-1)
C......
C......LOAD B-VECTOR
C......
      MP2=M+2
      B(1)=S0
      DO 85 K=2,MP1,2
      KP1=K+1
      B(K)=T(K-1)
      IF(K.GT.MP1) GOTO 85
      B(K+1)=S(K)
85    CONTINUE
      DO 86 K=MP2,MN1,2
      B(K)=0.D0
      KP1=K+1
      IF(KP1.GT.MN1)GOTO 86
      B(KP1)=U(K-M)
86    CONTINUE
C......
C......CALL GAUSSIAN ELIMINATION ROUTINE
C......TO INVERT MATRIX SO THE POLYNOMIAL
C......COEFFICIENTS CAN BE FOUND
C......
      CALL REDUCE(A,MN1,B,NDIM)
C......
C......CALCULATE CONVERGENCE ERROR FOR THIS ITERATION
C......
      AERR=0
      BERR=0
      DO 95 I=1,MP1
95    AERR=(B(I)-ACOF(I))**2+AERR
      DO 97 I=MP2,MN1
97    BERR=(B(I)-BCOF(I-M-1))**2+BERR
      ERR=AERR+BERR
      IF(ERR.LE.EPS.OR.IT.EQ.ITMAX)GOTO 350
```

```
C......
C......TRANSFER B(I)'S TO COEFFICIENT MATRICES
C......
       DO 90 I=1,MN1
C      IF(B(I).LT.0)B(I)DABS(B(I))
       IF(I.GE.MP2)GOTO 87
       ACOF(I)=B(I)
       AACOF(I)=B(I)
       GOTO 90
87     BCOF(I-MP1)=B(I)
       BBCOF(I-MP1)=B(I)
90     CONTINUE
       IT=IT+1
C......
C......WRITE ITERATION NUMBER AND
C......CONVERGENCE ERROR VALUE
C......
       WRITE(6,999) IT,ERR
999    FORMAT(3X,'IT=',I3,5X,'ERR=',E12.6)
       GOTO 1
C......
C......SET FIRST DENOMINATOR COEFFICIENT, BO,
C......EQUAL TO ONE
C......
350    XCOF(1)=1
       BBCO(1)=1
       NP1=N+1
       DO 355 I=2,NP1
       XCOF(I)=BCOF(I-1)
355    BBCO(I)=BCOF(I-1)
       WRITE(6,96)
96     FORMAT(' ')
       WRITE(6,301)
301    FORMAT('ROOTS OF DENOMINATOR ARE:'/ ' ')
C......
C......FIND THE ROOTS OF THE DENOMINATOR POLYNOMIAL
C......
       CALL ROOTS(XCOF,COF,N,ROOTR,ROOTI,IER)
C......
C......FIND THE RESIDUES OF THE RATIONAL FUNCTION
C......
       CALL RESIDU(AACOF,BBCOF,M,N,ROOTI,ROOTR,RES,FMAX,FNORM
      1,ALENG)
C......
C......FIND THE ROOTS SCALED TO THE RADIUS OF
C......THE MINIMUM CIRCUMSCRIBING SPHERE
C......
       PI=3.1415926535
       DO 28 I=1,N
       ROOTEN(I)=ROOTR(I)*FMAX/FNORM*ALENG/(PI*300.0)
```

```
      ROOTIN(I)=ROOTI(I)*FMAX/FNORM*ALENG/(PI*300.0)
28    CONTINUE
C......
C......WRITE NORMALIZE ROOTS AND RESIDUES
C......INTO DEVICE 10.
C......
      WRITE(10,192) FNAME
      WRITE(10,188)
      WRITE(10,185)
      WRITE(10,187) M,N
      WRITE(10,192) TITLE
      WRITE(10,400) (ROOTRN(I),ROOTIN(I),RES(I),I=1,N)
      WRITE(10,403)
403   FORMAT(12H DC TERM IS:)
C......
C......CALCULATE THE PREDICTED ZERO FREQUENCY
C......VALUE OF THE RESPONSE
C......
      A0=ACOF(1)
      WRITE(10,402) A0
402   FORMAT(1X,E12.4)
      WRITE(6,401) (ROOTRN(I),ROOTIN(I),I=1,N)
      WRITE(6,223)
223   FORMAT(' ')
C......
C......WRITE THE RESIDUES ON THE
C......INTERACTIVE TERMINAL(DEVICE 6)
C......
      WRITE(6,302)
302   FORMAT('RESIDUES ARE, RESPECTIVELY:'/ ' ')
      WRITE(6,202) (RES(I),I=1,N)
202   FORMAT(2X,2E12.4)
      WRITE(6,2200)
2200  FORMAT(' ')
400   FORMAT(4(1X,E12.4))
401   FORMAT(2(1X,E12.4))
188   FORMAT(27H NORMALIZED POLE LOCATIONS ,
     813H AND RESIDUES)
187   FORMAT(1X,2I5)
192   FORMAT(1X,18A4)
185   FORMAT(11H      M     N)
C......
C......CONSTRUCT FREQUENCY RESPONSE USING THE
C......RATIONAL FUNCTION APPROXIMATION TO THE
C......MEASURED DATA
C......
      CALL CONDA(NFREQ,FMAX,FLO,FNORM,N,AACOF,BBCO,M,FNAME
     5,TITLE,ALENG,SS)
      STOP
      END
```

```
C=======================================================================
C......
C......THIS SUBROUTINE SOLVES A*X=B BY GAUSSIAN
C......ELIMINATION. N IS THE MATRIX SIZE. X IS
C......REDUCED IN B.  A IS DESTROYED. A IS CONVERTED
C......TO UPPER TRIANGULAR FORM AND BACK SUBSTITUTION
C......IS PERFORMED.
C......
C=======================================================================
      SUBROUTINE REDUCE(A,N,B,NDIM)
      IMPLICIT REAL*8(A-H,O-Z)
      DIMENSION A(100,100),B(100)
      NM1=N-1
      DO 1 J=1,NM1
C......
C......FIND LARGEST ELEMENT IN JTH COLUMN
C......
      AMAX=DABS(A(J,J))
      LSAVE=J
      IJ=J+1
      DO 7 L=IJ,N
      IF(DABS(A(L,J)).LE.AMAX)GO TO 7
      AMAX=DABS(A(L,J))
      LSAVE=L
7     CONTINUE
      IF(AMAX.LT.1.D-61)WRITE(6,10)
      IF(LSAVE.EQ.J)GO TO 8
C......
C......EXCHANGE ROWS OF A AND B
C......
      DO 9 L=J,N
      TEMP=A(J,L)
      A(J,L)=A(LSAVE,L)
9     A(LSAVE,L)=TEMP
      TEMP=B(J)
      B(J)=B(LSAVE)
      B(LSAVE)=TEMP
8     DO 1 I=IJ,N
      ALPHA=A(I,J)/A(J,J)
      DO 2 K=IJ,N
2     A(I,K)=A(I,K)-ALPHA*A(J,K)
1     B(I)=B(I)-ALPHA*B(J)
C......
C......PERFORM BACK SUBSTITUTION
C......
      DO 5 J=1,N
      LAST=N-J+1
      LAST1=LAST+1
      IF(LAST1.GT.N)GO TO 5
      DO 3 I=LAST1,N
```

```
 3      B(LAST)=B(LAST)-A(LAST,I)*B(I)
 5      B(LAST)=B(LAST)/A(LAST,LAST)
        RETURN
10      FORMAT('SMALL-OR ZERO-VALUED PIVOT')
        END
C=====================================================================
C......
C......THIS ROUTINE SOLVES FOR THE COMPLEX
C......ROOTS OF A NTH ORDER POLYNOMIAL.
C......THE ROOTS ARE RETURNED IN REAL AND IMAGINARY
C......PARTS.
C......
C=====================================================================
        SUBROUTINE ROOTS(XCOF,COF,M,ROOTR,ROOTI,IER)
        IMPLICIT REAL*8(A-H,O-Z)
        DIMENSION XCOF(40),COF(40),ROOTR(40),ROOTI(40)
        IFIT=0
        N=M
        IER=0
        IF(XCOF(N+1))10,25,10
10      IF(N)15,15,32
15      IER=1
20      RETURN
25      IER=4
        GO TO 20
30      IER=2
        GO TO 20
32      IF(N-40)35,35,30
35      NX=N
        NXX=N+1
        N2=1
        KJ1=N+1
        DO 40 L=1,KJ1
        MT=KJ1-L+1
40      COF(MT)=XCOF(L)
45      XO=.00500101
        YO=0.01000101
        IN=0
50      X=XO
        XO=-10.0*YO
        YO=-10.0*X
        X=XO
        Y=YO
        ICT=0
        IN=IN+1
        GO TO 60
55      IFIT=1
        XPR=X
        YPR=Y
60      ICT=0
```

```
      UX=0.0
      UY=0.0
      V=0.0
      YT=0.0
      XT=1.0
      U=COF(N+1)
      IF(U)65,130,65
   65 DO 70 I=1,N
      L=N-I+1
      TEMP=COF(L)
      XT2=X*XT-Y*YT
      YT2=X*YT+Y*XT
      U=U+TEMP*XT2
      V=V+TEMP*YT2
      FI=I
      UX=UX+FI*XT*TEMP
      UY=UY-FI*YT*TEMP
      XT=XT2
   70 YT=YT2
      SUMSQ=UX*UX+UY*UY
      IF(SUMSQ)75,110,75
   75 DX=(V*UY-U*UX)/SUMSQ
      X=X+DX
      DY=-(U*UY+V*UX)/SUMSQ
      Y=Y+DY
   78 IF(DABS(DY)+DABS(DX)-1.0D-12)100,80,80
   80 ICT=ICT+1
      IF(ICT-500)60,85,85
   85 IF(IFIT)100,90,100
   90 IF(IN-5)50,95,95
   95 IER=3
      GO TO 20
  100 DO 105 L=1,NXX
      MT=KJ1-L+1
      TEMP=XCOF(MT)
      XCOF(MT)=COF(L)
  105 COF(L)=TEMP
      ITEMP=N
      N=NX
      NX=ITEMP
      IF(IFIT)120,55,120
  110 IF(IFIT)115,50,115
  115 X=XPR
      Y=YPR
  120 IFIT=0
  122 IF(DABS(Y/X)-1.0D-10)135,125,125
  125 ALPHA=X+X
      SUMSQ=X*X+Y*Y
      N=N-2
      GO TO 140
```

```
130   X=0.0
      NX=NX-1
      NXX=NXX-1
135   Y=0.0
      SUMSQ=0.0
      ALPHA=X
      N=N-1
140   COF(2)=COF(2)+ALPHA*COF(1)
      IF(N)155,155,145
145   DO 150 L=2,N
150   COF(L+1)=COF(L+1)+ALPHA*COF(L)-SUMSQ*COF(L-1)
155   ROOTI(N2)=Y
      ROOTR(N2)=X
      N2=N2+1
      IF(SUMSQ)160,165,160
160   Y=-Y
      SUMSQ=0.0
      GOTO 155
165   IF(N)20,20,45
      END
C=====================================================================
C......
C......THIS SUBROUTINE READS IN THE FREQUENCY RESPONSE
C......TO BE FIT. DATA CAN BE SUBMITTED IN TWO DIFFERENT
C......FORMS. THE FIRST FORM IS FOR FREQ.(MHZ), AMP., PHASE,
C......AT THREE DATA SETS PER LINE AND THE FORMAT
C......SPECIFICATION IS 3(2F8.3,F8.2).
C......THE SECOND FORM IS FOR FREQ.(MRAD.), REAL
C......PART, IMAGINARY PART, AT ONE DATA SET PER
C......LINE AND THE FORMAT SPECIFICATION IS 3F12.6
C......
C=====================================================================
      SUBROUTINE DATA2(R,X,OMEGA,NFREQ,FREQ,FLO,FMAX,FNORM,
     2AMPMIN,AMPMAX,PHAMIN,PHAMAX,AVEC,PVEC,FNAME,TITLE,IANSW)
      IMPLICIT  REAL*8(A-H,O-Z)
      DIMENSION FREQ(1000),R(1000),X(1000),AVEC(1000),PVEC(1000)
     1,OMEGA(1000),RFREQ(1000)
      INTEGER FNAME(4),WHICH,N,NM2,NFREQ
      INTEGER CMNT1(18),CMNT2(18),TITLE(18)
      INTEGER YES/'Y'/
C......
C......READ FILE NAMES, TITLES, AND COMMENTS
C......
      READ(9,109)FNAME
      WRITE(6,110)FNAME
      READ(9,109)CMNT1
      READ(9,109)CMNT2
      READ(9,109)TITLE
      WRITE(6,110)TITLE
      WRITE(6,98)
```

```
98    FORMAT(' ')
C......
C......READ IN MIN. AND MAX. VALUES
C......READ NUMBER OF DATA POINTS
C......
      READ(9,101)FLO,FMAX,AMPMIN,AMPMAX,PHAMIN,PHAMAX,NFREQ
      II=NFREQ
      WRITE(6,121)
121   FORMAT(' IS DATA IN THE FORM OF FREQ(MRAD),REAL,IMAG. ?')
      READ(5,122) IANSW
122   FORMAT(A1)
      IF(IANSW.EQ.YES) GO TO 322
      WHICH= MOD(II,3)-1
      NM2= II-2
      DO 20 I= 1,NM2,3
      READ(9,107)FREQ(I),AVEC(I),PVEC(I),FREQ(I+1),AVEC(I+1),
     1PVEC(I+1),FREQ(I+2),AVEC(I+2),PVEC(I+2)
20    CONTINUE
      IF(WHICH)21,22,23
22    READ(9,107)FREQ(II),AVEC(II),PVEC(II)
      GO TO 21
23    READ(9,107)FREQ(II-1),AVEC(II-1),PVEC(II-1),FREQ(II),
     1AVEC(II),PVEC(II)
21    CONTINUE
101   FORMAT(4F8.3,2F8.2,I5)
107   FORMAT(3(2F8.3,F8.2))
109   FORMAT(18A4)
110   FORMAT(1X,18A4)
      FNORM=(FMAX/(FLO*2.*3.1415926535))**.5
      WRITE(6,93)
93    FORMAT(' ')
      DO 30 I=1,NFREQ
      OMEGA(I)=2.*3.1415926535*FREQ(I)/FMAX*FNORM
      A=AVEC(I)
      P=PVEC(I)*3.1415926535/180.
      R(I)=A*DCOS(P)
      X(I)=A*DSIN(P)
30    CONTINUE
      GOTO 29
322   FNORM=(FMAX/FLO)**.5
      WRITE(6,93)
      FLO=FLO/(2.*3.1415926535)
      FMAX=FMAX/(2.*3.1415926535)
      DO 325 I=1,II
      READ(9,324) RFREQ(I),R(I),X(I)
      AVEC(I)=DSQRT(R(I)**2+X(I)**2)
      PHASE=DATAN2(X(I),R(I))
      PVEC(I)=PHASE*180./3.1415926535
C......
C......CONVERT FREQUENCY IN RAD. TO  HERTZ
```

```
C......
      FREQ(I)=RFREQ(I)/(2.*3.14159)
      OMEGA(I)=RFREQ(I)/FMAX*FNORM
325   CONTINUE
324   FORMAT(3F12.6)
29    RETURN
      END
C========================================================================
C......
C......THIS ROUTINE CALCULATES THE RESIDUES OF
C......THE POLES OF A RATIONAL FUNCTION GIVEN
C......THE POLES OF THE RATIONAL FUNCTION
C......
C========================================================================
      SUBROUTINE RESIDU(AACOF,BBCOF,M,N,ROOTI,ROOTR,RES,FMAX,
     @FNORM,ALENG)
      IMPLICIT REAL*8(A-H,O-Z)
      DIMENSION AACOF(40),BBCOF(40),ROOTI(40),ROOTR(40)
      COMPLEX*16 AA,BB,RESID
      COMPLEX RES(40)
      PI=3.1415926535
      II=1
      DO 11 J=1,N
      AA=DCMPLX(AACOF(1),0.D0)
      MM=M+1
      DO 12 I=2,MM
      AA=AA+DCMPLX(AACOF(I),0.D0)*DCMPLX(ROOTR(J),ROOTI(J))*
     1*(I-1)
12    CONTINUE
      BB=DCMPLX(BBCOF(1),0.D0)
      DO 13 I=2,N
      XX=I
      BB=BB+DCMPLX(BBCOF(I),0.D0)*DCMPLX(XX,0.D0)
     1*DCMPLX(ROOTR(J),ROOTI(J))**(I-1)
13    CONTINUE
      RESID=AA/BB
      RES(II)=RESID*FMAX/FNORM*ALENG/(PI*300.0)
      II=II+1
11    CONTINUE
      RETURN
      END
C========================================================================
C......
C......THIS ROUTINE TAKES THE RATIONAL FUNCTION
C......WHICH BEST FIT THE DATA AND CONSTRUCTS THE
C......FREQUENCY RESPONSE OF THE FITTED FUNCTION
C......
C========================================================================
      SUBROUTINE  CONDA(NFREQ,FMAX,FLO,FNORM,N,AACOF,BBCO,M,
     2FNAME,TITLE,ALENG,SS)
```

```
      IMPLICIT REAL*8(A-H,O-Z)
      DIMENSION FVEC(1000),PVEC(1000),AVEC(1000),FVECN(1000)
      DIMENSION AACOF(40),BBCO(40)
      INTEGER FNAME(4),TITLE(18)
      COMPLEX*16 SS(1000),CONST,A2,B2,CI
      INTEGER WHICH
      AMPMIN=1200.0
      AMPMAX=-1200.0
      PHAMIN=1200.0
      PHAMAX=-1200.0
      II=NFREQ
      PI=3.1415926535
      CI=(0.D0,1.D0)
      FLO=(FLO/FMAX)*FNORM
      FHI=FNORM
      DF=(FHI-FLO)/(NFREQ-1)
      DELOM=2.*PI*DF
      OM=2.*PI*FLO
      MM=M+1
      NN=N+1
      DO 150 L=1,NFREQ
      SS(L)=CI*OM
      A2=DCMPLX(AACOF(1),0.D0)
      DO 12 I=2,MM
      A2=A2+DCMPLX(AACOF(I),0.D0)*SS(L)**(I-1)
12    CONTINUE
      B2=DCMPLX(BBCO(1),0.D0)
      DO 13 I=2,NN
      B2=B2+DCMPLX(BBCO(I),0.D0)*SS(L)**(I-1)
13    CONTINUE
      CONST=A2/B2
      RR=DREAL(CONST)
      XX=DIMAG(CONST)
      PHASE=DATAN2(XX,RR)
      PVEC(L)=PHASE*180.0/PI
      FVEC(L)=DIMAG(SS(L))/(2.0*PI)*(FMAX/FNORM)
      AVEC(L)=CDABS(CONST)
      OM=OM+DELOM
      IF(AMPMIN .GT. AVEC(L)) AMPMIN=AVEC(L)
      IF(AMPMAX .LT. AVEC(L)) AMPMAX=AVEC(L)
      IF(PHAMIN .GT. PVEC(L)) PHAMIN=PVEC(L)
      IF(PHAMAX .LT. PVEC(L)) PHAMAX=PVEC(L)
150   CONTINUE
      DO 15 I=1,NFREQ
      FVECN(I)=FVEC(I)*ALENG/150.
15    CONTINUE
      FLO=FVECN(1)
      FMAX=FVECN(II)
      WRITE(8,109) FNAME
      WRITE(8,111)
```

```
          WRITE(8,110)
          WRITE(8,109) TITLE
C......
C......WRITE DATA ON DEVICE 8 .
C......
          WRITE(8,101)FLO,FMAX,AMPMIN,AMPMAX,PHAMIN,PHAMAX,NFREQ
          WHICH= MOD(II,3)-1
          NM2=II-2
          DO 20 I= 1,NM2,3
          WRITE(8,107)FVECN(I),AVEC(I),PVEC(I),FVECN(I+1),AVEC(I+1)
         1,PVEC(I+1),FVECN(I+2),AVEC(I+2),PVEC(I+2)
20        CONTINUE
          IF(WHICH)21,22,23
22        WRITE(8,107)FVECN(II),AVEC(II),PVEC(II)
          GO TO 21
23        WRITE(8,107)FVECN(II-1),AVEC(II-1),PVEC(II-1),FVECN(II),
         1AVEC(II),PVEC(II)
21        CONTINUE
101       FORMAT(4F8.3,2F8.2,I5)
107       FORMAT(3(2F8.3,F8.2))
109       FORMAT(1X,18A4)
110       FORMAT(25H                          )
111       FORMAT(44H RATIONAL FUNCTION RESPONSE WITH NORMAILIZED,
         110H FREQUENCY)
          RETURN
          END
C=====================================================================
C......
C......THIS ROUTINE NORMALIZES THE EXPERIMENTAL
C......DATA TO THE RADIUS OF THE MINIMUM
C......CIRCUMSCRIBING SPHERE.
C......
C=====================================================================
          SUBROUTINE NORMA(NFREQ,AMPMIN,AMPMAX,PHAMIN,PHAMAX,
         3FREQ,AVEC,PVEC,FNAME,TITLE,ALENG)
          IMPLICIT REAL*8(A-H,O-Z)
          DIMENSION FREQ(1000),PVEC(1000),AVEC(1000),FNEW(1000)
          INTEGER FNAME(4),TITLE(18),WHICH,NFREQ
          II=NFREQ
          WRITE(6,124)
124       FORMAT('ENTER RADIUS OF MINIMUM CIRCUMSCRIBING SPHERE')
          READ(5,125) ALENG
125       FORMAT(F10.3)
          WRITE(6,98)
98        FORMAT(' ')
C......
C......FIND W*L/PI*C, THE NORMALIZED FREQUENCY
C......
          DO 29 I=1,NFREQ
          FNEW(I)=2*FREQ(I)*ALENG/300.
```

```
 29   CONTINUE
      FLO=FNEW(1)
      FMAX=FNEW(II)
      WRITE(7,111) FNAME
      WRITE(7,112)
      WRITE(7,110)
      WRITE(7,111) TITLE
C......
C......WRITE NORMALIZED DATA ON DEVICE 7 .
C......
      WRITE(7,101)FLO,FMAX,AMPMIN,AMPMAX,PHAMIN,PHAMAX,NFREQ
      WHICH= MOD(NFREQ,3)-1
      NM2=NFREQ-2
      DO 20 I= 1,NM2,3
      WRITE(7,107)FNEW(I),AVEC(I),PVEC(I),FNEW(I+1),AVEC(I+1),
     1PVEC(I+1),FNEW(I+2),AVEC(I+2),PVEC(I+2)
 20   CONTINUE
      IF(WHICH)21,22,23
 22   WRITE(7,107)FNEW(II),AVEC(II),PVEC(II)
      GO TO 21
 23   WRITE(7,107)FNEW(II-1),AVEC(II-1),PVEC(II-1),FNEW(II),
     1AVEC(II),PVEC(II)
 21   CONTINUE
 101  FORMAT(4F8.3,2F8.2,I5)
 107  FORMAT(3(2F8.3,F8.2))
 112  FORMAT(30H NORMAILIZED EXPERIMENTAL DATA)
 110  FORMAT(25H                         )
 111  FORMAT(1X,18A4)
      RETURN
      END
```

References

Baum, C. E. (1976), "The singularity expansion method," in Transient Electromagnetic Fields (ed. L. B. Felsen), Springer-Verlag, Berlin.

Bowman, J. J., T.B.A. Senior and P.L.E. Uslenghi (1969), "Electromagnetic and acoustic scattering by simple shapes," North-Holland Pub. Co., Amsterdam.

Brittingham, J. N., E. K. Miller and J. L. Willows (1980), "Pole extraction from real-frequency information," Proc. IEEE 68, No. 2, 263-273.

Cho, K. S., and J. T. Cordaro (1980), "Calculation of the SEM parameters from the transient response of a thin wire," IEEE Trans. Antennas Propagat. AP-28, No. 6, also (1977) AFWL Interaction Note 379.

Levy, E. C. (1959), "Complex curve fitting," IRE Trans. Automatic Control AC-4, 37-44.

Liepa, V. V. (1980), "Scale model measurements of the B-52," University of Michigan Radiation Laboratory Report NO. 017463-2-F; AFWL Interaction Application Memo 36.

Martinez, J. P., Z. L. Pine and F. M. Tesche (1972), "Numerical results of the singularity expansion method as applied to a plane wave incident on a perfectly conducting sphere," AFWL Interaction Note 112.

Sancer, M. I., and A. D. Varvatsis (1980), "Toward an increased understanding of the singularity expansion method," AFWL Interaction Note 398.

Senior, T.B.A. (1975), Far field bistatic scattering by a sphere," The University of Michigan Radiation Laboratory Report No. 013741-1-F.

Sharpe, C. B., and C. J. Roussi (1979), "Equivalent circuit representation of radiation systems," AFWL Interaction Note 361.

Stratton, J. A. (1941), "Electromagnetic theory," McGraw-Hill Book Co., Inc., New York.

☆U.S. GOVERNMENT PRINTING OFFICE : 1982–576-115/522